CORN-BASED DEICERS

Final Report
IHRB Project TR-754
July 2020

Sponsored to
The Iowa Highway Research Board

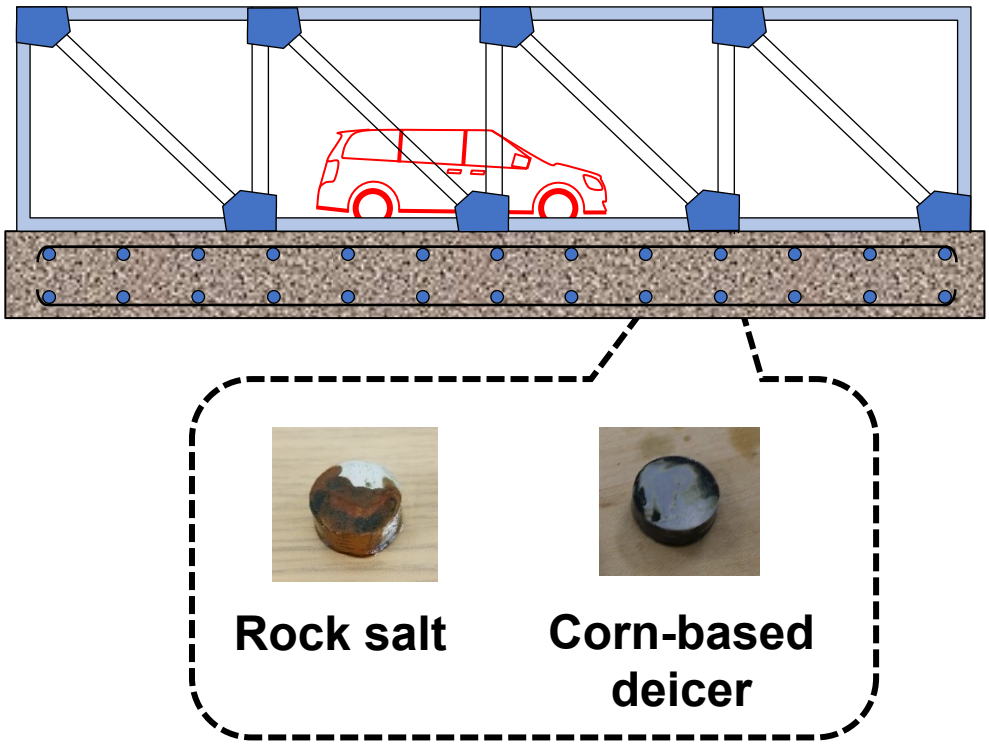

Disclaimer Notice

The contents of this report reflect the views of the authors, who are responsible for the facts and the accuracy of the information presented herein. The opinions, findings, and conclusions expressed in this publication are those of the authors and not necessarily those of the sponsors.

The sponsors assume no liability for the contents or use of the information contained in this document. This report does not constitute a standard, specification, or regulation. The sponsors do not endorse products or manufacturers. Trademarks or manufacturers' names appear in this report only because they are considered essential to the objectives of the document.

Statement of Non-Discrimination

Federal and state laws prohibit employment and/or public accommodation discrimination on the basis of age, color, creed, disability, gender identity, national origin, pregnancy, race, religion, sex, sexual orientation or veteran’s status. If you believe you have been discriminated against, please contact the Iowa Civil Rights Commission at 800-457-4416 or Iowa Department of Transportation's affirmative action officer. If you need accommodations because of a disability to access the Iowa Department of Transportation’s services, contact the agency's affirmative action officer at 800-262-0003.

TECHNICAL REPORT DOCUMENTATION PAGE

1. Report No. IHRB Project TR-754	**2. Government Accession No.**	**3. Recipient's Catalog No.**
4. Title and Subtitle Corn-Based Deicers		**5. Report Date** July 2020 **6. Performing Organization Code**
7. Author(s) Ravi Kiran Yellavajjala, Ph.D., P.E. https://orcid.org/0000-0001-8300-0767 Dayakar Naik Lavadiya, Ph.D. https://orcid.org/0000-0003-0558-3893 Hizb Ullah Sajid. https://orcid.org/0000-0002-2370-8592		**8. Performing Organization Report No.**
9. Performing Organization Name and Address North Dakota State University, 1340 Administration Ave, Fargo, ND-58105		**10. Work Unit No.** **11. Contract or Grant No.**
12. Sponsoring Agency Name and Address Iowa Highway Research Board Iowa Department of Transportation 800 Lincoln Way Ames, IA 50010.		**13. Type of Report and Period Covered** 10/1/2018-7/31/2020 **14. Sponsoring Agency Code**
15. Supplementary Notes		

16. Abstract

Scaling up the production of agro-byproduct-based deicer is challenging as their yield is far less than the demand. Since corn is the most planted crop in the United States, the current study focuses on developing corn-based deicers that possess lower freezing point depression, enhanced ice melting capacity, and corrosion inhibition properties. The PI hypothesizes that the sugar alcohols/polyols like Sorbitol, Maltitol and Mannitol produced from the corn starch can enhance salt-brine deicer. Various blends of deicers referred to as corn-based deicers are generated by combining corn juice, corn-derived polyols, and salt-brine in different weight fractions and their deicing properties are determined experimentally by performing five tests, namely, freezing point depression, corrosion inhibition, ice melting capacity, skid resistance, viscosity and, dissolved oxygen. Based on the results obtained, a blend of deicer prepared from 27 wt. % Sorbitol+23.3 wt. % salt-brine is recommended to achieve freezing point depressions as low as -38.1°C and, 27 wt. % Maltitol+23.3 wt. % salt-brine is recommended for freezing point depressions between -25°C to -35.6°C. In corrosion-prone zones such as bridge decks, concrete pavements and steel bridges a blend of deicer prepared by adding 0.5-2 wt. % Mannitol to 23.3 wt. % salt-brine is recommended. A blend of deicer prepared from 27 wt. % Mannitol+23.3 wt. % salt-brine is recommended at sub-freezing temperatures of -10°C and -20°C for improved ice melting capacity.

17. Key Words Deicing chemicals (Rbmnj); Snow and ice control (Fmbs); Corrosion resistant materials (Rbmdyse); Skid resistance tests (Gbks); and Organic materials (Rbmdm)	**18. Distribution Statement** No restrictions.

19. Security Classif. (of this report) Unclassified	**20. Security Classif. (of this page)** Unclassified	**21. No. of Pages** 75	**22. Price**

Form DOT F 1700.7 (8-72) Reproduction of completed page authorized

CORN-BASED DEICERS

Final Report
July 2020

Principal Investigator

Ravi Kiran Yellavajjala, Ph.D., P.E.
Assistant Professor
Department of Civil and Environmental Engineering
North Dakota State University

Co-authors

Dayakar Naik Lavadiya, Ph.D.*
Hizb Ullah Sajid*

*Graduate Research Assistant
Department of Civil and Environmental Engineering
North Dakota State University

Sponsored by

the Iowa Highway Research Board
(IHRB Project TR-754)

A Report from

Damage in Materials and Structures Laboratory
Department of Civil and Environmental Engineering
CIE 201, 1410 North 14th Avenue
Fargo, ND 58105-5285
Phone: 701-231-7878
Fax: 701-231-6185
www.ndsu-dams.org

Table of Contents

List of Figures

List of Tables

Acknowledgements

The PI would like to thank the Iowa Highway Research Board (IHRB) for sponsoring this research. The PI acknowledges the valuable comments and suggestions provided by the TAC members Ms. Tina Greenfield and Mr. Craig Bargfrede. PI thankfully acknowledges constant support provided by Ms. Vanessa Goetz during the execution of the project. The authors thank Ms. Jan Lofberg (CEE, NDSU) for administrating this grant. Further, the authors would also like to acknowledge the support from Pilot Plant and the laboratory staff from Research Park at North Dakota State University (NDSU). Technical support and guidance from Polymers and Coatings Department to carry out polarization tests is highly appreciated. The authors would like to thank the Department of Civil and Environmental Engineering and North Dakota State University for providing laboratory facilities to carry out the experiments.

CHAPTER 1
INTRODUCTION

1.1 Background

Snow and icy pavements disrupt the smooth flow of traffic, rendering the traffic network dysfunctional (Izumi et al. 1997; Kao and Sung 2017). This may result in massive economic losses, discomfort to the public, and sometimes even loss of life (Salt and Deicing 1991). Commercial vehicle operators lose about 32.6 billion driving hours each year due to the traffic delays caused by adverse road conditions resulting in a loss of $2.2 to $3.5 billion (FHWA 2018). According to United States Federal Highway Administration (FHWA), about 10%, 8% and 9% of weather-related crashes that occurred between 2005 and 2014 can be attributed to snow/sleet, ice and snow/ slush on pavements, respectively as shown in Figure 1.1 (FHWA 2018). The number of fatalities that are caused by snow/ sleet on pavements alone in the last 20 years is considerably high and the actual fatality trends are provided in Figure 1.2 (Administration 2018). The local and state bodies regularly perform maintenance routines to improve the pavement surface conditions during winter months. The maintenance routines include either deicing of pavement after a snow event or adding anti-icing agents to the roadways prior to a snow event. Deicing is the process of removing snow, frost, or ice from the surface of the pavement by plowing. In contrast, anti-icing is the process of delaying the formation of ice or its adhesion to surface by applying chemical/ abrasive agents to the surface of pavements (Fischel 2009). Each year, the Iowa Department of Transportation spends around $14 million on the deicing of roadways (IowaDoT 2018).

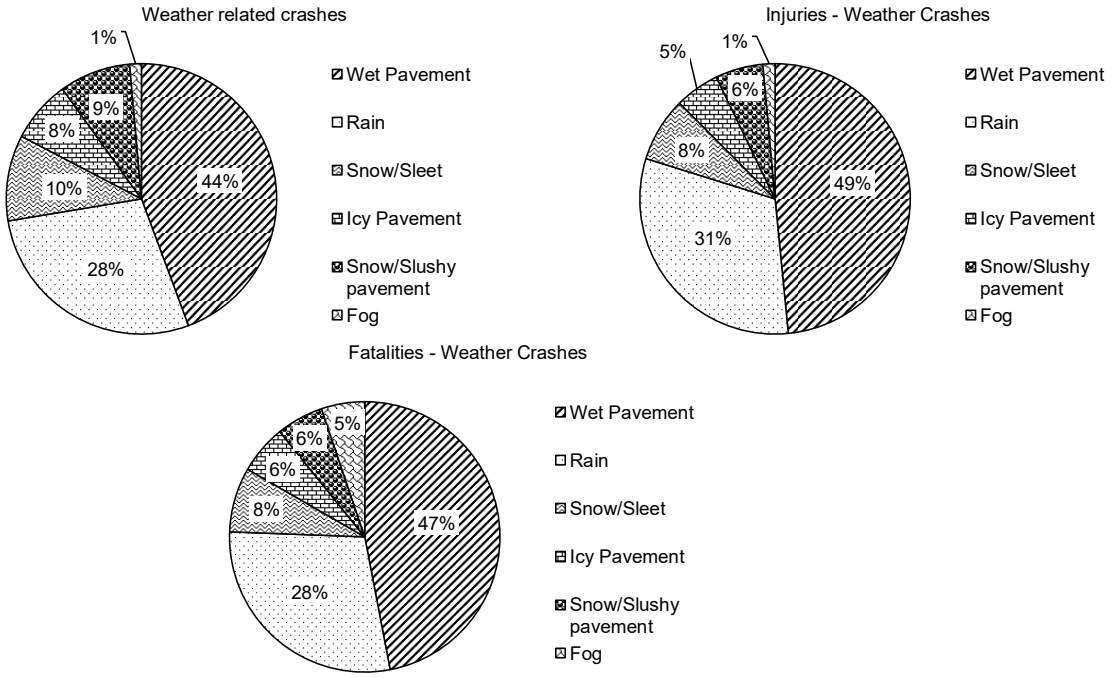

Figure 1.1. Weather-related crashes in the USA between 2005-2014 (FHWA 2018).

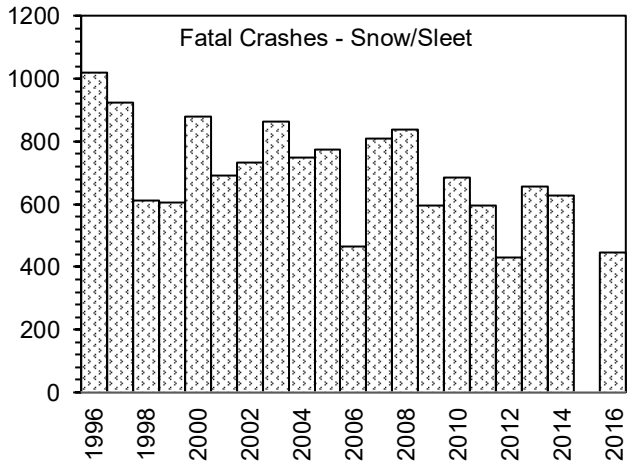

Figure 1.2. Snow/sleet related fatalities between 1996-2016 (NHTSA 2018)).

1.2 Traditional Chloride and Acetate-Based Deicers and their Limitations

Deicing methods that are practiced by various state Department of Transportation (DoT) for winter maintenance can be broadly classified into three categories, namely, mechanical, thermal, and chemical methods (Shi and Fu 2018). While mechanical and chemical methods are more commonly used in practice, thermal methods are least popular. One of the mechanical methods of deicing is to spread sand or other abrasive materials on the roadway with the intention of improving friction between the vehicle tires and the icy pavements. This method has been used for decades and proved to be effective on low traffic volume roads, unpaved roads, and low speed paved roads (Public Sector Consultants 1993). However, on high traffic volume roads, the effectiveness of this method is reduced by the continuous flow of traffic. In addition to this, applied sand can drain into the adjacent sewer systems clogging them in the long run. Chloride and acetate-based deicers are commonly used as chemical-based methods (Shi and Fu 2018) (see Table 1.1). On an average, a state Department of Transportation (DoT) in the United States apply as much as 44,000 pounds of deicing salt per lane mile in winter season (Kelting 2010). Further, an increasing trend of total annual consumption of sodium chloride for roadway operations in the US also reveals the volume of demand for deicers (see Figure 1.3). Chloride-based salts like sodium chloride (NaCl), magnesium chloride ($MgCl_2$), and calcium chloride ($CaCl_2$) are used to break down the ice and snow by lowering the freezing point of the water (Goff 2018). Water molecules on the surface of the ice readily react with the salt to form a thin layer of salty water when the chloride-based salt comes in contact with the surface of ice crystals (Kimbrough 2006). This reaction is facilitated by the presence of loosely bonded unstable and mobile water molecules on the surface of ice crystals. The freezing temperature of the salt solution is lower than the freezing point of pure water as the salt molecules hinder the nucleation and growth of ice crystals (Kimbrough 2006). The process of ice melting continues as the saltwater spreads on the ice surface occupying more surface area and melting more ice.

Chloride based deicers are efficient and economical but are detrimental to concrete pavements (Sumsion and Guthrie 2013), steel bridges, vehicles (Shi and Fu 2018), soil quality (Amrhein et al. 1992) and aquatic life (MPCA 2018). In 2010, the annual cost of automobile corrosion due to deicing salt alone was estimated to be $11.7 billion (Kelting 2010). Every ton of deicing salt applied on pavements is estimated to cost damages ranging from $803 to $3,341/ton to transportation infrastructure, automobiles, and environment (Stefan et al. 2008). A detailed study conducted by Nixon et al. (Wang et al. 2006) revealed that the use of chloride based deicing chemicals result in physical damage (scaling and cracking) to concrete pavements from the development of osmotic pressure due to uneven salt concentrations along the depth of concrete, hydraulic pressure due to over saturation of concrete pores and crystallization pressure due to salt crystallization in cracks during the freeze-thaw cycles. In addition to this, loss of mass, reduction in compressive strength and formation of precipitates was also reported (Wang et al. 2006). Chloride ion penetration is determined to be a major source of corrosion in rebars embedded in concrete (sumsion and Guthrie ; Sumsion and Guthrie 2013) and vehicles (Nixon and Xiong 2009) (see Figure 1.4). In addition to this, accumulation of chloride ions in the agricultural lands can result in low soil permeability, reduced fertility, and increased soil alkalinity that adversely effects crop productivity (Bäckström et al. 2004). Chloride based deicers are found to pollute ground water (Corsi et al. 2010) and cause acute chloride concentrations in surface waters adversely affecting the aquatic life, plants, and invertebrates (Consultants 1993).

Table 1.1. Traditional deicers and their properties (MPCA 2018).

	Deicer	Freezing point (°F)	Corrosive	Environmental Impact	Cost per ton
Chloride based	Sodium Chloride	-6	High	Moderate to high and potential for metals to mobilize in soils	$70
	Magnesium Chloride	-10	High	Low to Moderate and potential for metals to mobilize in soils	$111
	Calcium Chloride	-60	High	Low to Moderate and potential for metals to mobilize in soils	$140
Acetate based	Calcium Magnesium Acetate	20	Low	Low to Moderate and potential for metals to mobilize in soils	$1500
	Potassium Acetate	-15	Low	Depletion of oxygen in water	$800
	Sodium Acetate	-20	Low	Depletion of oxygen in water	$1900
Formates	Sodium Formate	-4	Low	Depletion of oxygen in water	$400
	Potassium formate	-76	Low	Depletion of oxygen in water	$70/gallon

Note: The reported freezing point depressions of each individual deicer may have been obtained for a specific weight concentration of deicer (when diluted with water) and may vary from one deicer to another. For instance, the freezing point depression of sodium chloride and calcium chloride listed in this table were obtained for 23.3 wt. % (-6°F) and 30 wt. % (-60°F), respectively.

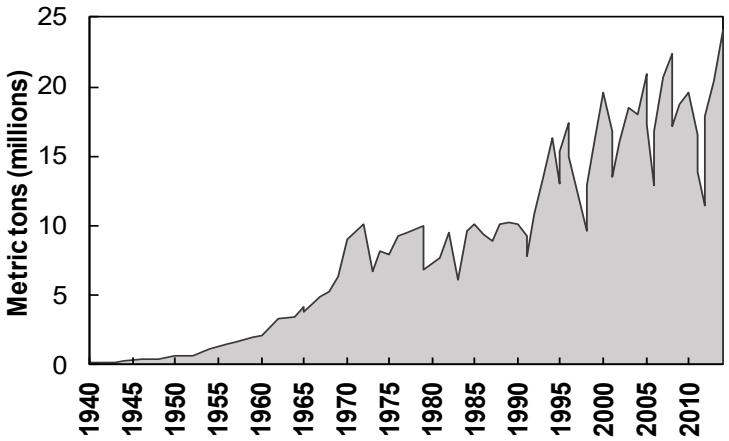

Figure 1.3. Annual salt (NaCl) consumption in the US for roadway deicing during the 1940-2014 period (data source: US Geological Survey).

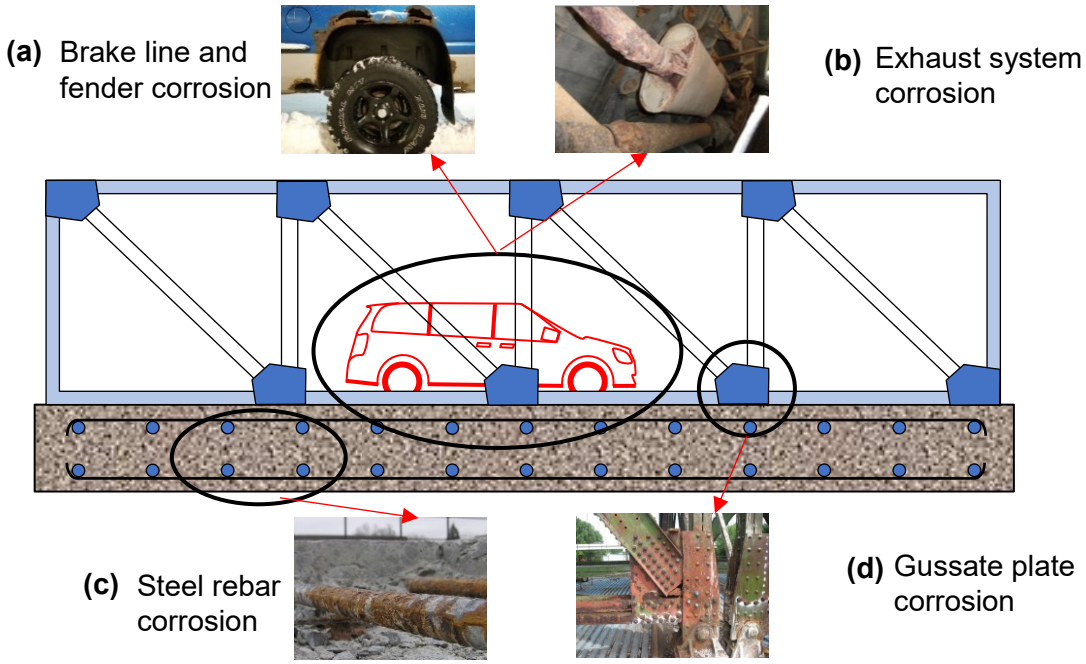

Figure 1.4. Typical corrosion damage in the transportation infrastructure: (a) corroded brake line and fender in cars, (b) corroded exhaust system (Shi et al. 2012), (c) corroded steel rebar (Gucunski et al. 2013), and (d) corroded gusset plate (Mateega 2013).

Acetate-based deicers like sodium acetate (CH_3COONa) potassium acetate (CH_3COOK) and calcium magnesium acetate (CMA) are generally viewed as environment-friendly counterparts of

chloride-based deicers due to their biodegradable nature. They are primarily used for their attractive anti-icing properties, non-corrosiveness, and low toxicity to terrestrial and aquatic vegetation (Fischel 2001). The acetic acid in acetate-based deicers prevent the formation of a bond between the pavement surface and the ice (Fay et al. 2008), making them effective anti-icers. However, acetate-based deicers are expensive and have slow-melting rates when compared to chloride-based deicers. Furthermore, acetate-based deicers are found to chemically deteriorate concrete when used in high concentrations (Darwin et al. 2008) and are corrosive to galvanized steel (Shi 2008) (Shi et al. 2009). Specifically, the use of CMA as a deicer produces brucite ($Mg(OH)_2$) in the concrete pores, which exerts pressure on the concrete leading to cracking and strength reduction (Peterson 1995; sumsion and Guthrie).

Although chloride and acetate based deicers are the two most commonly employed deicers in practice, there are other chemical deicers that are noticed in the literature, namely (1) Formates (e.g. sodium formate (CHO_2Na) and potassium formate (CHO_2K)), (2) urea ($CO(NH_2)_2$) (Kerti et al. 2001), (3) ammonium nitrate (Standish and Cross 1965), (4) ammonium sulphate, and (5) various blends of chlorides, acetates and Formates (Shi et al. 2009) (see Table 1.1). However, a very limited amount of information is available in the literature about these deicers and hence is not discussed in detail.

1.3 Sustainable Agro-based Deicers

Considering the disadvantages of traditional chloride and acetate-based deicers and owing to the demand for more sustainable and environment-friendly deicers, research efforts have been directed towards examining the potential of agricultural or bio-based products to replace/enhance the traditional deicers (Muthumani et al. 2015; Shi and Fu 2018). Examples include pure desugared molasses (Bloomer 2000), corn steep water (Janke and Johnson Jr 1997; Janke and Johnson Jr 1998), sugar beet juice (Talor et al. 2010), particulate plant material (Koefod 2000), alkalinically reduced sugars (Yang and Montgomery 2003), succinate salts (Berglund et al. 2001), etc. In this section, a brief summary of agro-based deicers is provided.

1.3.1 Summary of Literature Review on Agro-based Deicers

Bloomer et al. (Bloomer 2000) proposed the use of pure desugared molasses and desugared molasses mixed with chloride salts as a deicing material (see (Talor et al. 2010) for composition). Desugared molasses is the waste product obtained during the sugar removal process from molasses. Desugared molasses showed good performance when used as a stand-alone deicer and when used in conjunction with rock salt or $MgCl_2$ based on ice melting tests.

Janke et al. (Janke and Johnson Jr 1997; Janke and Johnson Jr 1998) investigated the effectiveness of three different agricultural byproducts namely, corn steep water (obtained from corn wet milling process), cheese brewing byproducts (whey) and vintners condensed soluble (wine processing byproduct) as potential deicers. An ice-melting temperature as low as -14°C was reported for corn steep water, and a low freezing point of -29°C was reported for vintners condensed soluble (Shi and Fu 2018). Further, it was suggested that both corn steep water deicer and cheese brewing byproducts could be mixed with chloride salts to enhance the corrosion inhibition.

Yang et.al. (Yang and Montgomery 2003) enhanced the freezing point depression of corn steep water by mixing it with the biodegradable organic acid salts. These organic salts were extracted by treating the reducing sugars (e.g. glucose and xylose) with the alkali metal hydroxides. In their study, the potential of both monovalent (KOH or NaOH) and divalent (CaO or MgO) alkali metal hydroxides were investigated. Among the three metal alkali hydroxides CaO, KOH, and NaOH, KOH was reported to be effective. The freezing point depression experiments carried out for different concentrations ranging between 5 wt.% and 55 wt. % of glucose obtaining freezing point temperatures in the range of -5°C to -30°C.

Hartley (Hartley and Wood 2001) developed an agricultural product based deicing solution composed of three parts namely, inorganic freezing point depressants like $CaCl_2$, NaCl etc. (weight fraction of 5% to 35%), Brewers Condensed soluble (BCS) (weight fraction of 25%), Distiller Condensed soluble (DCS) (weigh fraction of 8%), Condensed Corn Steep Liquid (CCSL) (weight fraction 6%) and thickeners like sand and aggregate. The Brewer's Condensed Soluble (BCS) mixed with magnesium chloride ($MgCl_2$) aqueous solution exhibited a freezing point of -35.5°C./-31.9°F.

Various succinate salt-based deicers such as potassium succinate, ammonium succinate, sodium succinate, and combinations of these were also reported in the literature. For instance, Berglund et al. (2003) developed a deicer composed of succinic acid and/or succinic anhydride and a neutralizing base. When the deicer comes in contact with the water, a certain amount of heat is generated, thereby melting the ice. Recently, Fay et al. (Fay and Akin 2018) investigated the potential of potassium succinate (KSu) as a deicer in the field. One gram of succinate is generated from a biological fermentation process of 1 gram of glucose from biomass such as corn stalks, corn fiber, and sugarcane (Potera 2005). The freezing point of a 50% solution of KSu is -12°C, while a mix of water, KSu, potassium acetate, and potassium formate at a ratio of 50:30:10:10, respectively, provided the lowest depression of freezing point to -19°C (BioAmber Inc. 2011). Based on these findings, the use of a blended product that includes KSu warrants consideration.

Koefod et al. (Koefod 2000; Koefod and Rose III 2004) developed a deicer consisting of salt and a radiation absorber, which absorbs and converts solar radiation to heat. An example formulation is composed of concentrations by weight of 90–99% NaCl, up to 5% $MgCl_2$, up to 1000 ppm triethanolamine (corrosion inhibitor), and up to 1000 ppm Naphthol Green B (radiation absorber).

Taylor et al. (2010) evaluated brines of glycerol, NaCl, $MgCl_2$, and commercial deicers and their blends. A mixture composed of 80% glycerol with 20% NaCl showed great promise with good laboratory performance and limited negative impacts. The addition of succinate salts and glycerol to salt brine was reported to enhance the anti-icing performance at cold temperatures to the level comparable to $MgCl_2$ or potassium acetate at reasonable costs, while producing substantial savings through reduced application rates, reduced corrosion to metals, and reduced impact on concrete or asphalt pavement.

Nazari et al. (Nazari and Shi 2019) developed anti-icing liquids from a blend of chemicals such as renewable agro-based compounds (Concord grape extract and glycerin), sodium chloride, sodium metasilicate, and sodium formate. Twenty-one different mixture compositions were investigated.

The best-performing anti-icer mixture was reported to be composed of 0.89% Concord grape extract, 4.57% glycerin, 4.54% sodium formate, 0.19% sodium metasilicate, 18.4% NaCl, and water. When compared to 23% NaCl brine and the beet juice/salt brine blend (the two controls), the suggested mixture outperformed in terms of ice melting, COD and BOD5 values thus posing less risk of oxygen depletion in the receiving water bodies. Further differential scanning calorimetry thermograms revealed the critical role of glycerin and sodium formate in the relatively low critical temperature of this mixture (−23.9°C). The importance of this role remained the same even after the aging of the anti-icer.

A deicing composition comprising of lignocellulosic byproducts was formulated by Lewis et al. (Lewis et al. 2019). The proposed formulation includes a solvent, a blend of an inorganic salt, low molecular weight lignin, and sugar compound. The solvent could either be water or alcohol. The inorganic salt could be any of the traditionally used deicing salts or their blends such as chlorides, acetates, formates, etc. Lignin and hemicellulose could be derived from any non-wood source such as wheat straw, rice straw, barley straw, oat straw, ryegrass, coastal Bermuda grass, Arundo donax, miscanthus, bamboo, sorghum, banana harvest residue, pineapple residue, sugarcane bagasse, industrial hemp, recreational cannabis waste, nutshell residue, kenaf, switchgrass, succulents, alfalfa, corn stover, and flax straw. The ice melt capacity (at 28°F) and corrosion inhibition were reported for 40 NaCl-60WSL mix and 30$MgCl_2$-70WSL, where WSL refers to wheat straw liquor. While no significant difference in ice melt capacity was reported, 15% to 50% reduction in corrosivity was found when compared to the control NaCl solution.

Christopher et al. (Bradt et al. 2014) provided deicing formulation utilizing coproducts obtained during the conversion process of lignocellulosic to biofuel. Biomass to fuel processes typically uses a physiochemical process to treat the biomass and to hydrolyze the sugar polymers in preparation for fermentation. A significant amount of residual materials, such as pentose sugars, are produced in the lignocellulosic biomass to fuel process and must be disposed at additional cost. This affords a dilute side stream that is predominantly hemicellulose and hydrolyzed parts of the hemicellulose polymer consisting primarily of xylooligosaccharides and xylose. The dilute side stream is preferably concentrated and then mixed with salt or salt solutions of Calcium Chloride, Magnesium Chloride or Sodium Chloride, or any combination thereof. Freezing points for three different mixes consisting of 57.77% side stream solids and 30% CaCl2, 57.77% side stream solids, and 23% NaCl a 57.77% side stream solids and a mixture of 15.1% CaCl2, 3% MgCl2 and 9.2% NaCl was reported. The 23% sodium chloride solution exhibited a substantial decrease in the freezing point at -25.1°C versus -20.9°C from the original 23% sodium chloride concentration. Further, it was reported that a deicer composition of calcium chloride aqueous solution containing 25%-38% by weight calcium chloride mixed up to 50% by volume of hemicellulose hydrolysis side stream can reduce the corrosivity of calcium chloride to 70% less that of a sodium chloride solution.

Klyosov et al. (Klyosov et al. 2000) determined that deicer compositions using organic (lactic, succinate, acetic, and formic) acids obtained from the fermentation of commercially available glucose feature effective ice-melting and anti-corrosive properties. Water solubility, biodegradable nature, and non-corrosiveness are some of the advantages of organic-based deicers. In addition to

the above discussed bio-based deicers, there are other commercially available bio-based deicing materials whose composition is proprietary and not open in the public domain. Geomelt®, Iceban®, Ice Gone®, etc. belong to this category. High viscosity (Talor et al. 2010), creation of temporary anaerobic soil conditions (Shi and Fu 2018), high quantities of phosphorous and nitrates that accelerate the growth of algae and reduce the supply of oxygen for aquatic biota are some of the disadvantages of bio-based deicers. Most importantly, the average cost of bio-based deicers is around $880.00 per ton, which is more than ten times higher than the traditional chloride-based deicers.

Considering the fact that about 200,000 tons of salt (in Iowa) (IowaDoT 2018) is used for deicing purposes, scaling-up the production of bio-based deicers is challenging as they are generally manufactured from byproducts of various processes or directly from the agricultural products with current yields in the United States far lesser than the actual demand. So, bio-based deicers should be produced from agricultural products that are abundantly grown in the United States.

1.4 The motivation for Alternative Ag-based Deicer

Corn is the second most planted crop in the world, and the United States is the largest producer of corn with annual harvests exceeding 4.125 billion tons (140 billion bushels, 1 bushel-66 pounds) in the year 2017 with yields close to 176.6 bushels/ acre (NCGA 2018). Among all the states in the US, Iowa has the highest corn production and accounts for about 18% of total US corn production (NASS/USDA 2018). In this study, the efficiency of corn-based products as deicers will be investigated. The PI hypothesizes that the sugar available in the raw corn and sugar alcohols that are produced from corn may be useful as a deicer. The process of depressing the freezing points in the case of sugar solutions is more or less similar to the freezing point depression in the case of salt solution (see Figure 1.5(a)). For the pure water to crystallize into ice, it should be undercooled initially below freezing temperature (32°F) so that a critical mass of ice crystal nuclei are formed to initiate the ice formation process. Subsequently, the ice nuclei lose latent heat faster than the rate at which the heat is being removed from the system bringing back the freezing point to 32^0F in the case of pure water. At this temperature, the nuclei then slowly grow into crystals forming ice in the case of pure water. However, the presence of solute (salt/ sugar) results in faster nucleation (i.e., less undercooling when compared to pure water - see Figure 1.5(a)) and lower freezing point. The lower freezing point can be attributed to the fact that the presence of solute particles hinders the growth of full-size ice crystals from nuclei. Furthermore, the nucleated ice crystals do not contain any solute (sugar/ salt), making the un-crystallized solution more concentrated, and hence freezing it into solid ice becomes much more difficult or needs even lower temperatures causing freezing point depression. The salt/ sugar solution instead of freezing into solid ice becomes a soft paste of a large number of very small ice crystals dispersed in a high concentration sugar/salt solution. This is the reason why anti-iced roads turn slushy after a snow event.

Raw sugar beets and corn have 7 and 5 grams of sugar, respectively, for every 100 grams of dry weight (Barclay et al. 2014). Beet juice is already found to be a viable alternative to traditional deicers due to its sugar content and is now being used by several municipalities in North America as a deicer (Sanburn 2018). Sugar beets are less expensive ($35.5 per ton in 2017) and could be

used as a deicer in places with high sugar beet production. However, only 35 million tons of sugar beets are produced in the US annually as many parts of the country are unsuitable for growing this crop, unlike corn. Hence, despite higher sugar content and low cost, sugar beet juice deicer cannot be scaled-up beyond individual municipalities/ counties where it is grown in abundance. On the other hand, with very high production and relatively reasonable cost ($108/ ton; $3.25 per bushel (NCGA 2018)), corn and its derivatives can be used as viable deicers.

Corn juice can be used as a deicer if there is a juice extraction process that can optimally extract the sugar from the corn. Further, sugar alcohols (polyols) manufactured by processing corn starch can also be added to the corn juice to improve its efficiency as a deicer. Currently, polyols are used as artificial sweeteners in the food industry. These polyols also aid in depressing the freezing point of water and improve the smoothness and texture of ice creams at low temperatures (Marshall et al. 2012). The depressed freezing points for some corn-based polyols are shown in Figure 1.5 (b) (URAJI et al. 1996). The deicing properties of corn juice and corn-based polyols are not fully explored, and this will be the subject of investigation in this project. *The main aim of this research is to develop an economical, efficient, environment friendly, and adaptable corn-based deicer to improve the travel safety, remediate traffic congestion and cut travel times during winter months in the state of Iowa.*

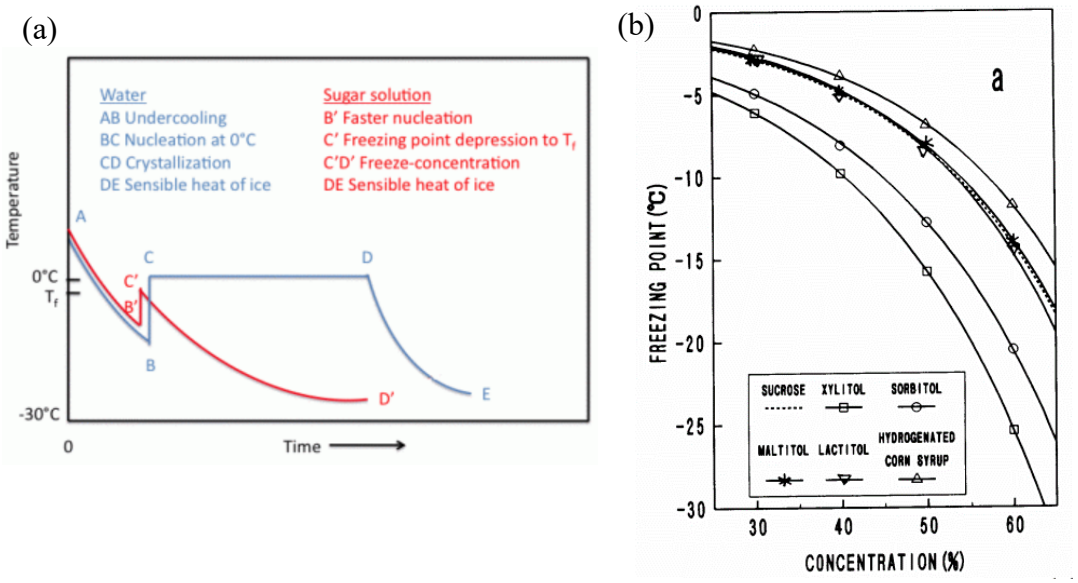

Figure 1.5 (a) Freezing process curve (Goff 2018) (b) freezing point depression curves of polyols (URAJI et al. 1996).

1.5 Research Gap

There is a necessity for the development of bio-based deicing materials with low freezing points, high ice melting rates, that are less detrimental to the steel infrastructure when compared to the traditional salt-brine deicers without compromising on skid resistance and oxygen demand.

1.6 Research Objectives

The above mentioned research gap is addressed in this project by fulfilling the following research objectives

(1) To quantify the improvement in the freezing point depression of salt brine deicer with the addition of polyols, corn juice and beet juice.
(2) To determine the type and weight percentage of polyol that should be added to salt brine solution to achieve the highest freezing point depression.
(3) To identify the weight percentage of polyols that should be added to the salt brine deicer to achieve maximum corrosion inhibition.
(4) To quantify the extent of corrosion inhibition achieved by adding polyols to the salt brine deicer.
(5) To quantify the improvement in the ice melting capacity of polyol-salt brine deicer at sub-freezing temperatures.
(6) To determine the skid resistance and oxygen demand of the developed polyol-salt brine deicers.

1.7 Organization of the Report

The rest of the report is organized as follows: In Chapter 2 the freezing point depression of different combinations of corn/polyol-brine deicer are determined, and the experimental results are discussed. In Chapter 3, the corrosivity of various combinations of corn/polyol-brine deicer are investigated for ASTM A572 steel (commonly used in bridge superstructures) using polarization tests, and the experimental results are discussed. In Chapter 4, the ice melting capacity, skid resistance, and the dissolved oxygen content of various combinations of corn/polyol-brine deicer are carried out, and the experimental results are discussed. Finally, Chapter 5 summarizes the key findings from the previous three chapters and presents research needs identified from this project, followed by suggestions and recommendations to the Iowa Highway Research Board (IHRB).

1.8 Research Products

The following journal articles are produced from this study

1) Abbas T.[#], Naik D.[#], and **Kiran R**[c]. (2020). "Exploring the use of polyols, corn, and beet juice for decreasing the freezing point of brine solution for deicing of pavements", (submitted to ASCE Journal of Cold Regions Engineering).

2) Sajid H.U.[#], Naik D.[#], and **Kiran R**[c]. (2020). "Improving the ice-melting capacity of traditional deicers" (submitted to Construction and Building Materials).

3) Sajid H.U.[#] and **Kiran R**[c], Qi X., Bajwa D.S., Battocchi D. (2020). "Employing corn derived products to reduce the corrosivity of pavement deicing materials", (revised manuscript submitted to Construction and Building Materials).

The following Conference/ poster talks are produced from this study:

C1 & P1) Sajid H.U.[#], and **Kiran R**. (2020). "Poster & talk - Bio-based additives for corrosion mitigation in transportation infrastructure", Graduate Research Symposium, North Dakota State University, Fargo, ND.

C2) Sajid H.U.[#], and **Kiran R**. (2020). "Bio-based additives for mitigating chloride-induced corrosion in transportation infrastructure", Engineering Mechanics Institute Conference – 2020, Columbia University, New York, NY (accepted-cancelled).

The following research recognition was received for the research conducted

R1) Hizb Ullah Sajid (graduate student) is one of the finalists for the 2020 NDSU 3-minute competition for his talk on "Bio-based additives for corrosion mitigation in transportation infrastructure".

The following outreach activity was conducted

OR1) "How to deice roads in winter" in Deer Creek elementary school (2/3/2020) as a part of "West Fargo Public Schools Engineer visits to local kindergarten" by P.I. Ravi Kiran Yellavajjala.

Figure 1.6. Outreach activity for kindergarten students by Ravi Yellavajjala and (b) Hizb Ullah Sajid with Ravi Yellavajjala after winning the 2020 NDSU 3-minute thesis competition.

[#]Graduate student funded on this project; [*]Corresponding author (P.I.).

CHAPTER 2
FREEZING POINT DEPRESSION OF POLYOL-BRINE DEICERS

Freezing point depression is the physicochemical characteristic of a deicer material that refers to the temperature at which the freezing of the solution is initiated i.e., formation of first ice crystals (Chappelow et al. 1992). In practice, the deicer possessing a lower freezing point depression is preferred since they remain in the liquid state for longer durations without freezing and can melt the snow/ice effectively. In this study, three different polyols (sugar alcohols) and two different agricultural products are employed to investigate their influence on the enhancement of the freezing point depression of the brine solution. This chapter focuses on describing the procedure adopted for the preparation of polyol-brine deicer samples and the experimental protocol followed for measuring freezing point depression of corn-based deicers. The results obtained from the experiments are discussed, and the conclusions are provided.

2.1 Materials and sample preparation

2.1.1 Materials

Three polyols, namely sorbitol, maltitol, and mannitol, are acquired from a commercial supplier in the United States, and two agricultural products, namely corn, and beet are acquired from local farmers in Fargo, North Dakota (USA). The chemical structures and the physio-chemical properties of all three polyols are presented in Figure 2.1 and Table 2.1, respectively. While both sorbitol and mannitol are observed to have similar molecular weights, the solubility of the former polyol is higher than the later one. Among all the three polyols that are chosen in this study, maltitol has a higher molecular weight, and mannitol has the lowest solubility. Unlike polyols, the physio-chemical properties of the corn and beet juices are not available in the literature. However, the sugar content/soluble solids of these two agricultural products is of interest in the context of the current study and are measured using the refractometer method. Details of sugar content/soluble solids measurement are provided later in this section.

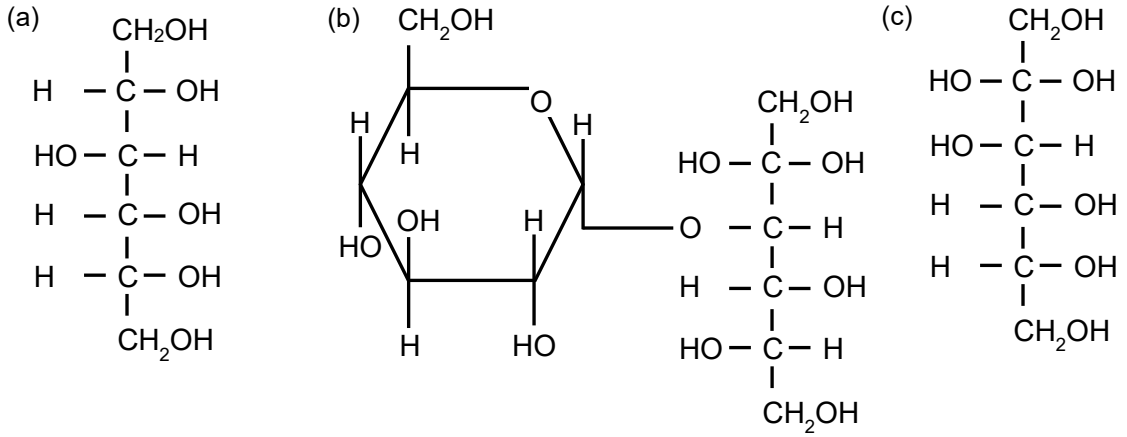

Figure 2.1. Chemical structures of polyols (a) sorbitol (Aliyu et al. 2015; Dewick 2006), (b) maltitol (BeMiller 2018; Guddat et al. 2008), and (c) mannitol (Kalsoom et al. 2016).

Table 2.1. Physiochemical properties of polyols used in this study

	Sorbitol	**Maltitol**	**Mannitol**
Molecular formula	$C_6H_{14}O_6$	$C_{12}H_{24}O_{11}$	$C_6H_{14}O_6$
Molecular weight (g/mol)	182.172	344.313	182.172
Water solubility (g/100 mL of water at 25 ºC) (Zumbe et al. 2001)	246.6	171.2	18.2

2.1.2 Sample preparation

The procedure adopted to prepare the aqueous solution samples for freezing point depression tests is as follows.

2.1.2.1 Polyol-brine solution

The following procedure is adopted to prepare an aqueous solution comprising of water, NaCl, and polyol. Firstly, a 23.3 wt.% of NaCl or brine solution is prepared by mixing 3 g of NaCl to a glass beaker containing 10 g of water. This weight fraction is considered as the brine solution achieves a maximum freezing point depression (-21.1 °C) at 23.3 wt.% (Ketcham et al. 1996). The resulting mix is then continuously stirred for 5 min using a magnetic stirrer at room temperature until the NaCl is completely dissolved. Followed by the preparation of brine solution, a specific weight fraction of a polyol is chosen and is added to the 23.3 wt.% of brine solution. The mix is continuously stirred for another 5 min using a magnetic stirrer at room temperature to achieve the complete solubility of polyol in brine. In this study, the weight fraction of polyol is defined as the ratio of the weight of polyol to the weight of combined brine and polyol solution and, following weights fractions are considered: sorbitol – 7.14%, 10.34%, 16.13%, 18.75%, 23.52% and 27.77 %; maltitol – 7.14%, 10.34%, 16.13%, 18.75%, 23.52% and 27.77 % and; mannitol – 7.14%, 10.34%and 13.34 %. Weight fractions higher than 13.34% is not considered for mannitol because of its low solubility in a brine solution (see Table 2.1).

2.1.2.2 Corn juice-NaCl solution

The following procedure is adopted to prepare an aqueous solution sample comprising NaCl and corn juice. To obtain the corn juice, first the dry corn kernels are soaked in the water for 24 hours, and this process is referred to as steeping. Depending on the quantity of the soaked corn kernels, different concentrations of corn juice can be achieved. In this study, ten different weights of corn kernels are chosen which are soaked in 250 g of water (corn steeping). These ten different weights of the corn kernels correspond to the 5%, 10%, 15%, 20%, 25%, 30%, 40%, 50%, 60% and 70% of corn kernels to water weight fractions. Followed by 24 hours of soaking, the steeped corn is transferred to the commercial blender and ground. The ground mixture is then centrifuged to separate the pulp and the juice. Followed by the extraction of corn juice, a mixture of corn juice-NaCl solution is prepared by adding 3g of NaCl to the 10g of corn juice.

2.1.2.3 Beet juice-NaCl solution

A commercial plunger-type juicer is employed to extract the concentrated beet juice. The raw beets are thoroughly washed before the juice extraction to avoid the presence of dust and other

impurities. From the extracted beet juice, different concentration(s) of juice is prepared by diluting it with tap water in an appropriate quantity. Following four concentrations of beet juice are prepared – 20%, 40%, 60%, and 80%. Pure beet juice is diluted with water to obtain these concentrations. For example, adding 2 mL of water to 8 mL of pure beet juice results in 80% beet juice. Similarly, other concentrations of beet juice are obtained by diluting the pure beet juice with water. Followed by the extraction of beet juice, a mixture of beet juice-NaCl solution is prepared by adding 3g of NaCl to the 10g of beet juice.

2.2 Freezing point depression test

In this study, two different types of experimental setups are employed to perform the freezing point depression tests: (1) an in-house experimental set up similar to the one demonstrated in (Telis et al. 2007; Villa-Vélez et al. 2012), and (2) the differential scanning calorimetry (DSC).

2.2.1 In-house experimental setup

An in-house experimental set up is built in this study which essentially consists of four major components (see Figure 2.2): (a) test tube to hold the aqueous solution sample, (b) a K-type thermocouple for measuring the temperature of the solution, (c) magnetic stirrer to stir the solution sample, and (d) cooling bath to facilitate the drop in temperature below 0°C in the test tube holding aqueous solution sample. Acetone has a freezing point close to -78°C and dry ice is added to acetone to achieve very low temperatures to serve the purpose of a cooling bath in this study. This set up was used to investigate the freezing point depression of different weight fractions of polyols in brine, and 70% corn juice and pure beet juice having 23.3 wt.% of NaCl in it.

To perform the freezing point depression experiment, six mL of the sample solution was transferred to a test tube, which is fixed on a vertical stand (see Figure 2.2). In the next step, a K-type thermocouple is immersed in the sample solution to measure the temperature of the solution. To ensure that a representative temperature of the solution is measured, the thermocouple is positioned at the center of the test tube, i.e., away from the test tube walls. The thermocouple is then connected to a data acquisition system that is obtained from Pico Instruments Inc. The test tube is then gradually lowered into the cooling bath that is maintained at -50°C, and the temperature of the solution is simultaneously acquired. In this study, the temperature of the sample solution was recorded for every 900 milliseconds. Note that the solution was continuously stirred using a magnetic stirrer during the experiment to maintain a homogeneous temperature in the sample solution. Before the deployment of this setup, a series of experiments were performed on brine solution alone that was prepared by adding various weight fractions of NaCl below 23.3 wt.% to tap water (see Section 2.5.1). This exercise was carried out for validation purposes.

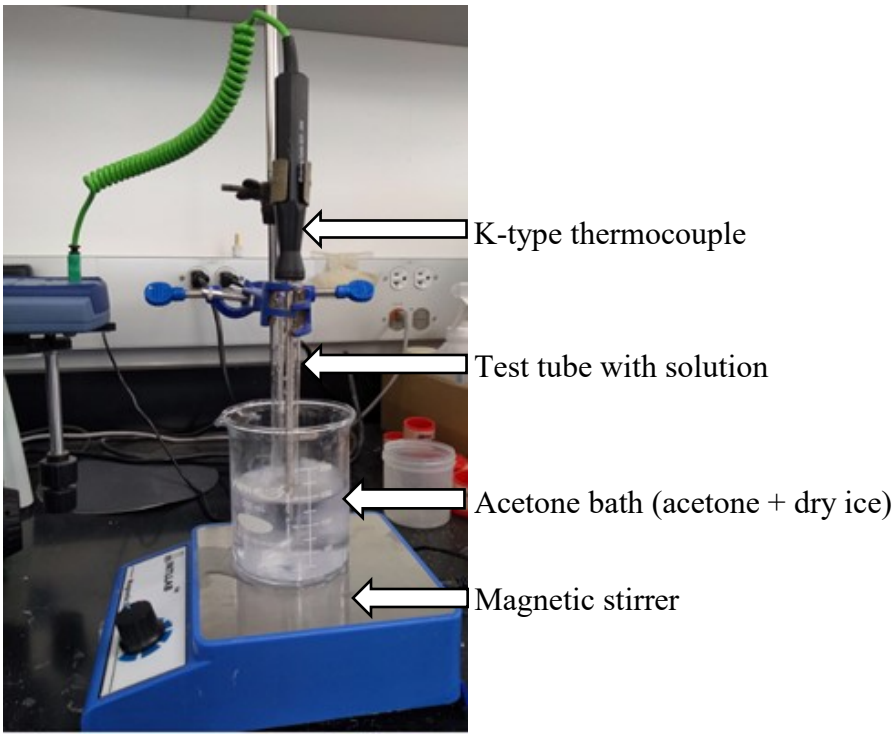

Figure 2.2. An in-house experimental set up employed in this study for evaluating freezing point depression.

2.2.2 Differential scanning calorimetry (DSC) analysis

Differential scanning calorimetry (DSC) is one of the thermo-analytical techniques often used to measure the phase transitions occurring in a material. While a calorimeter measures the heat flow into or out of a sample, a differential calorimeter measures the heat of a sample relative to a reference sample (generally air). For the sake of brevity, the working principle of DSC is not provided in this report and can be found elsewhere (Groenewoud 2001). In this study, the DSC technique is employed to determine the freezing point of corn and beet juice. The freezing temperatures for the following weight fraction(s) of corn 5%, 10%, 20%, 30%, 40%, 50%, 60% and 70% are determined using DSC. The freezing points for the following beet juice weight fractions: 20%, 40%, 60%, 80%, and 100% are evaluated using DSC. In addition to this, the freezing point of pure beet juice mixed with 23.3 wt.% of NaCl is also determined using DSC. This technique was also used to determine the freezing point of high concentration (27.77%) of polyols in brine due to ambiguous results obtained from the in-house experimental setup. For experimentation, the DSC (2920 Modulated DSC, TA Instruments, New Castle, DE, USA) equipment that is available in the Research Park-1 facility at North Dakota State University is used. A Universal Analysis Program (Version 1.11A, TA Instruments, New Castle, DE) was employed to monitor and process the heat flow-temperature curves. Aluminum Hermite sample pans were used for holding the sample during the DSC runs. Solution samples (10-25 mg) were transferred to aluminum DSC pans using a 25 µL syringe and are spread as films using tweezers,

and the resulting samples are sealed using Universal Crimper Press. Nitrogen gas (flow rate, 50 mL/min) was used for the cell purge, and helium (flow rate, 150 mL/min) was used for refrigerating the cooling system. The DSC was calibrated at 2 ºC/min using indium and water as standards. Two thermal events, namely, the cooling and heating cycle, are carried out on the samples during DSC runs. While the material samples were cooled to temperatures between -30 ºC and -60 ºC at a rate of -10 ºC/min in the cooling cycle, they were heated at a rate of 5 ºC/min in the heating cycle to obtain the DSC thermogram.

2.3 Measuring soluble solids in corn and beet juice

The quantity of total soluble solids present in corn and beet juices with various weight concentrations are determined using a refractometer. A refractometer is an optical instrument that uses the principle of refraction of light to measure the soluble solids in the juice. It provides the °Brix value of the juice, which represents the mass (g) of soluble solids in 100 ml of juice. For instance, a reading of 5 °Brix on refractometer implies that 5 g of soluble solids are present in a 100 g of juice. In this study, a fresh drop of extracted juice was placed on the glass slide of the refractometer, and the °Brix reading was recorded. This procedure was repeated for all different concentrations of corn and beet juices.

2.4 Description of typical a freezing point depression curve and DSC thermogram

In this section, the description of a typical freezing point depression curve of aqueous solutions that are obtained from an in-house experimental setup is provided, and the underlying mechanisms that govern each segment of the curve are briefly described. In addition to this, the description of a typical DSC thermogram of aqueous solutions obtained from DSC experiments is also provided.

2.4.1 Freezing point depression curve

Understanding a typical freezing point depression curve will aid in evaluating the freezing points of aqueous solutions from the in-house experimental setup. The schematic of a typical freezing point depression curve is shown in Figure 2.3. This curve comprises of three different segments or thermal events, namely (1) cooling period, (2) nucleation propagation and crystallization (also referred to as recalescence), and (3) solid freezing (Rahman et al. 2002). During the first thermal event, which extends from A to C, the temperature of the aqueous solution drops continuously, and the sensible heat is released. Sensible heat is the amount of heat absorbed or lost by a substance that results in a temperature change in the substance (Stewart 2014). Consequently, the thermal energy required for the molecular vibrations of the aqueous solution also decreases. While point A represents the room temperature of aqueous solution and point B represents the freezing point of water (i.e., 0 °C), point C represents the nucleation temperature achieved during cooling of the aqueous solution. Nucleation temperature is the temperature at which the formation of ice crystals begins. Note that the solution does not freeze at point B, i.e. at 0 °C and extends up to point C (see Figure 2.3). This difference in the temperature between points B and C is due to supercooling that occurs before nucleation. Supercooling is the stage in which the aqueous solution is still in a liquid state and is unstable, i.e. the molecules are still in a disorderly state. In other words, the ordered lattice structure required for the formation of ice crystals does not exist in this temperature range. The second event referred to as nucleation formation, propagation and crystallization occur from

point C to point E. During this stage, nucleation which has begun at point C spreads throughout the aqueous solution and crystal growth in the solution occurs until equilibrium is reached (formation of ice). A phase transition from liquid to solid state is observed in this process which results in the release of energy, also referred to as latent heat. Latent heat is the heat required for phase transition without an increase in the temperature (Louhenkilpi 2014). Note that there is a rapid rise in the temperature from C to D, which is attributed to the release of the heat from the crystallizing supercooled water after the start of nucleation (Srivastava 2002). Beyond point D, a horizontal plateau is observed up to point D, which is also referred to as freezing point depression (Rahman et al. 2002). The third event referred to as solid freezing occurs from point E to point F. During this stage, the temperature of the frozen solid can further drop until the temperature of the frozen solid, and the temperature of the cooling bath becomes equal.

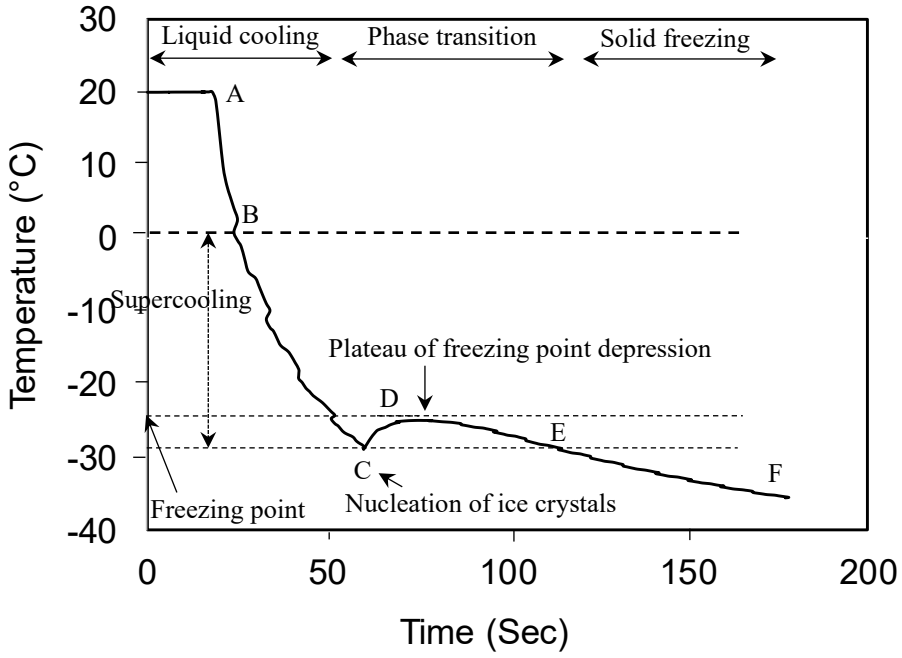

Figure 2.3. Typical freezing point depression curve obtained from in-house experimental set-up used for determining the freezing point of aqueous solutions.

2.4.2 Freezing point and DSC thermogram

A schematic of a typical DSC thermogram is shown in Figure 2.4. This thermogram comprises of two thermal events, namely (1) cooling event and, (2) heating event. While the cooling event involves the process of dropping the temperature of the sample to -60 °C and maintaining in isothermal equilibrium for two minutes (see Section 2.3), the heating event involves raising the temperature of the frozen sample gradually to 20 °C. The amount of differential heat absorbed by the sample with respect to reference material (in general air) as a function of temperature is then recorded by the DSC. In what follows, only the heating event of the thermogram is described in this paper because the current study focusses on freezing point determination, which is generally captured during the heating event. During the heating event, an endothermic peak is observed (see Figure 2.4(b)). The area under this peak represents the heat absorbed by the frozen sample relative

to the reference material in that temperature range. Upon drawing the steepest tangent to the left-hand side of the endothermic peak, an x-intercept is obtained, which represents the melting point. In other words, it represents the temperature at which maximum heat is absorbed with the least change of temperature, i.e. the heat absorbed is consumed primarily for ice to water phase transition. Hence the temperature corresponding to this event is the melting point of the sample solution. It should be noted that in the case of DSC melting point is obtained whereas, in the case of in-house set-up freezing point is obtained. This difference can be attributed to the difference in the heating or cooling cycles employed in the experimental process. In the case of the DSC, the frozen samples are heated, whereas the liquid sample solutions are cooled in the case of in-house set-up. However, it is important to note that the freezing points and the melting points obtained from in-house set-up and DSC are numerically equal (i.e., water freezes at 0 °C and ice melts at 0 °C).

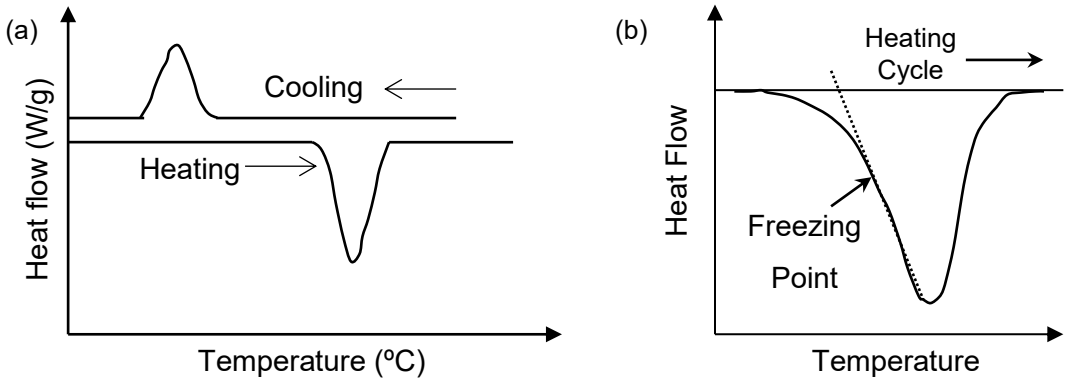

Figure 2.4. (a) A typical DSC thermogram, and (b) the endothermic peak used for the determination of freezing point depression. The units of heat flow and temperature are in W/g and ^{o}C.

2.5 Results

In this section, the calibration process of in-house experimental set up is described, and the time-temperature cooling curves of various aqueous solutions (see Section 2.2) are interpreted. Additionally, the influence of weight fractions of polyols, corn, and beet juice on freezing point depressions are discussed.

2.5.1 Validation of the experimental setup

Validation of in-house experimental set up is carried out in this study to ensure the reliability and consistency of results. For this purpose, the brine solution of five different weight concentrations is chosen: 5%, 10%, 15%, 20% and, 23.3% and the experiments are performed according to the procedure explained in Section 2.3.1. Because the freezing point depressions of brine solution at different weight concentrations is well-established in the literature (Ketcham et al. 1996), NaCl is preferred in this study for the sake of calibration purpose. The time versus temperature cooling curves are obtained for the chosen concentrations of brine solution (see Section 2.3.1), and the freezing point depressions are evaluated (see Section 3.1). The weight fraction versus freezing

point depressions are plotted in Figure 2.5 and are compared to the values provided by the Federal Highway Administration (Ketcham et al. 1996). From Figure 2.5, it is evident that the freezing point depression values obtained using the in-house experimental setup matched the values provided by the Federal Highway Administration validating the in-house set-up. In this study, the concentration of brine solution beyond 23.3 wt. % was not investigated, as it does not depress the freezing point of brine solution any further (Ketcham et al. 1996). The increase in the freezing point when the concentration of the brine solution is greater than 23.3 wt. % can be attributed to the reduction in ion disassociation of NaCl in water beyond this concentration (Belch et al. 1986; Kelley et al. 2015).

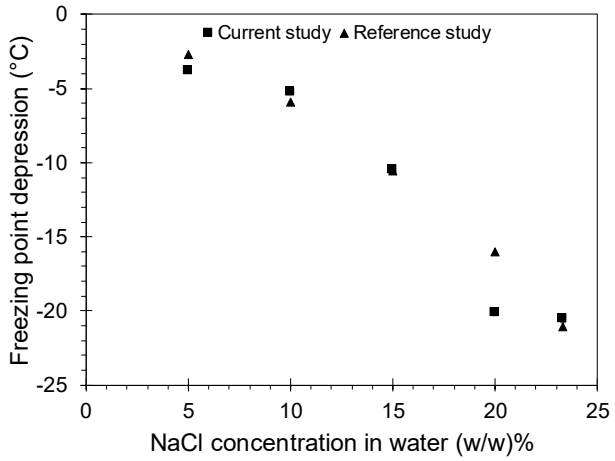

Figure 2.5. Validation of freezing point depressions of brine solution at different concentrations evaluated from in-house experimental setup by comparing it with the values provided in the reference study (Ketcham et al. 1996).

2.5.2 Freezing points of polyol-brine solutions

The time versus temperature cooling curves of polyol-brine solutions (see Section 2.2.1) is obtained from the experiments, and the results are provided in this section. Further, the freezing points and the influence of weight fractions of polyols in brine solution on freezing points are discussed.

2.5.2.1 Sorbitol-brine solutions

In this study, six different weight fractions of sorbitol (in 23.3% brine solution), 7.14%, 10.34%, 16.13%, 18.75%, 23.52% and, 27.77 % are considered, and their freezing points are determined. The time versus temperature cooling curves are obtained for each weight fraction of sorbitol, and the results are shown in Figure 2.6. From Figure 2.6, it is evident that the cooling curves are fairly repeatable for all the weight fractions of sorbitol that are considered in this study. Unlike all other weight fractions of sorbitol, 27.77% weight fraction of sorbitol did not exhibit a clear horizontal plateau on the cooling curve. Although the exact reason is not clear, this horizontal plateau represents the phase transition of a liquid into a solid and is important in determining the freezing point depression. Therefore, to evaluate the freezing point depression for this particular weight fraction, DSC is employed. The freezing point depressions evaluated for all six weight fractions

of sorbitol: 7.14%, 10.34%, 16.13%, 18.75%, 23.52%, and 27.77 % are: -23.8 ºC, -24.8 °C, -27.4 °C, -25.7 °C, -28.1 °C, and -38.1 °C, respectively. These values are provided in the form of a bar chart in Figure 2.7 to illustrate the trend of freezing points with respect to the weight fractions of sorbitol.

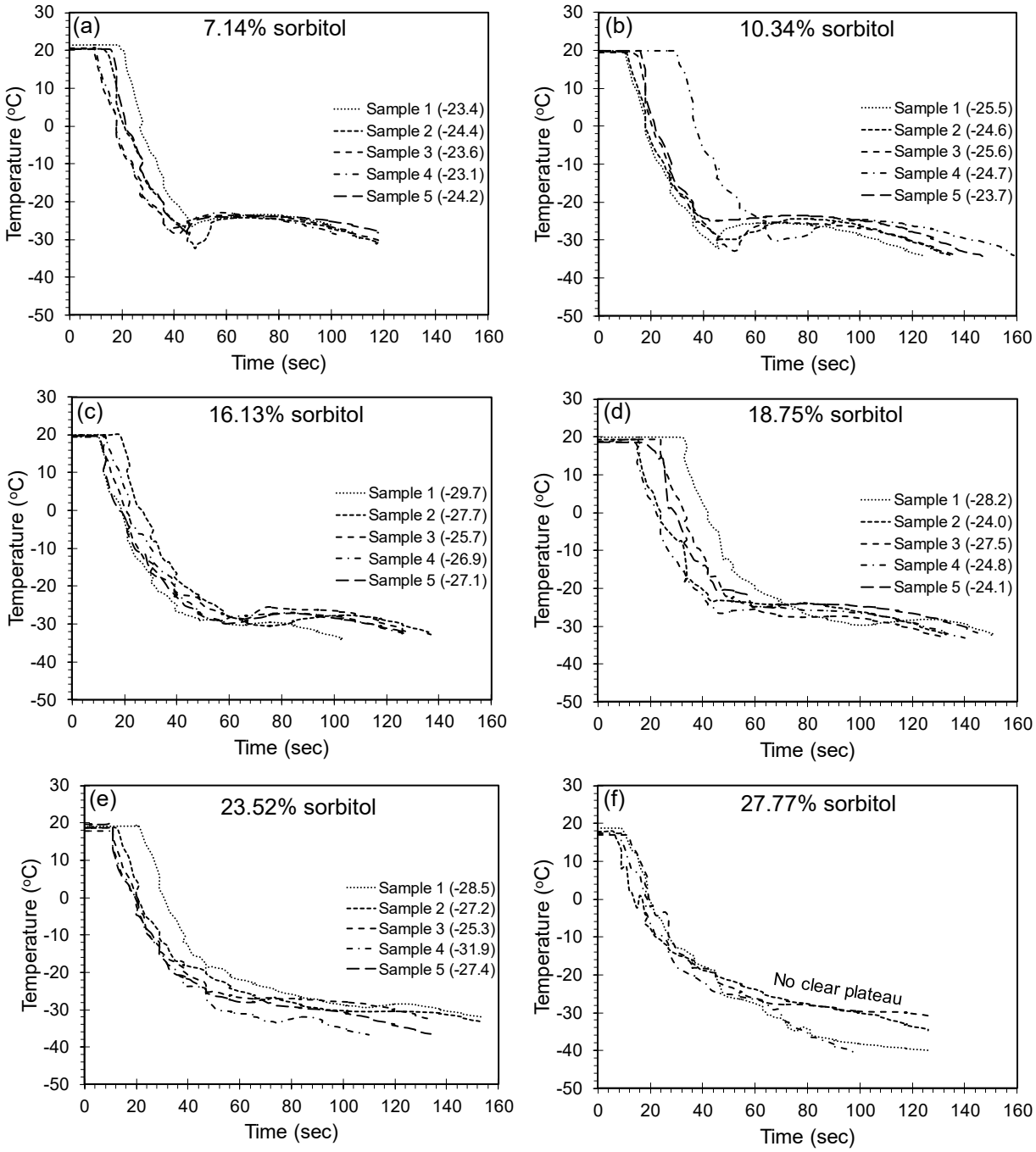

Figure 2.6. Effect of different weight fractions of sorbitol on freezing point depression of brine solution (23.3% NaCl in water).

From Figure 2.7, it can be inferred that the freezing point of the sorbitol-brine solution drops with an increase in the weight fraction of the sorbitol. While a drop of 15.13% is observed when sorbitol weight fraction is increased from 7.14% to 16.13%, a drop of 35.59% is observed when sorbitol weight fraction increased from 23.52% to 27.77%. However, a small dip in trend was observed at 18.75% weight fraction of sorbitol. The temperature at which solution freezes depends upon the concentration and type of solute present in the mixture. The extent of freezing point depression is based on the number of solute molecules and their size. Molecules of a comparatively smaller size have the greatest effect; the higher the concentration of these small molecules, the lower the freezing point (Hui and Sherkat 2005). The increase in the freezing point depression with an increase in the weight fraction of sorbitol can be attributed to the increased number of dissolved sorbitol molecules which inhibit the bonding of water molecules thereby hindering the growth of ice crystals (Pappas 2006).

Figure 2.7. Influence of weight fractions of sorbitol on depressing the freezing point of brine (all experiments (7.14 wt% to 23.52 wt%) were performed in triplicate using an in-house experimental setup except the one with 27.77 wt% of sorbitol in brine as it was performed using DSC).

2.5.2.2 Maltitol-brine solutions

In this study, six different weight fractions of maltitol (in 23.3% brine solution): 7.14%, 10.34%, 16.13%, 18.75%, 23.52%, and 27.77% are considered and their freezing points are determined. The time versus temperature cooling curves are obtained for each weight fraction of maltitol, and the results are shown in Figure 2.8. From Figure 2.8, it is evident that the cooling curves are fairly repeatable for all the weight fractions of maltitol that are considered in this study. Similar to sorbitol, at 27.77% weight fraction, the maltitol-brine solution also did not exhibit a clear horizontal plateau in the cooling curve. Therefore, to evaluate the freezing point depression for this particular weight fraction, DSC is employed. The freezing point depressions evaluated for all six weight fractions of maltitol, 7.14%, 10.34%, 16.13%, 18.75%, 23.52%, and 27.77 % are: -22.6 °C, -25.2 °C, -28.5 °C, -24.4 °C, -29.8 °C, and -35.6 °C, respectively. These values are provided in the form of a bar chart in Figure 2.9 to illustrate the trend of freezing points with respect to the weight fractions of maltitol.

From Figure 2.9, it can be inferred that the freezing point of the maltitol-brine solution drops with an increase in the weight fraction of the maltitol. While a drop of 26.11% is observed when maltitol

weight fraction is increased from 7.14% to 16.13%, a drop of 19.46% is observed when maltitol weight fraction increased from 23.52% to 27.77%. Similar to sorbitol, a small dip in trend was again observed in the case of 18.75% weight fraction of maltitol-brine solution. The drop in the freezing point depression with an increase in the weight fraction of maltitol can be attributed to the high concentration of solute (maltitol in this case) molecules in the water which hinders the bonding of water molecules from forming ice crystals (Jayawardena et al. 2017; Pappas 2006).

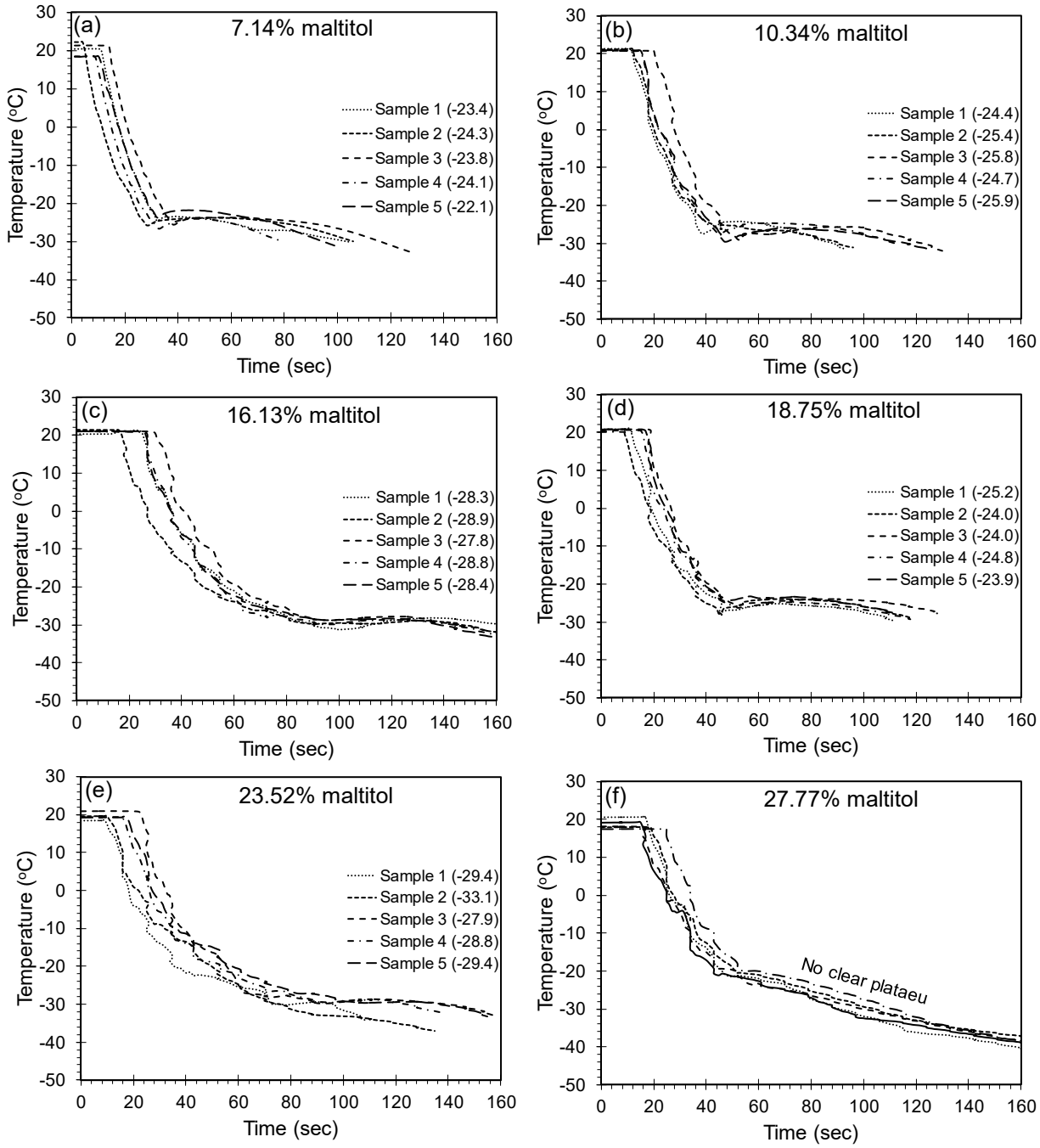

Figure 2.8. Effect of different weight fractions of maltitol on freezing point depression of brine (23.3% NaCl in water).

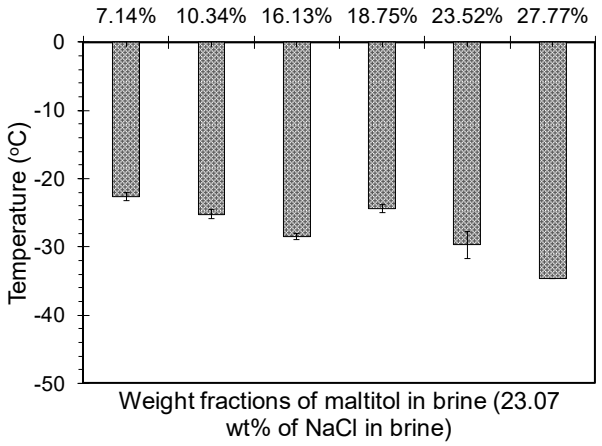

Figure 2.9. Influence of weight fractions of maltitol on depressing the freezing point of brine solution. (all experiments (7.14 wt% to 23.52 wt%) were performed in triplicate using an in-house experimental setup except the one with 27.77 wt% of maltitol in brine solution as it was performed using DSC).

2.5.2.3 Mannitol-brine solutions

In this study, three different weight fractions of mannitol (in 23.3% brine solution) 7.14%, 10.34%, and 13.33% are considered, and their freezing points are determined. Weight fractions beyond 13.33% are not considered due to the low solubility of mannitol in the brine solution. The time versus temperature cooling curves are obtained for each weight fraction of mannitol, and the results are shown in Figure 2.10. From Figure 2.10, it is evident that the cooling curves are fairly repeatable for all the weight fractions of mannitol considered in this study. The freezing point depressions evaluated for the three weight fractions of mannitol, 7.14%, 10.34% and, 13.33% are -23.10 °C, -26.70 °C, and -27.00 °C, respectively. These values are provided in the form of a bar chart in Figure 2.11 to illustrate the trend of freezing points with respect to the weight fraction of mannitol. From Figure 2.11, it can be inferred that the freezing point of a mannitol-brine solution drops with an increase in the weight fraction of the mannitol. While a drop of 15.08% is observed when maltitol weight fraction is increased from 7.14% to 10.34%, only a drop of 1.13% is observed when maltitol weight fraction is increased from 10.34% to 13.33%. Again the drop in the freezing point depression with an increase in the weight fraction of mannitol can be attributed to the presence of more solute molecules in the solution which inhibit the formation of ice crystals (Jayawardena et al. 2017; Pappas 2006).

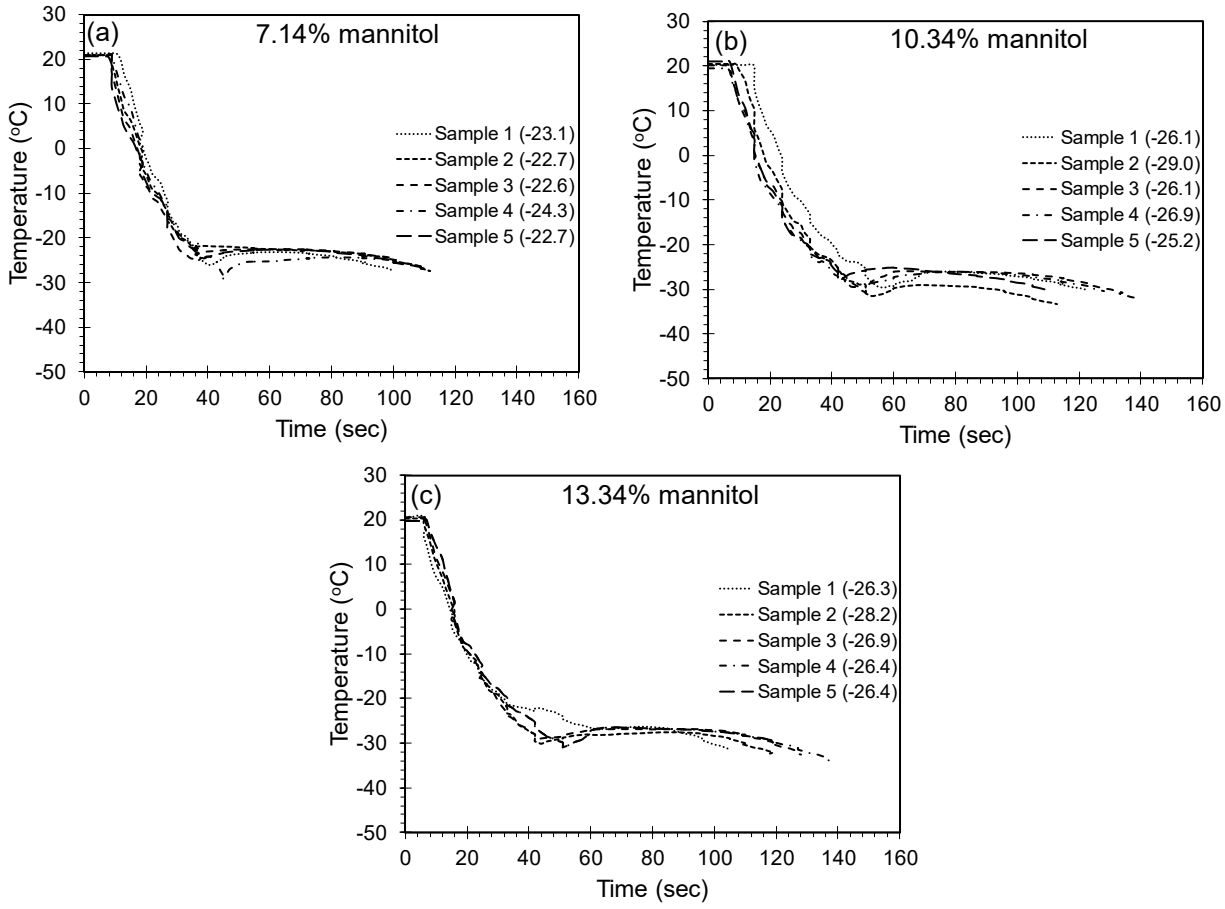

Figure 2.10. Effect of different weight fractions of mannitol on freezing point depression of brine solution (23.3% NaCl in water).

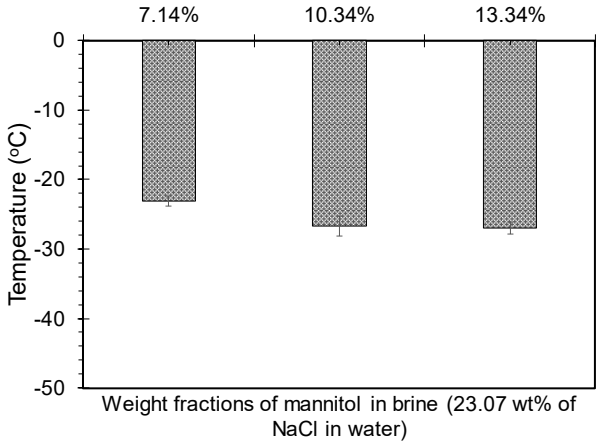

Figure 2.11. Influence of weight fractions of mannitol on freezing point depression of brine solution.

2.5.3 Freezing points of corn and beet juice

The freezing points of different concentrations of corn and beet juices are determined, and the influence of total soluble solids on their freezing points is investigated. In addition to this, the role of NaCl in depressing the freezing point of corn juice is also investigated. The freezing point depressions evaluated for different concentrations of corn and beet juice is shown in Figure 2.12(a). It can be observed that the freezing point of corn juice drops with an increase in the weight fraction of corn kernels. While the freezing point depression of corn juice is found to be -0.88 °C at 5% weight fraction, it is found to be -2.87 °C at 70% weight fraction (see Figure 2.13). The drop in the freezing points with an increase in the weight fraction of corn can be attributed to the increased quantity of total soluble solids present in the solution with high corn juice concentration (Auleda et al. 2011). Note that the composition of soluble solids is not determined as it falls outside the scope of the current study. Total soluble solids measured for different concentrations of corn juice is provided in Figure 2.12(b). The °Brix value at 70 wt. % of corn juice (°3.8) is found to be ten times higher than 5 wt. % of corn juice (°0.4).

A similar trend in the decrease of freezing points is noticed in the case of beet juice with the increase in weight concentration. While the freezing point of beet juice is found to be -2.43 ºC at 20% weight fraction, it is found to be -6.7 ºC at 100% weight fraction (Figure 2.13(b)). It can be seen in Figure 2.12(b) that °Brix value for pure beet juice was higher (º15) than 20% beet juice (º3.5). It has been proposed in the literature that the higher °Brix value, which represents total sugar solids such as sucrose, fructose, and glucose in fruit juices, lower the freezing point of fruit juice (Auleda et al. 2011). Therefore, it can be concluded that beet juice has a lower freezing point than corn juice because of the higher Brix value.

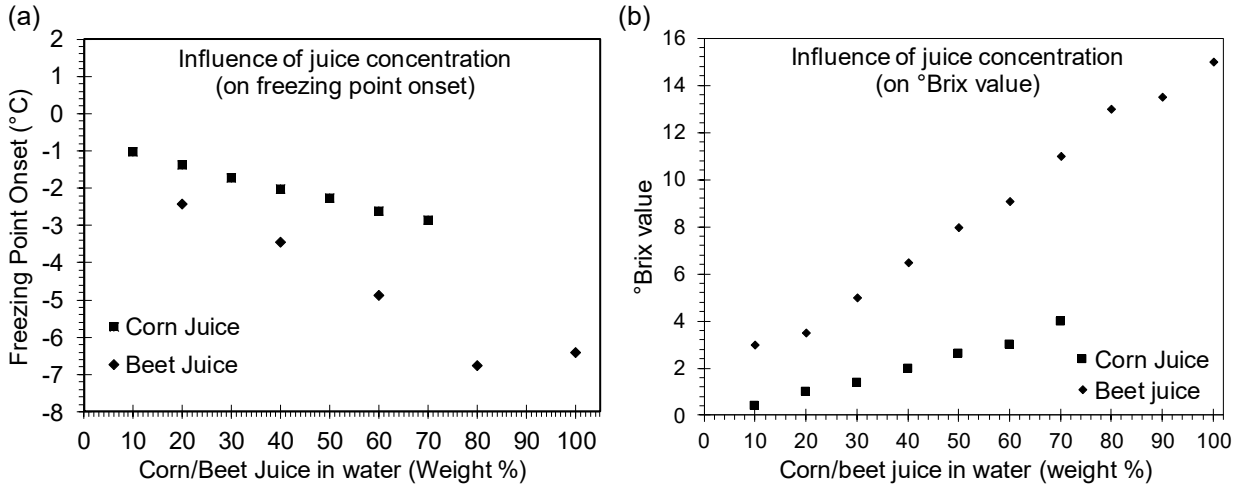

Figure 2.12. (a) Onset of freezing in corn and beet juices with different weight concentrations and (b) ºBrix value for different weight fractions of corn and beet juice concentrations.

2.5.3.1 Influence of NaCl on freezing point of corn and beet juice

The influence of the addition of NaCl to corn and beet juices is presented in this sub-section. As discussed earlier, pure beet juice and 70% of corn juice had a lower freezing point depression than corresponding diluted juices. Therefore, only these two juice concentrations are considered. Figure 2.14(a) and Figure 2.14(b) show the cooling curves of 70% corn juice-NaCl solution and DSC thermogram of pure beet-NaCl solution. It is evident that cooling curves are repeatable for corn-NaCl, and the freezing point depression of corn juice-NaCl is found to be -23.5 °C, the freezing point depression of pure beet juice-NaCl is found to be -28 °C. As discussed in Section 3, the presence of NaCl and soluble solids in fruit juice NaCl solutions hinder the formation and growth of ice crystals lowering the freezing points below -21.1 °C.

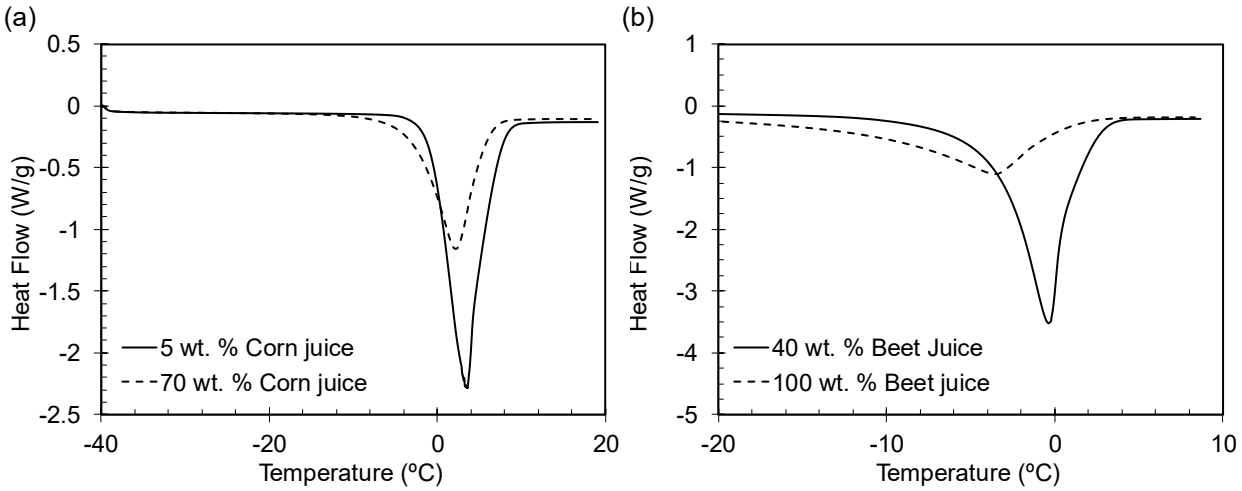

Figure 2.13. (a) DSC thermogram of corn juice for 5% and 70 % weight concentrations, and (b) DSC thermogram of beet juice at 40% and 100% weight concentrations.

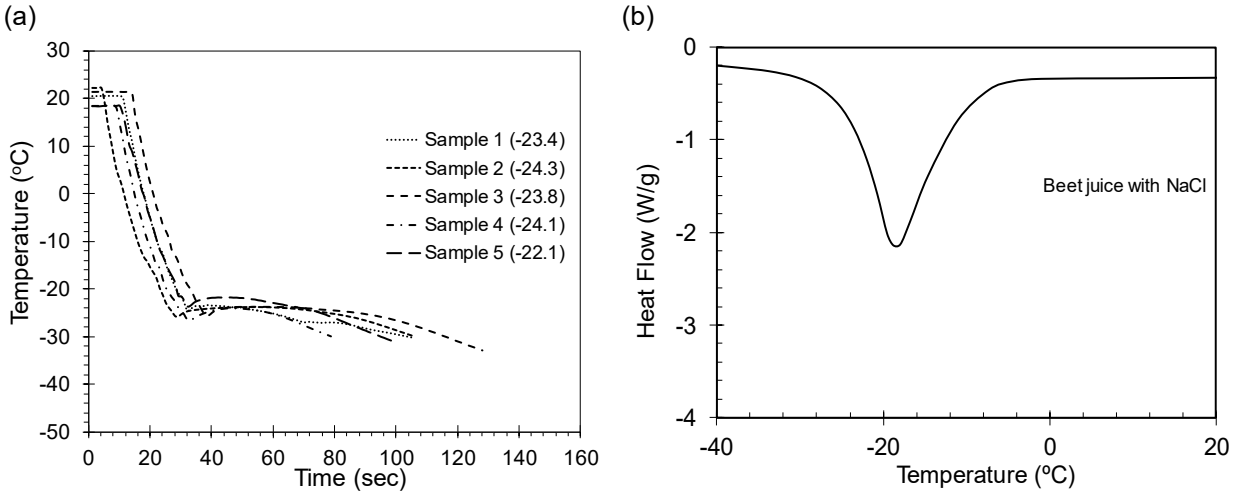

Figure 2.14. Freezing point depression of corn and beet juices in brine solution (23.3% wt.): (a) 70% corn juice, and (b) pure beet juice.

2.6 Conclusions

In this chapter, the influence of different weight fractions of polyols such as sorbitol, maltitol, and mannitol on the freezing point depression of brine solution is investigated. In addition to this, the freezing point of corn and beet juice was also determined, and the influence of NaCl in lowering their freezing points below -21.1 °C is investigated. The following conclusions can be drawn from this chapter:

1. Addition of polyols to the 23.3% wt. brine solution is observed to lower the freezing point below -21.1 °C. The freezing point decreased until the solubility limit of polyols is reached. While a 15.13%, 26.11%, and 15.08% drop in the freezing point was observed when the weight fraction was increased from 7.14% to 16.13% for sorbitol, maltitol, and mannitol respectively, 35.39% and 19.46% drop was observed in the freezing point depression when the weight fraction was increased from 23.52% to 27.77% for sorbitol and maltitol, respectively.
2. The minimum freezing points achieved by sorbitol, maltitol, and mannitol when combined with 23.3% wt, brine solution are -38.1 °C, -35.6 °C, and -26.7 °C, respectively at weight fractions of 27.77%, 27.77%, and 13.33%, respectively.
3. The freezing points of corn and beet juice are observed to decrease with an increase in their weight concentration. This phenomenon can be attributed to the higher quantity of the total soluble solids in the higher concentration juices. While corn juice exhibited a freezing point of -2.87 °C at 70% weight fraction of corn kernels, 100% concentration beet juice exhibited a freezing point of -6.8 °C.
4. The addition of NaCl to corn and beet juice further depressed their freezing points. The 70% wt. corn and 100% concentration beet juice with 23.3% wt. NaCl lowered the freezing points to -23.5 °C, and -28 °C, respectively.

CHAPTER 3
CORROSIVITY OF POLYOL-BRINE DEICERS

Traditional brine deicers are known for their adverse impacts on the corrosivity of the metals and the transportation infrastructure. In practise, a low corrosive deicer or a deicer with corrosion inhibiting additive is often desirable. This chapter focuses on the determination of the corrosion inhibition performance of polyols-brine deicers. To this end, the process of preparing the specimens and the test protocols adopted for conducting the experiments are described in detail. The results obtained from the corrosion tests are discussed and the conclusions are provided.

3.1 Materials and Specimen Preparation

ASTM A572 Gr. 50 (ASTM 2018) high strength low alloy steel is employed in this study to explore the corrosivity of polyols-brine deicer. ASTM A572 Gr. 50 steel is commonly used in the US construction industry particularly in bridges (Sajid and Kiran 2018; Sajid and Kiran 2019) and has properties that are similar to Q460 (Wang et al. 2012), Q345B and S355JR steel grades that are used in Chinese and European construction industry. For the purpose of experiments, two sets of ASTM A572 steels specimens are prepared in this study. While the first set of specimens are in cylindrical (disc) in shape with diameter 19mm, the second set of specimens are square in shape with dimensions 3" × 3" × 5/16". The cylindircal disc shaped specimens are used for accelerated corrosion tests and the square-shaped steel plates are used for potentiodynamic polarization tests, as shown in Figure 3.1(a) and Figure 3.1 (b), respectively (see Section 3.2.1). The chemical composition of ASTM A572 steels that are used in this study is provided in Table 3.1. The microstructure of ASTM A572 Gr. 50 steel used herein is primarily composed of ferrite and pearlite phases with an average ferrite grain size of 13 μm and an average pearlite colony size of 3 μm (Sajid et al. 2020). To avoid the influence of surface roughness on corrosion behavior (Sajid and Kiran 2018), the surfaces of both sets of steel specimens are prepared through successive grinding using Silicon Carbide (SiC) papers in the following grit order: #60, #120, #220, #400, #600 and #800. After grinding, the specimens are thoroughly cleaned using warm water and acetone to remove any residue present on the surface of specimens. In total, 13 disc-shaped specimens are prepared for accelerated corrosion tests whereas 20 steel plates are prepared for potentiodynamic polarization tests. The test procedures for both accelerated corrosion tests and potentiodynamic polarization tests are discussed in the next section.

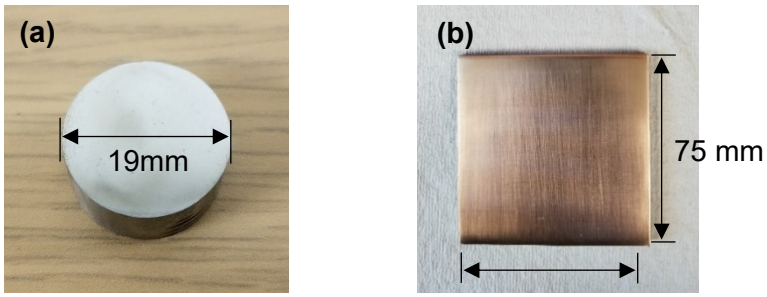

Figure 3.1. Test specimens for corrosion tests: (a) cylindrical specimens for accelerated corrosion tests, and (b) steel plates for potentiodynamic polarization tests.

Table 3.1. Chemical composition of ASTM A572 steel.

Element	Composition (%)
Carbon (C)	0.0500
Manganese (Mn)	1.3400
Phosphorous (P)	0.0110
Sulphur (S)	0.0040
Silicon (Si)	0.1500
Copper (Cu)	0.2800
Chromium (Cr)	0.1900
Nickel (Ni)	0.1300
Molybdenum (Mo)	0.0400
Vanadium (V)	0.0830
Titanium (Ti)	0.0010
Niobium (Nb)	0.0030
Iron (Fe)	97.7180

3.2 Corrosion Tests

3.2.1 Accelerated Corrosion Test

The experimental setup of an accelerated corrosion test employed in this study consists of a feed reservoir for holding the deicing solution, a peristaltic pump for producing a recurring flow of deicing solution, and a disc-shaped test specimen placed on an inclined steel plate, in accordance with ASTM B117 (ASTM and International 2016) standard. The test setup employed for the accelerated corrosion tests is shown in Figure 3.2. In this test set up, the feed reservoir is filled with the desried polyols-brine deicer solution that is prepared by mixing 23% wt. brine with following weight concentrations of polyols (sorbitol, mannitol, and maltitol): 0%, 0.5%, 1.0%, 2.0%, and 3.0% and subsequently is allowed to flow constantly on to a disc-shaped test specimen.

All accelerated corrosion tests are conducted in a highly corrosive environment inside an environmental chamber wherein the temperature and relative humidity levels are maintained at 85°F and 100%, respectively. The inclination of the plate allows the flow of deicing media on the grinded top surface of test specimens and inhibits accumulation of deicing media on the specimen during the experiment. The test specimens are exposed to the deicing media for 48 hours at an average flow rate of 0.5 mL/min and images are taken at regular intervals to visually monitor the corrosion damage in steel specimens. These images are visually examined to study the corrosion inhibition and will be discussed in Section 3.3.

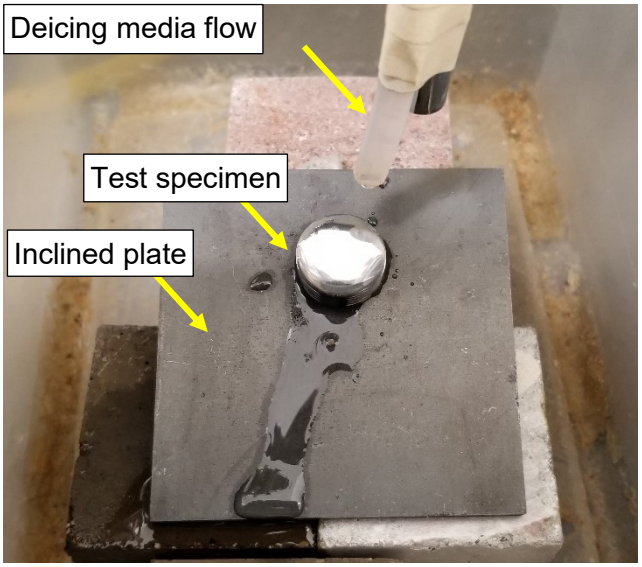

Figure 3.2. Typical cylindrical specimen subjected to flowing deicing media (23.0% NaCl brine + polyol) inside an environmental chamber at 30 °C temperature and 100% relative humidity conditions.

3.2.2 Potentiodynamic Polarization Test

To quantify the corrosion rates of polyol-brine deicer solution, potentiodynamic polarization tests are conducted on the grinded steel plates. Among the various electrochemical techniques that are available such as linear polarization resistance tests, potentiodynamic polarization tests, electrochemical impedance spectroscopy, etc. (Roberge 2000), potentiodynamic polarization tests is commonly preferred as they provide useful information regarding corrosion mechanisms, corrosion rates, passivation range, pitting potential, and susceptibility of metals to corrosion in a specific corrosive environment. Moreover, potentiodynamic polarization tests are quick and inexpensive to run and yield fairly reproducible results (HOLLAND 1991). In potentiodynamic polarization tests, the potential of the working electrode is varied at a selected rate (typically expressed as mV/s) by applying current through the electrolyte. The potential of the working electrode can be varied in either anodic direction (anodic polarization), cathodic direction (cathodic polarization), or both the anodic and cathodic directions (cyclic polarization). The boundaries of the potential scan (initial potential and final potential) are usually selected based on

the desired polarization (anodic or cathodic). In this study, the potentiodynamic polarization tests are carried out using Gamry's potentiostat Interface E1000. The potentiodynamic polarization tests are performed using a conventional 3-electrode electrochemical cell which employs ASTM A572 steel plates with an exposed area of 7.07 cm^2 as a working electrode (WE). All potentials are measured against a saturated calomel electrode (SCE) whereas a stainless steel wire mesh is used as a counter electrode (CE). The potentiodynamic polarization test setup used in this study is provided in Figure 3.3. All potentiodynamic polarization tests are conducted at room temperature (25 °C). Before starting the electrochemical tests, the working electrode (steel plate) is kept immersed in the polyol-based deicing solution for an average period of 2 hours to achieve a steady-state potential. For each polyol concentration in the deicing solution, the potentiodynamic polarization tests are repeated thrice on separate steel plates. During potentiodynamic polarization tests, the potential of the working electrode (steel plates) is varied from cathodic to the anodic direction (anodic scan) within a range of ± 500 mV with reference to the steady-state potential at a scanning rate of 10 mV/s. A high potential window of ± 500 mV is adopted in this study to capture the passivation and pitting behavior of steel plates. The corrosion rates, corrosion inhibition efficiencies and the corrosion inhibition mechanisms corresponding to each polyol is then determined using the electrochemical measurement procedures that are specified in ASTM G102 and will be discussed in section 3.3.2.

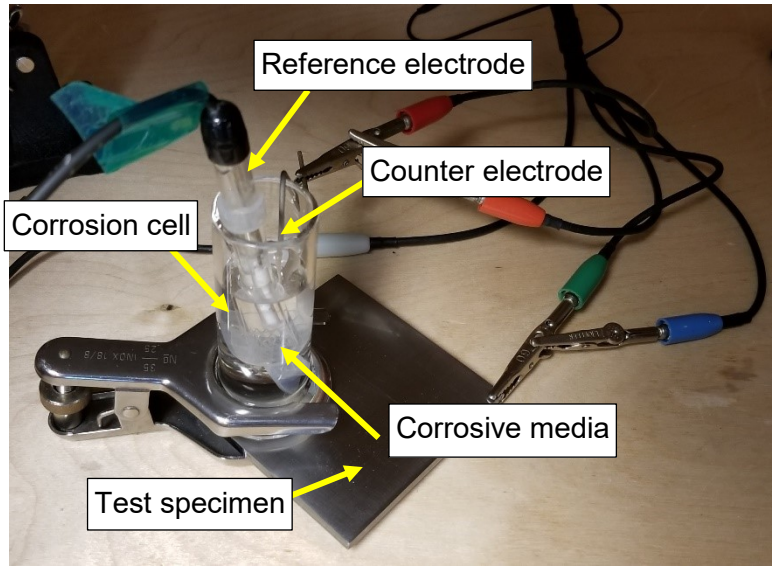

Figure 3.3. Typical corrosion cell with steel plate as working electrode (WE) (exposed area: 7.07 cm^2), saturated calomel electrode as reference electrode (RE) and stainless steel wire mesh as counter electrode (CE).

3.3 Results and Discussion

The results obtained from both accelerated corrosion tests and potentiodynamic polarization tests corresponding to each polyol-brine deicer combination are discussed in this section. Moreover, the corrosion inhibition mechanism is explained using adsorption isotherms.

3.3.1 Accelerated Corrosion Tests

Accelerated corrosion tests are carried out in this study for the purpose of visual observation of corrosion damage in the steel specimens. Specimens are subjected to a constant flow of traditional deicing media (23% wt. NaCl brine) in the absence and presence of different concentrations of polyols inside an environmental chamber for a period of 48 hours. The corrosion damage is visually observed by taking images of specimens at regular intervals. These images are presented in Figure 3.4 through Figure 3.7. It should be noted that for 23% wt. NaCl brine solution and sorbitol+23% wt. NaCl brine solutions, images are taken at 8 hours interval. After confirming the lower corrosion damage in the specimens that are exposed to sorbitol+23% wt. NaCl brine solutions, the images for the remaining polyols (maltitol and mannitol) are obtained at longer time intervals. At the beginning of each test (time $t = 0$ hours), the disc-shaped steel specimens are observed to be free of any contamination or apparent corrosion distress. Varying amount of corrosion is observed in the specimens as the test progressed. As observed in Figure 3.4, the specimens subjected to traditional deicing solution (23% wt. NaCl brine) exhibited noticeable corrosion damage after only 16 hours of exposure when compared to the deicing solutions which contain small quantities of polyols. In the case of deicing solutions containing 0.5% polyol, the corrosion damage is visually observed to initiate after 24 hours and the amount of corroded area increases with an increase in the exposure time period (see Figure 3.5 through Figure 3.7). For higher concentrations of polyol in the brine solution (1.0% to 3.0%), the corrosion damage is noticed at 24 hours around the periphery of test specimens and there is no considerable increase in the corroded area during the remaining duration of the test. In summary, delayed corrosion initiation is observed in ASTM A572 steels that are exposed to the deicing solution containing a small weight concentration of polyols. Moreover, only a small amount of corrosion in these specimens occurred during the exposure period. The accelerated corrosion tests are conducted to visually monitor the corrosion damage in steel specimens exposed to the deicing solutions containing polyols. To quantify the corrosion rates in steel specimens in the absence and presence of polyols in the salt deicing solutions and to elucidate the corrosion inhibition mechanism, potentiodynamic polarization tests are conducted and are discussed in the next section.

Figure 3.4. Visual appearance of ASTM A572 steel specimens exposed to traditional deicing solution (23% NaCl brine).

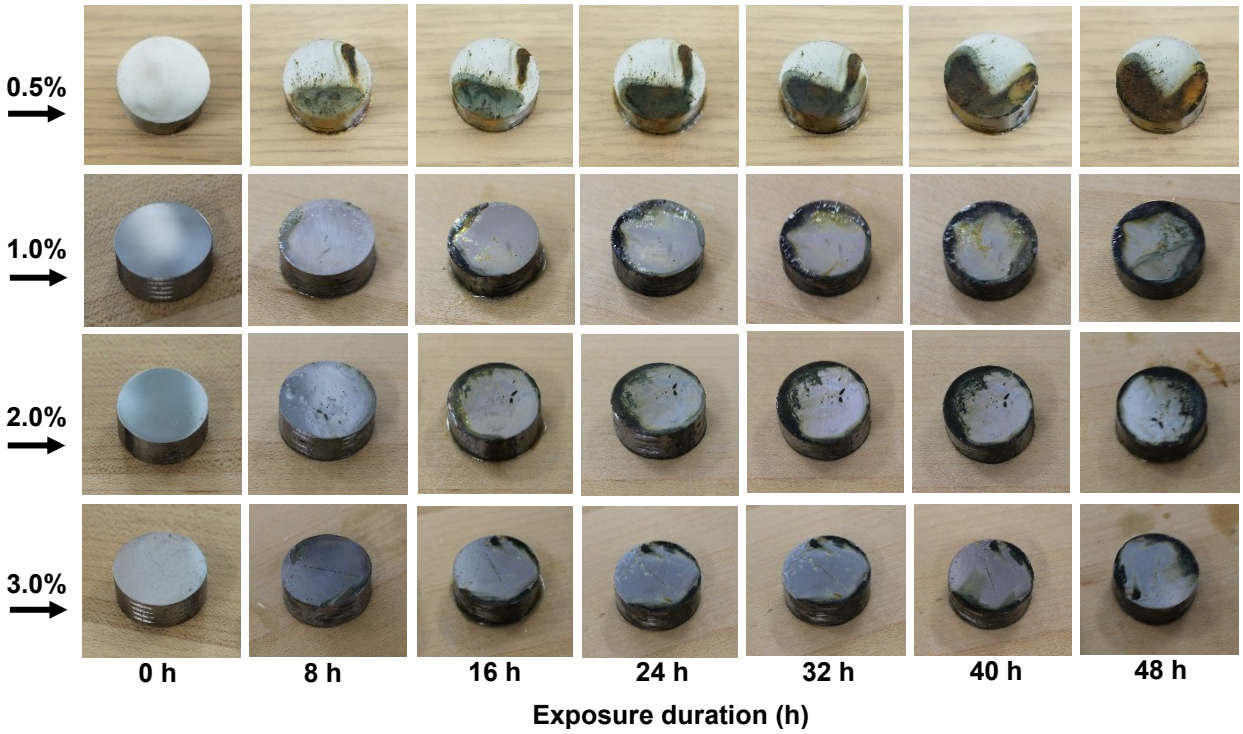

Figure 3.5. Visual appearance of ASTM A572 steel specimens exposed to deicing solution containing 0.5%, 1.0%, 2.0% and 3.0% sorbitol.

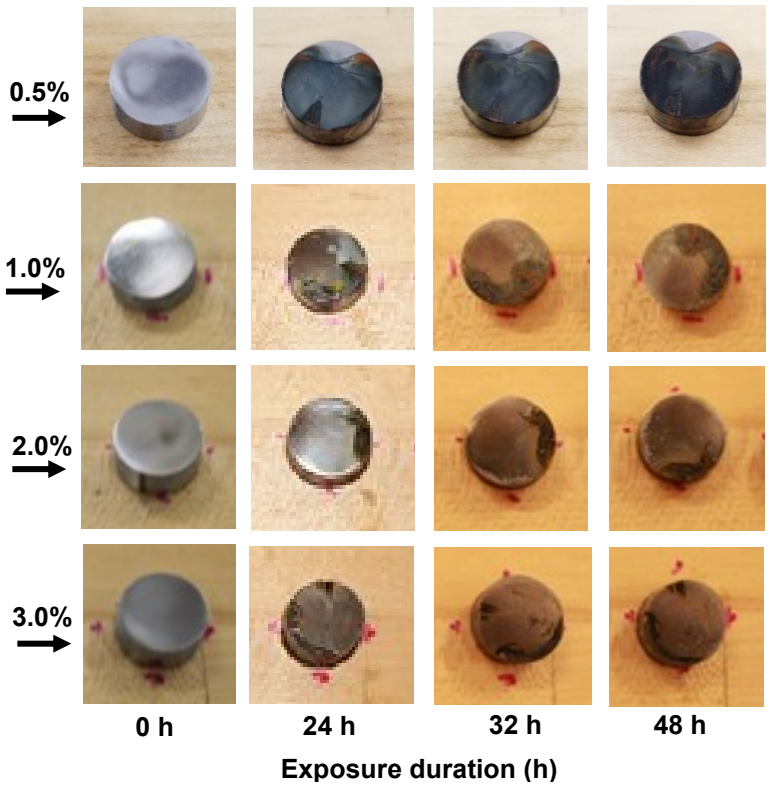

Figure 3.6. Visual appearance of ASTM A572 steel specimens exposed to deicing solution containing 0.5%, 1.0%, 2.0% and 3.0% mannitol.

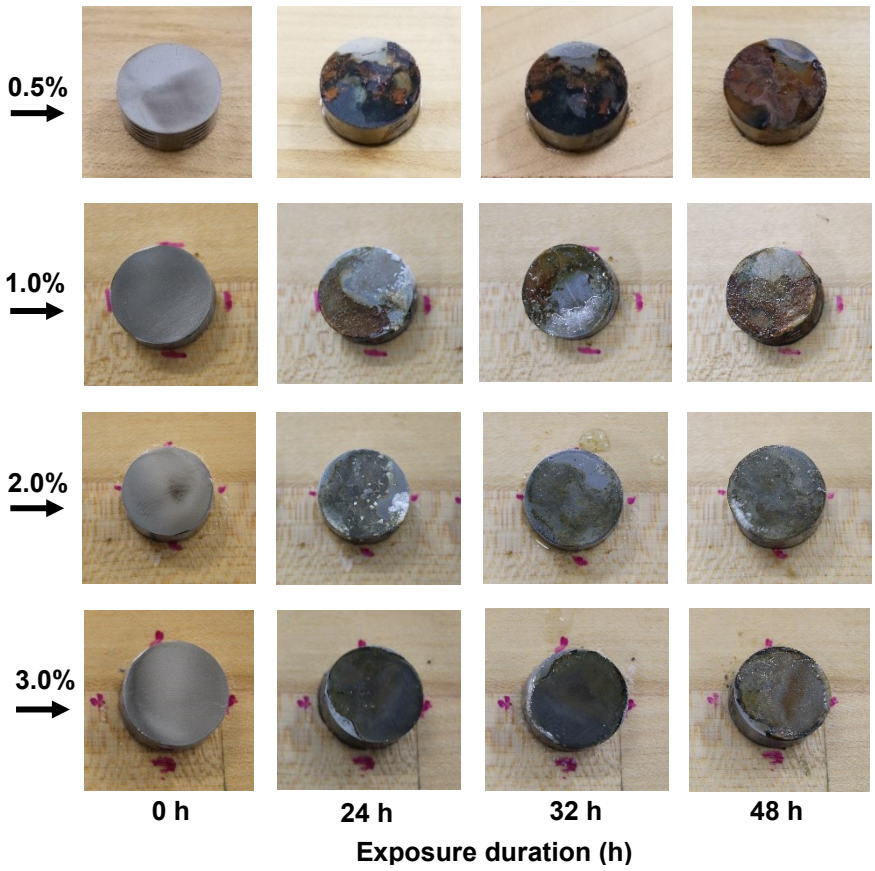

Figure 3.7. Visual appearance of ASTM A572 steel specimens exposed to deicing solution containing 0.5%, 1.0%, 2.0% and 3.0% maltitol.

3.3.2 Potentiodynamic Polarization Tests

The potentiodynamic polarization tests are conducted to evaluate the corrosion current densities, corrosion rates and subsequent corrosion inhibition mechanism using the procedure discussed in Section 3.2.2. The polarization curves obtained from the potentiodynamic polarization tests usually provide insights on the important processes that occur at the anodic and cathodic sites. A schematic polarization curve that can be obtained for steels in the electrolytic environment simulated in this study is provided in Figure 3.8. As observed in Figure 3.8, the cathodic branch exhibits two regions: 1) hydrogen evolution, and 2) reduction of passive film and dissolved oxygen (McCafferty 2010). On the other hand, the anodic branch exhibits an initial active corrosion region wherein the current density increases which is followed by the formation of a passive region wherein the current density values remain almost constant and the potential decreases. The passive

region represents the formation of the passivation layer. Finally, a marked increase in the current density is observed which reveals the breakdown of the passivation layer, active anodic dissolution, and the formation of pits.

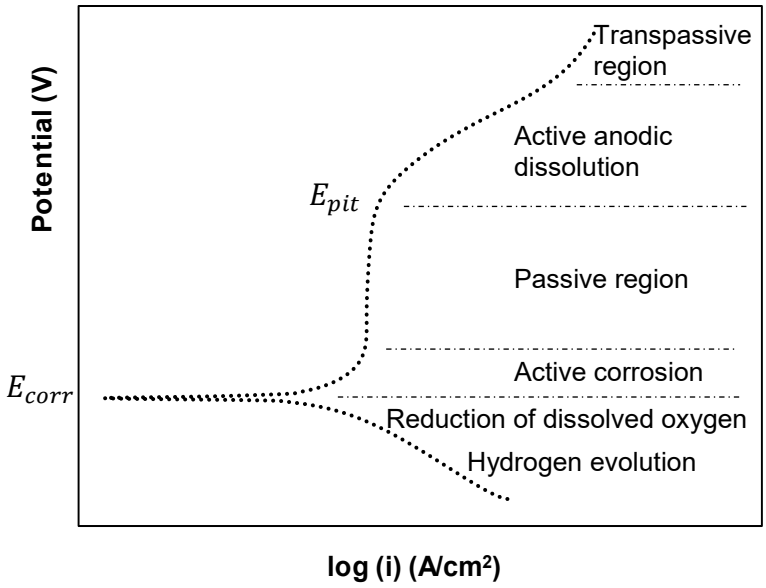

Figure 3.8. Schematic polarization curve of a typical test specimen.

The potentiodynamic polarization curves of ASTM A572 steels in the deicing solution in the absence and presence of small concentrations of different polyols are presented in Figure 3.9. For each polyol concentration, three potentiodynamic polarization tests are conducted and only one curve is presented corresponding to each polyol concentration herein for the sake of clarity as the three curves almost overlapped. As observed in Figure 3.9, a typical Tafel behavior is observed in the cathodic branches for all polarization curves wherein the logarithmic current density varies linearly with the potential. Moreover, the shapes of cathodic and anodic branches remain the same for all cases. In most of the cases, the cathodic and anodic branches exhibited distinct regions that are illustrated in the schematic polarization diagram in Figure 3.8. The cathodic branches exhibited hydrogen evolution, and reduction of dissolved oxygen whereas the anodic branches exhibited an initial active corrosion region which is followed by the formation of a passive region and finally the breakdown of the passivation layer and the formation of pits. The polarization curves shifted towards lower current regions in the presence of the polyols (see Figure 3.9) which indicates corrosion inhibition. Moreover, in the presence of polyols, the corrosion potentials (E_{corr}) are observed to shift in the noble direction which indicates that the presence of polyols has a noticeable influence on retarding the electrochemical reactions (anodic dissolution of steel) happening at the anodic sites. The polarization curves are used to obtain necessary electrochemical parameters corresponding to each polyol concentration in the deicing solution that are discussed in the next section.

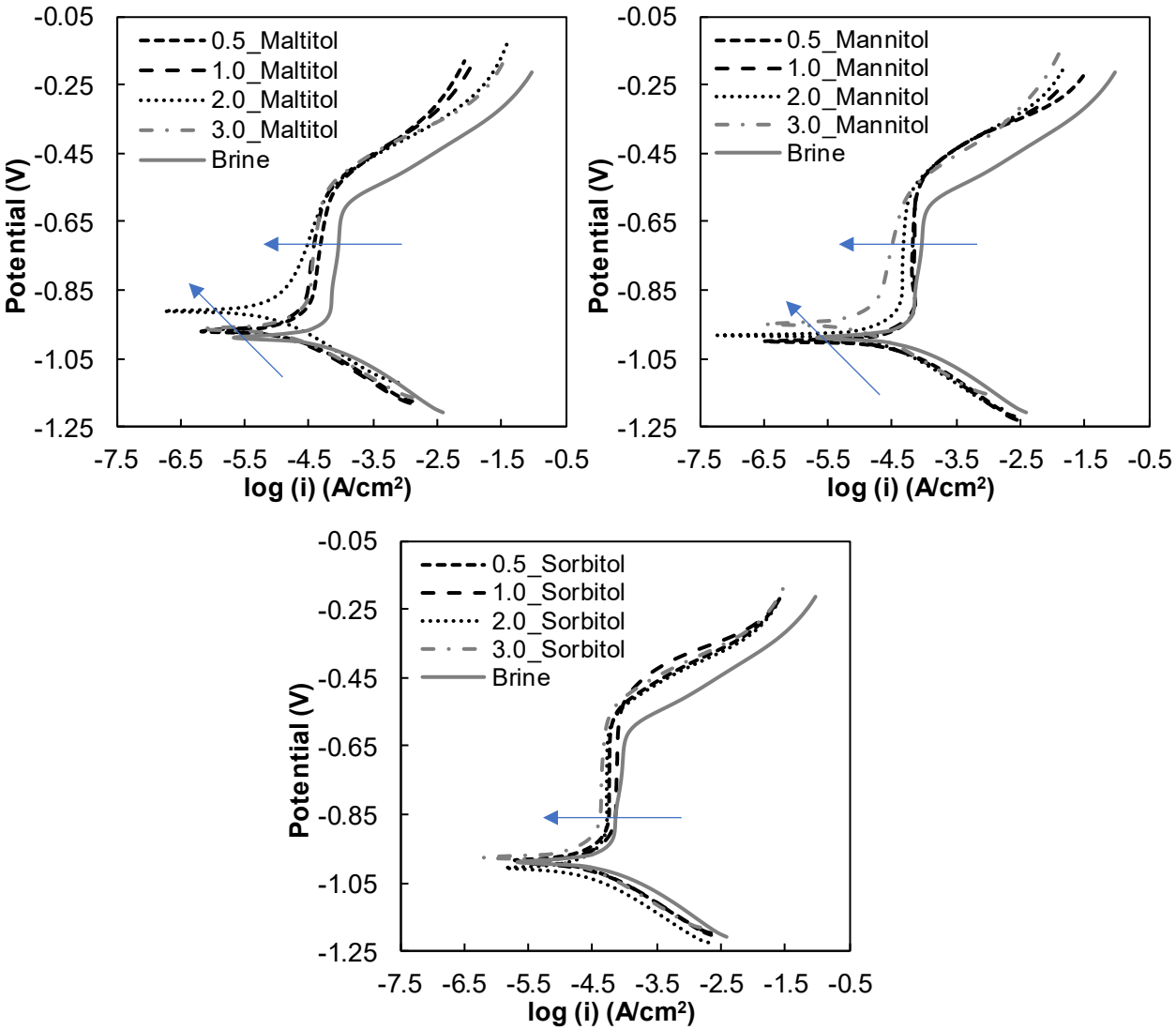

Figure 3.9. Potentiodynamic polarization curves of ASTM A572 steel specimens in deicing solution (23% NaCl brine) in the absence and presence of various polyols concentrations (0.5%, 1.0%, 2.0%, and 3.0%).

3.3.3 Tafel Extrapolation Results

Tafel extrapolation is performed to determine important electrochemical parameters that include corrosion potential (E_{corr}), corrosion current density (i_{corr}), anodic Tafel slope (β_a), and cathodic Tafel slope (β_c). For Tafel extrapolation, at least one branch (either cathodic or anodic) is required to exhibit Tafel behavior wherein the logarithmic current density varies linearly with the potential of the working electrode (McCafferty 2005). It is desirable to use both cathodic and anodic curves in determining Tafel slopes. However, either cathodic or anodic branch can also be used in Tafel extrapolation to determine the Tafel slope and the subsequent corrosion current density. When

using a single branch (cathode or anode) for Tafel extrapolation, the cathodic branch is generally preferred over the anodic branch for two reasons: 1) the cathodic branches usually exhibit a more pronounced Tafel region as compared to the anodic branch, and 2) the anodic branch usually exhibits passivation and pitting behavior, and roughening of the specimen surface, all of which can result in deviation of the anodic branch from the Tafel behavior (McCafferty 2005). It can be observed from Figure 3.9 that the polarization curves obtained for ASTM A572 steels exhibited a more pronounced Tafel behavior in the cathodic curves and relatively small Tafel region in the anodic curves. For these reasons, only cathodic curves are considered in Tafel extrapolation. To minimize the errors that are usually encountered in Tafel extrapolation due to the logarithmic nature of the current density, the extrapolating region is selected at least 50 mV away from the corrosion potential (E_{corr}) and the Tafel region extends at least over one decade of the corrosion current density (Kelly et al. 2002). The polarization parameters obtained after following the above procedure are provided in Table 3.2. The corrosion current densities are presented in Figure 3.10.

Table 3.2. Polarization parameters obtained from Tafel extrapolation.

Corrosion inhibitor	**Concentration (%)**	$\boldsymbol{E_{corr}}$ **(V)**	$\boldsymbol{-i_{corr}}$ **(μA/cm^2)**	$\boldsymbol{-\beta_c}$ **(V/dec)**	**Corrosion rate (mm/yr)**
None (23% NaCl salt brine only)	----	-1.002	71.189	0.137	0.829
Maltitol	0.5	-0.961	12.045	0.111	0.140
	1.0	-0.936	8.738	0.110	0.102
	2.0	-0.907	5.334	0.103	0.062
	3.0	-0.978	10.734	0.094	0.125
Mannitol	0.5	-0.993	20.378	0.105	0.237
	1.0	-0.975	11.597	0.095	0.135
	2.0	-0.988	11.311	0.085	0.132
	3.0	-0.956	7.654	0.096	0.089
Sorbitol	0.5	-0.953	15.230	0.099	0.177
	1.0	-0.954	15.409	0.126	0.179
	2.0	-0.975	11.564	0.090	0.135
	3.0	-0.933	5.979	0.092	0.069

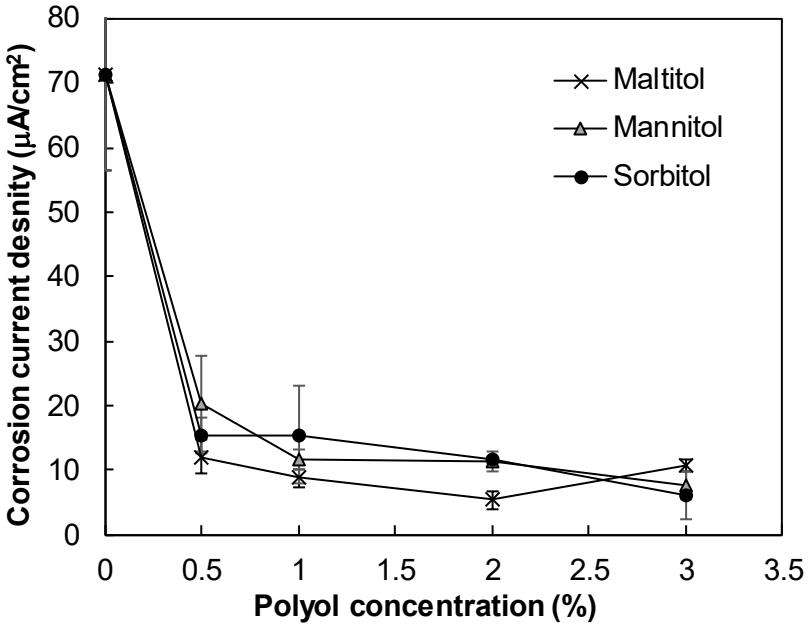

Figure 3.10. Corrosion current densities of ASTM A572 steel specimens as a function of polyols concentration in deicing solution.

From Figure 3.10 and Table 3.2, it is clear that the corrosion current densities decrease substantially when small quantities of polyols are added to the salt brine which confirms their corrosion inhibition potential. In the absence of polyols, an average corrosion current density of 70 μA/cm^2 is observed for steel specimens. When small amounts of polyols are added to the deicing solution the average corrosion current density is observed to be in the range of 6-20 μA/cm^2. The corrosion inhibition performance corresponding to different concentrations of each polyol is quantified by evaluating the corrosion inhibition efficiency (IE) which is defined as the relative reduction in the corrosion current density and is it determined by using the following equation

$$\text{IE}\ (\%) = \frac{i_{corr}^{0} - i_{corr}^{inh}}{i_{corr}^{0}} \times 100 \qquad (3.1)$$

where, IE = inhibition efficiency corresponding to a particular concentration of polyol in the deicing solution (in %), i_{corr}^{0} and i_{corr}^{inh} are corrosion current densities in the absence and presence of polyols in the deicing solutions, respectively (in μA/cm^2). The average inhibition efficiencies determined using the above equations are provided in Figure 3.11. It is clear from Figure 3.11 that the addition of even a small amount (0.5% wt.) of polyols that are investigated in this study result in an average corrosion inhibition efficiency of 71%. When the concentration of polyols is increased up to 3.0% wt., the average inhibition efficiencies reached 92%. These results indicate that a pronounced effect on corrosion rates is observed at 0.5% wt. concentration of polyols and a

small but steady increase in corrosion inhibition efficiencies is observed when the weight concentrations of polyols are increased from 0.5% to up to 3.0% wt.

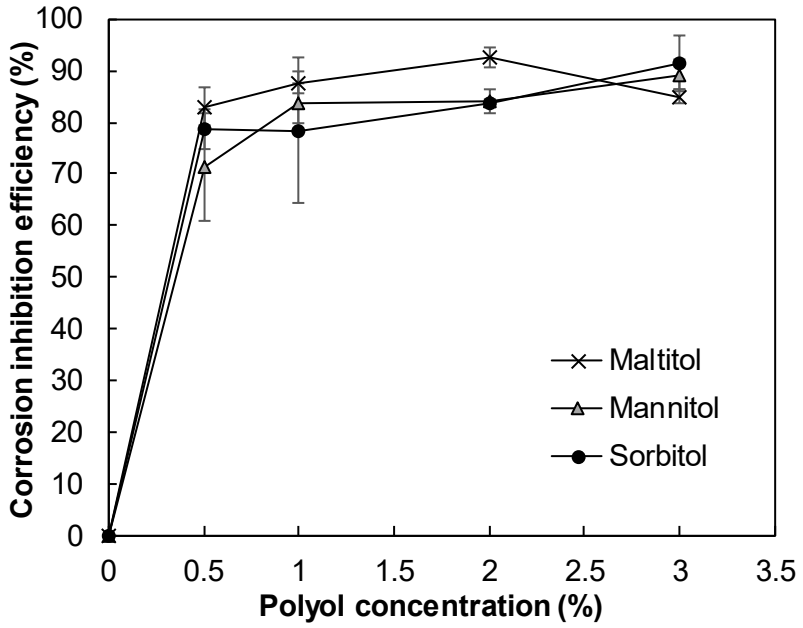

Figure 3.11. Corrosion inhibition efficiencies of polyols as a function of polyols concentration in deicing solution.

The corrosion rates in ASTM A572 steel specimens in the absence and presence of polyols in the deicing solution are determined by using the following equations in accordance with the ASTM G102 procedure (ASTM-G102-89-e1 2015)

$$CR = K_1 \frac{i_{corr}}{\rho} EW \tag{3.2}$$

where, CR = corrosion rate in mm/yr, $K_1 = 3.27 \times 10^{-3}$, i_{corr} = corrosion current density in $\mu A/cm^2$, ρ = density of steel in g/cm^3, and EW = equivalent alloy weight which is a dimensionless parameter and is determined from the mass percent of each alloy component in the steel using the following equation

$$EW = \left(\sum \frac{n_i f_i}{W_i} \right)^{-1} \tag{3.3}$$

where, n_i = valence of the ith element of the steel alloy, f_i = mass fraction of the ith element of the steel, and W_i = atomic weight of the ith element in the steel. The average corrosion rates determined using Eq. (3.2) are plotted in Figure 3.12. As observed in Figure 3.12, ASTM A572 steel specimens exhibited a higher average corrosion rate (0.83 mm/yr on average) in the absence

of polyols in the deicing solution. The corrosion rates decreased substantially (up to 92%) in the presence of polyols. The lowest corrosion rate is noticed in the case of 2.0% maltitol in the deicing solution (0.062 mm/yr) and 3.0% sorbitol in the deicing solution (0.069 mm/yr). The mechanisms that led to the reduction of corrosion rate in the presence of polyols in the deicing solutions are discussed in the next section.

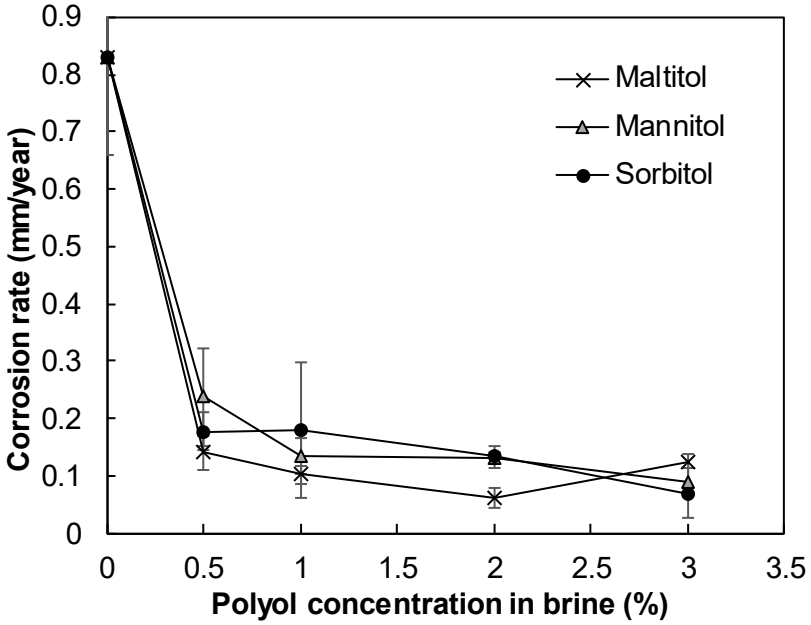

Figure 3.12. Corrosion rates in ASTM A572 steels as a function of polyols concentrations in deicing solution.

3.3.4 Corrosion Inhibition Mechanism of Polyols

In the aqueous solution, the loss of iron at anodic sites (also referred to as anodic dissolution of iron) is given by Eq. (3.4).

$$Fe \rightarrow Fe^{2+} + 2e^{-} \tag{3.4}$$

The reactions at the cathodic sites are usually governed by the PH level of the solution. In the case of acidic solution, the reduction of hydrogen ions occurs Eq. (3.5) whereas reduction of dissolved oxygen is usually noticed in neutral or basic solutions Eq. (3.6).

$$2H^{+} + 2e^{-} \rightarrow H_2 \tag{3.5}$$

$$O_2 + 2H_2O + 4e^{-} \rightarrow 4OH^{-} \tag{3.6}$$

The hydroxyl ions formed as a result of reduction of dissolved oxygen can migrate to anodic sites and react with the iron ions thus leading to initial corrosion products formation in the form of ferrous hydroxide $Fe(OH)_2$. Brine solution has substantially less solubility of dissolved oxygen due to high concentration of sodium ions (Na^+) and chloride ions (Cl^-) (Revie and Uhlig 2008). As a result, the reduction of dissolved oxygen can be less prominent when compared to the hydrogen evolution reaction. In such a case, the hydrogen evolution can also occur by direct reduction of water (Eq. (3.7)) (Jones 1996; Kim and Kim 2017).

$$2H_2O + 2e^- \rightarrow H_2 + 2OH^- \tag{3.7}$$

The presence of abundant sodium ions (Na^+) and chloride ions (Cl^-) in the traditional deicing solution (23% wt. NaCl) notably increases the conductivity of the electrolyte and hence the rate of anodic and cathodic reactions increases. In addition, in the presence of these ions, ferrous chloride ($FeCl_2$) can also be formed apart from the formation of ferrous hydroxide and sodium hydroxide ($NaOH$). Ferrous chloride can hydrolyze and form hydrochloric acid (Eq. (3.8)) which increases the acidity and subsequent corrosivity of the solution (Alcántara et al. 2017; Revie and Uhlig 2008).

$$FeCl_2 + H_2O \rightarrow FeO + 2HCl \tag{3.8}$$

With the addition of polyols in the deicing solution, the polyol molecules compete with the hydroxyl ions and oxygen atoms for attaching with the iron ions via physical and/or chemical adsorption. Polyols are known to have a chelating affinity for metal (Dwyer and Mellor 1964; Hodge et al. 1963). In neutral or alkaline media, polyol molecules can provide anionic regions which are known to bind multivalent metal ions (Hodge et al. 1963). In addition, sugar-derived molecules can provide nucleophilic atoms that tend to bind metal ions more readily as compared to oxygen (Hodge et al. 1963). Both of these phenomena result in the formation of stable complexes of iron and thereby block active sites for anodic and/or cathodic reactions.

The electrochemical parameters obtained from potentiodynamic polarization tests are used to further elucidate the corrosion inhibition mechanism of the polyols that are studied herein. The Tafel plots are observed to shift towards the lower current region and slightly shift towards positive potential in the presence of polyols. However, the shape of the Tafel curves remain the same. The average change in the corrosion potential observed in the case of maltitol is 56.5 mV whereas an average shift of 24 mV and 48.2 mV in the anodic direction is observed in the case of mannitol and sorbitol, respectively. The average corrosion potential shift for all three polyols is less than 85 mV which is usually considered as a benchmark potential value for categorizing a corrosion inhibitor either as cathodic or anodic (Awad et al. 2017; Lai et al. 2017). From these observations, it can be inferred that the polyols acted as mixed-type corrosion inhibitors. The slightly positive potential shift in the polarization curves reflect that the anodic inhibition is more dominant. The

corrosion inhibition mechanism of mixed-type inhibitors is achieved via either physisorption or chemisorption of corrosion inhibitor molecules on the steel surface (Brycki et al.).

The adsorption behavior of the polyols corrosion inhibitors on the steel surface can be quantified with the help of adsorption isotherms. An adsorption isotherm is a graphical plot between the amount of adsorbate (corrosion inhibitor molecules) on the adsorbent (metal surface) and the concentration of the adsorbate and is usually determined experimentally (Butt et al. 2013). Adsorption isotherms quantify the interaction between the metal surface and the corrosion inhibiting molecules (Christov and Popova 2004; Marzorati et al. 2019). Adsorption isotherms describe the relationship between the surface coverage θ and the concentration of corrosion inhibitors. The surface coverage θ represents the thin layer of adsorbed inhibitors on the steel surface and it can be determined from the corrosion inhibition efficiency (IE) using Eq. (3.9).

$$\theta = \frac{\mathrm{IE}(\%)}{100} \tag{3.9}$$

The most commonly used isotherms for studying the adsorption of corrosion inhibitors on the steel surfaces include Temkin isotherm, Langmuir isotherm, Frumkin isotherm, Flory–Huggins isotherm, and Freundluich isotherm (Christov and Popova 2004; Freundlich 1906; Langmuir 1916). The surface coverage θ and corrosion inhibition concentration data obtained in the current study can be fitted to Langmuir isotherm (Langmuir 1916). It is worth mentioning that most organic corrosion inhibitors studied in the literature usually fit the Langmuir adsorption isotherm (straight-line model) (Christov and Popova 2004) which is provided in Eq. (3.10).

$$\frac{\mathrm{C_{inh}}}{\theta} = \frac{1}{\mathrm{K_{ads}}} + \mathrm{C_{inh}} \tag{3.10}$$

where, $\mathrm{C_{inh}}$ is the corrosion inhibitor concentration, θ is the surface coverage and $\mathrm{K_{ads}}$ is the standard adsorption equilibrium constant. The standard adsorption equilibrium constant is determined from the Langmuir isotherm model and is then used to evaluate the standard free energy of adsorption ($\Delta \mathrm{G^0_{ads}}$). The standard free energy of adsorption ($\Delta \mathrm{G^0_{ads}}$) quantifies the interaction between adsorbate and the metal surface (Biresaw and Mittal 2011). The standard free energy of adsorption ($\Delta \mathrm{G^0_{ads}}$) and the standard adsorption constant ($\mathrm{K_{ads}}$) are related by Eq. (3.11) (Liu 2009).

$$\Delta \mathrm{G^0_{ads}} = -\mathrm{RT ln}(55.5 \mathrm{K_{ads}}) \tag{3.11}$$

where, R = universal gas constant, T = absolute temperature and 55.5 is the molar concentration of water. The adsorption isotherms for ASTM A572 steels in the absence and presence of different polyols in the deicing media are provided in Figure 3.13, along with Langmuir model fitted

equations. The linear behavior observed in Figure 3.13 confirms that the Langmuir model accurately represents the adsorption behavior. The adsorption parameters obtained from the adsorption isotherms are provided in Table 3.3. The negative value of ΔG^0_{ads} indicates the spontaneity of the adsorption process and stability of the adsorbed film on the metal surface. Different studies have suggested that the analysis of ΔG^0_{ads} helps establish the adsorption type between a metal and an inhibitor (Christov and Popova 2004). If the ΔG^0_{ads} values are close to −20 kJ/mol or lower, the adsorption process is physical. On the other hand, if the values are close to −40 kJ/mol or higher, a chemisorption process takes (Sliem et al. 2019). In many recent studies, the ΔG^0_{ads} value falling between -28 kJ/mol and -38 kJ/mol is linked to mixed adsorption (Kaczerewska et al. 2018; Lgaz et al. 2017; Sliem et al. 2019). The ΔG^0_{ads} values corresponding to each polyol corrosion inhibitor are closer to -20 kJ/mol. This suggests that that polyols inhibited the corrosion in ASTM A572 steels in deicing media via physical adsorption on the steel surface which prevented interaction between the steel and corrosive media.

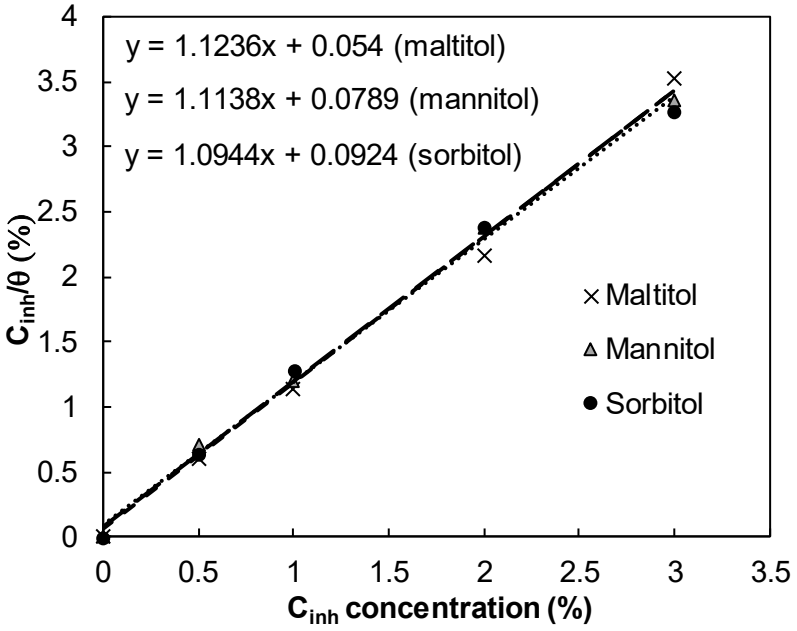

Figure 3.13. Langmuir adsorption isotherm plots for steel specimens in brine solution containing various concentrations of polyols in deicing solution.

Table 3.3. Calculated thermodynamic parameters from the Langmuir isotherm.

CI type	Molar conversion factor	$1/K_{ads}$	$\Delta G_{ads}{}^0$
Maltitol	0.029	0.054	-25.95
Mannitol	0.0549	0.0789	-23.43
Sorbitol	0.0549	0.0924	-23.04

3.4 Conclusions

In this study, the corrosion inhibition performance is quantified for three corn-derived polyols, namely, maltitol, mannitol, and sorbitol in the traditional deicing solution (23% wt. NaCl brine). Following are the important conclusions that can be drawn from this work:

1. The visual observations from accelerated corrosion tests indicated delayed corrosion initiation and less corrosion damage in the steel specimens that are subjected to polyols-mixed deicing solutions (polyol+23% wt. NaCl) inside a corrosive environment.
2. The results obtained from the potentiodynamic polarization tests revealed that the presence of even small amounts of polyols (0.5% wt.) in the deicing media results in an average corrosion inhibition efficiency of up to 71%. When the concentration of polyols is increased up to 3.0% wt., the inhibition efficiencies reached up to 92%.
3. In the presence of 0.5% wt. sorbitol in the deicing solution, ASTM A572 steels exhibited a 79% reduction in the average corrosion rate (0.18 mm/yr) when compared to the average corrosion rate observed in the absence of sorbitol in the deicing solution (0.83 mm/yr). The average corrosion rate in steel specimens decreased by 92% (0.06 mm/yr) when the concentration of sorbitol in the deicing solution is increased from 0.5% to 3.0% wt.
4. The average corrosion rates in the steel specimens decreased by 83% after the addition of 0.5% wt. maltitol to the deicing solution (23% wt. NaCl). The lowest average corrosion rate in maltitol-mixed deicing solutions (0.06 mm/yr) is observed corresponding to 2.0% wt. concentration in the deicing solution.
5. The average corrosion rates in steel specimens decreased by 71% (0.24 mm/yr) in the presence of 0.5% wt. mannitol in the deicing solution. The average corrosion rate further decreased (up to 89%, 0.09 mm/yr) when the concentration of mannitol in the deicing solution is increased up to 3.0% wt.
6. The corrosion inhibition, corrosion potentials and corrosion rates obtained from the Tafel extrapolation revealed that the corn-derived polyols studied herein acted as mixed-type corrosion inhibitors in the deicing media. The corrosion inhibition is achieved via physisorption of polyols molecules on the steel surface.

CHAPTER 4
ICE MELTING CAPACITY, SKID RESISTANCE AND DISSOLVED OXYGEN OF POLYOL-BRINE DEICERS

The fundamental properties of deicers are not rigorously related to the mode of interactions between ice or snow and deicers (Chappelow et al. 1992). Besides this, the frictional characteristics of pavement surfaces exposed to deicer solutions are also of concern from a safety standpoint. Therefore, this chapter focuses on the investigation of ice melting cpacity and skid resistance of polyols-brine deicer solution. To this end, the process of preparing the specimens and the test protocols adopted for conducting the experiments are described in detail. The results obtained from the experiments are discussed and the conclusions are provided.

4.1 Experimental setup

4.1.1 Ice Melting Capacity Test

The ice melting capacity (IMC) of salt brine deicer after the addition of corn-derived polyols and juices is investigated by performing ice melting tests using an in-house built test setup, as shown in Figure 4.1. First, the deicing solutions are prepared by adding corn-derived polyols (sorbitol, mannitol, and maltitol) and juices (beet juice and corn juice) to the salt brine deicer in the following weight concentrations: 0%, 5%, 10%, 15%, and 27.7%. Corn juice and beet juice are prepared by employing the same procedure mentioned in Section 2.1.2.2 and Section 2.1.2.3 respectively. Different ice melting test setups are currently used in ice melting tests of deicing chemicals and some of these test methods involve insulated containers or thermos containing the deicing solution at various subfreezing temperatures and shaking of ice cubes in the deicing solutions (Chappelow et al. 1992; Gerbino-Bevins et al. 2012). In the current study, each deicing solution is kept at 10 °C to mimic the temperature of the deicer just before application on road. The ice melting behavior of each bio-based deicer (salt brine+polyol or salt brine+corn juice or salt brine+ beet juice) is evaluated for the following temperatures: 0 °C, -10 °C, -20 °C, and -30 °C. For this purpose, ice cubes with approximately 38 mm length are first formed in a commercially available freezer by setting the temperature around -5 °C. The ice cubes are then immersed in acetone solution which is preset to the target temperature by using dry ice. The ice cubes are kept immersed at the target temperatures for 2 minutes. After the ice cubes reach the target temperature, the ice cubes are removed from acetone and are placed in the vicinity of dry ice to maintain the target temperature. The temperature of the acetone solution and the ice cubes is constantly monitored using K-type thermocouples to ensure the target temperature is maintained. One ice cube is then immersed in a 70 ml test solution (salt brine+polyol or juice, set a 10 °C) for 2 minutes. The weights of the ice cube before and after immersion in the test solution are obtained which are used to quantify the ice melting potential of the test solution. In total, 68 different combinations of salt brine + polyols solutions, brine + beetroot juice solutions, brine + corn juice solutions, and temperatures are tested for ice melting capacity, and each test is repeated twice. The results obtained from ice melting capacity tests are discussed in Section 4.2.1.

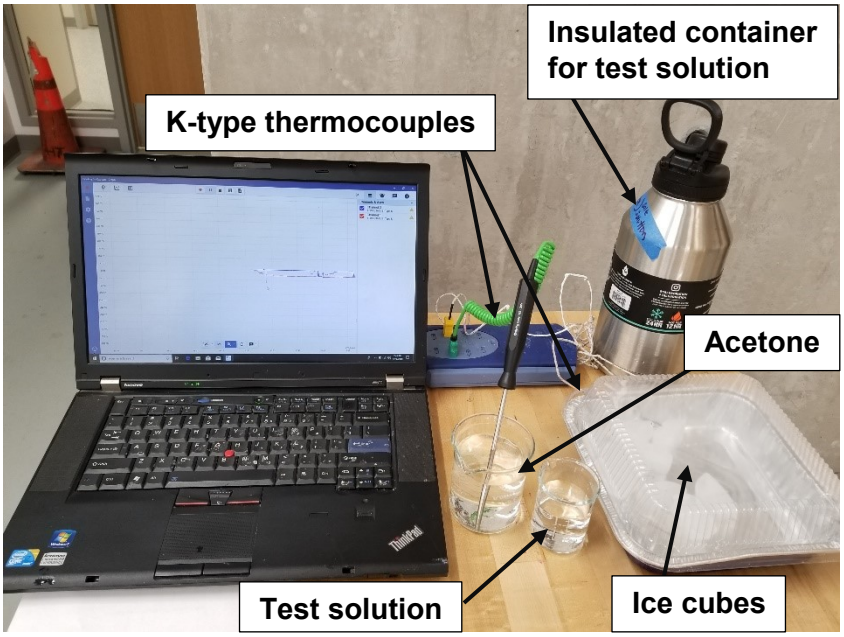

Figure 4.1. Test setup for conducting ice melting tests.

4.1.2 Skid Resistance Test

Skid resistance is a measure of the frictional force that is generated when a tire slides on a wet pavement surface (Henry 2000). Skid resistance quantifies the slipperiness of a pavement surface and is considered a primary contributory factor to road accidents (Kokkalis and Panagouli 1998). High skid resistance prevents skidding of the vehicle tires on the pavement surface and thus ensures adequate control for operating vehicles on highways. The skid resistance of pavements can be evaluated using field and laboratory testing methods that include Locked Wheel Tester (ASTM E274) ((E274M-15 2020; Henry 2000), Spin Up Tester (Wambold et al. 1990), Side Force Method (e.g. MuMeter and the Sideway Force Coefficient Routine Investigation Machine (SCRIM)) (Henry 2000; Hosking and Woodford 1976), Fixed Slip Method (Henry 2000), Variable Slip Method (ASTM E1859) (E1859/E1859M-11 2015), British Pendulum Tester (ASTM E303) (ASTM 2018; Liu et al. 2004), and Dynamic Friction Tester (ASTM E1911) (E1911-19 2019). In this study, the skid resistance of deiced pavement surfaces is determined using the British Pendulum Tester in accordance with the procedure specified in ASTM E303 (see Figure 4.2). The skid resistance of the pavement surfaces is determined for the reference deicing solution (23.3% wt. NaCl) and bio-based deicing solution combinations that led to higher ice melting (23.3% wt. NaCl + 27.7% wt. sorbitol, 23.3% wt. NaCl + 27.7% wt. maltitol, and 23.3% wt. NaCl + 27.7% wt. mannitol). The skid resistance tests are performed on a cleaned Portland cement pavement (PCC) pavement surface on the premises of the North Dakota State University. The pavement surface is first cleaned then the deicing solution is applied and left on the surface for a settling time of 10 minutes. The British Pendulum Tester is then employed to obtain the skid resistance values in terms of British Pendulum Number (BPN). BPN is an indirect measure of skid resistance and higher BPN values indicate higher skid resistance of a road surface. For each deicing solution

combination, different locations of PCC pavement surface are chosen and each test is repeated 5 times. The skid resistance of pavements results for both reference deicing solution and polyol-brine deicing solutions are discussed in Section 4.2.2.

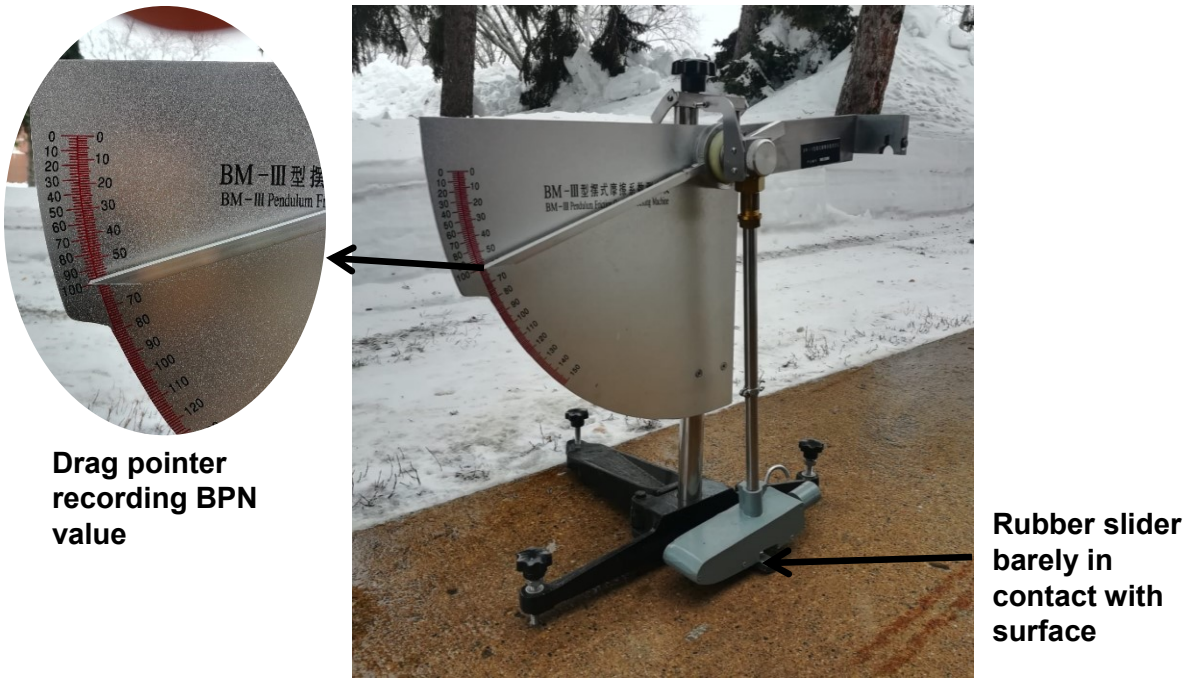

Figure 4.2. British Pendulum Tester for measuring skid resistance of pavement surface.

4.1.3 Viscosity Test

The viscosity of a fluid is a measure of its resistance to the deformation at a given rate. The viscosity of the deicing solution affects the handling and transportation of deicing solutions to the field. It further affects the workability and uniform spreading of a deicing solution on the pavement surface. In this study, the viscosity of the bio-based deicing solutions and reference deicing solution is determined using HAAKE Viscotester® 550 (see Figure 4.3). HAAKE viscotester® 500 consists of a standard cylindrical spindle and the data acquisition (DAQ) system that measures and records the shear stress and shear rate of a given fluid. The viscosity is then evaluated using the following equation

$$\text{viscosity (MPa.s)} = \frac{\text{shear stress}}{\text{shear rate}} \times 1000 \qquad (4.1)$$

To perform the viscosity test, 50 ml of the deicing solution is filled in a 13.5 mm diameter centrifuge tube. The cylindrical spindle of the viscotester is then gradually lowered in the solution until a desired depth, as specified by the equipment manufacturer, is achieved. The spindle is then set to undergo rotations at a speed of 1032 rpm and the associated shear stress (Pa) magnitude is recorded. For each deicer solution, the test is repeated three times. All viscosity tests are conducted

at a constant temperature of 20 °C. The viscosity tests are conducted for the salt brine deicer and the bio-based deicing solutions that resulted in higher ice melting capacity. The results obtained from the viscosity tests are discussed in Section 4.2.3.

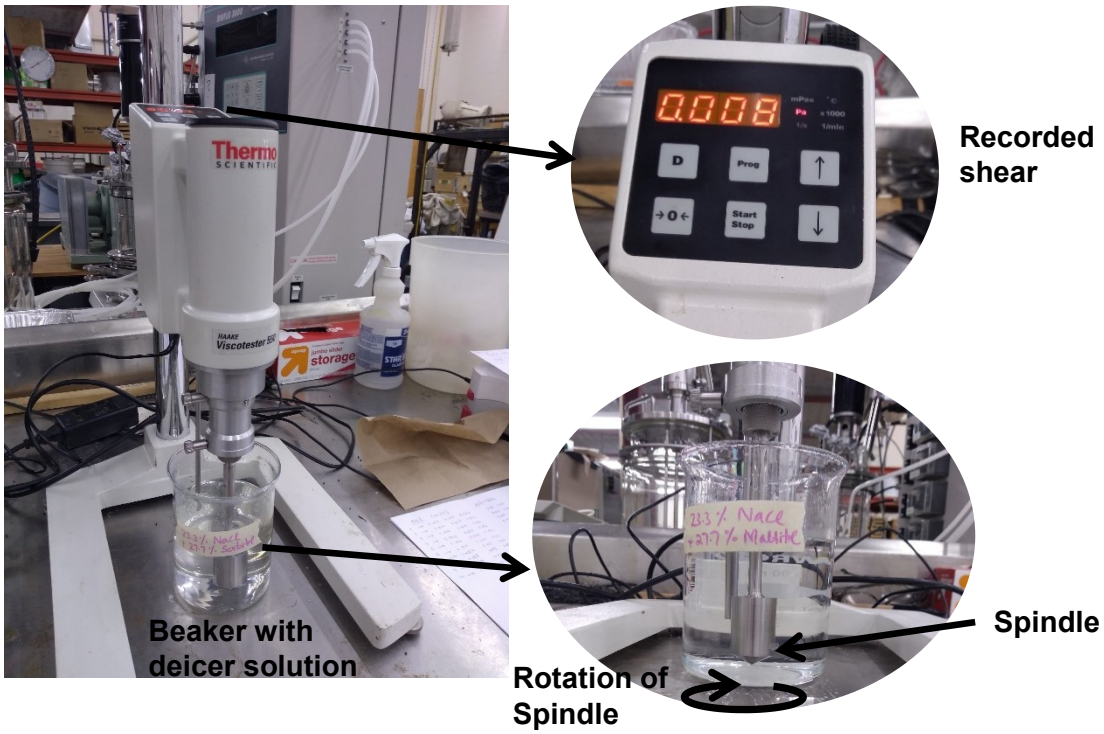

Figure 4.3. Viscosity test set up.

4.1.4 Dissolved Oxygen Test

Dissolved oxygen (DO) is a measure of the level of free, non-compound oxygen available in the water i.e. the oxygen that is not bonded to any other element. It is considered as an important preliminary parameter for assessing the water quality. Dissolved oxygen is necessary to many forms of aquatic life including fish, invertebrates, bacteria, and plants. These organisms use oxygen in respiration. Too high or too low can harm aquatic life and affect water quality. The deicers that are sprayed on the pavements may reach the stagnant water bodies or river streams adjacent to roads through surface run-off or soil infiltration and may reduce their DO levels which can cause adverse impacts. In this study, the influence of optimal combinations of corn-based polyol+brine solution on the change in the DO levels of the natural stream water (Red river) is investigated. Red river stream water is chosen for the reason that it runs parallel to the majority of the road network in the city of Fargo, ND, and mimics the real-world scenario where the deicers are run-off into the nearby stream.

For carrying out a Dissolved Oxygen experiment in the laboratory the following test protocol is adapted. About 45 ml of raw Red river water sample that was acquired from the Fargo water treatment plant was first filled in a centrifuge tube of 50 ml capacity. Then a 2µl of deicer solution is drawn into the 2-200 µl micropipette and is added to the raw water sample to obtain a

concentration of 45 mg/L. This concentration is chosen as per the study performed by Bang et. al. (Bang, 1998). Then the DO level of the mix containing raw water and deicer solution is measured using a Thermo Scientific Orion Star® benchtop DO meter (see Figure 4.4) available in the environmental engineering laboratory at the Civil Engineering Department of North Dakota State University (NDSU). The initial reading is referred to as 'Day 0' reading. The mix is then left undisturbed for the next 72 hours to obtain a 'Day 3' reading. The difference in the DO level indicates the amount of oxygen consumed by the aquatic microorganisms in 72 hours. The test procedure is adapted for all four deicer solutions namely, (1) 23.3 wt. % brine, (2) 23.3 wt. % brine + 27.7 wt.% sorbitol, (3) 23.3 wt.% brine + 27.7 wt.% maltitol, (4) 23.3 wt.% brine + 13.33 wt.% mannitol and were repeated in triplicates. For reference purpose, the DO levels of the control sample (without the addition of deicer) was also measured.

Figure 4.4. Benchtop Dissolved Oxygen Meter (Source: Thermo Fisher Scientific™).

4.2 Results and Discussion

4.2.1 Ice Melting Capacity

The ice melting capacity corresponding to different concentrations of corn-derived polyols in the salt brine deicer is determined using the procedure discussed in Section 4.1. The percentage decrease in the weight of the ice cube immersed in the salt brine deicer (salt brine deicer) and corn-derived polyol solutions (salt brine+polyol) is provided in Figure 4.5. In addition, the percent change in the weight of ice cube polyols-based deicing solutions with respect to the salt brine deicer (salt brine deicer) is provided in Figure 4.6. As observed in Figure 4.5, the addition of polyols led to a higher decrease in the weight of ice cube at almost all target temperatures with the exception of -30 °C. The ice melting capacity of salt brine with 27.7% sorbitol increased by 43% at -10 °C (see Figure 4.6 (a)). At -20 °C, the presence of 27.7% sorbitol in the salt brine led to a 13% increase in the ice melting capacity of the deicing solution. At -30 °C, the sorbitol-based deicing solutions are observed to have similar ice melting capacity as that of salt brine. In the case of mannitol-based deicing solutions, the ice melting capacity is observed to increase by up to 93% and 112% at -10 °C and -20 °C, respectively (see Figure 4.6 (b)). Moreover, at -30 °C, the presence of 27.7% mannitol in the salt brine led to an increase of 81% in the ice melting capacity. The higher increase in the ice melting capacity of mannitol-based deicing solutions can be attributed to the

lower solubility of mannitol in the salt brine when compared to other polyols which lead to the presence of the undissolved mannitol solute particles in the salt brine. The undissolved mannitol particles in the salt brine can melt the ice and form a solution that can further contribute to the melting of ice. The ice melting capacity of salt brine increased by 17% at -10 °C and -20 °C when 27.7% maltitol is added to the salt brine deicer (see Figure 4.6 (c)). However, beyond -20 °C, the ice melting capacity of maltitol-based deicing solutions is observed to decrease, which indicates that salt brine+maltitol solution is no more effective for ice melting at -30 °C (see Figure 4.6 (c)). These results illustrate that the ice melting capacity of the salt brine deicer increased with the addition of various concentrations of corn-derived polyols. Among the polyols, mannitol and sorbitol resulted in higher ice melting even at lower temperatures (-20 °C and -30 °C). The maximum ice melting capacity is obtained when 27.7% wt. mannitol is added to 23.3% wt. brine solution for -20 °C target temperature wherein two times more ice melting is observed when compared to the traditional 23.3% wt. salt brine deicer.

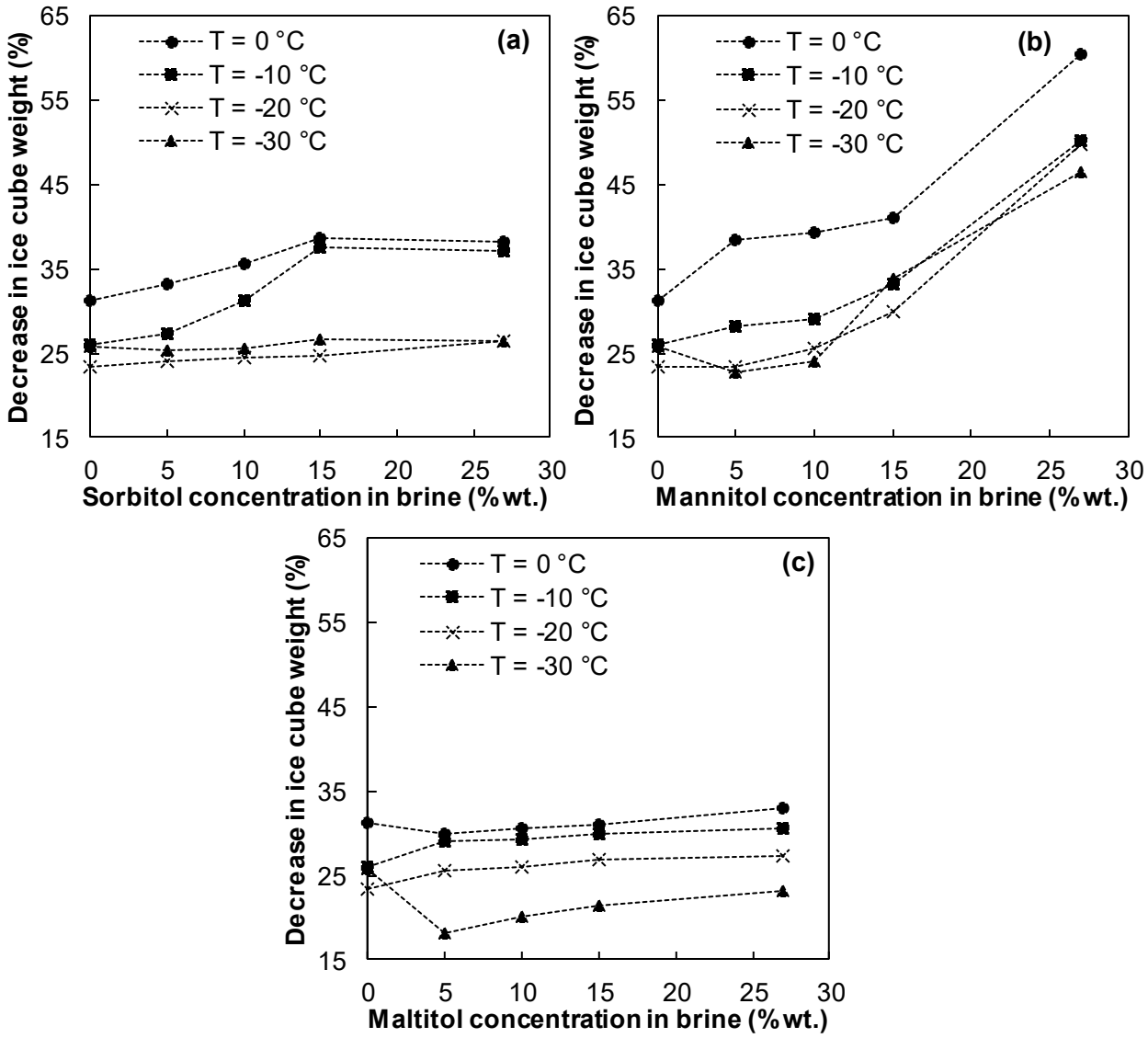

Figure 4.5. Percent decrease in weight of ice cube with an increase in the concentration of (a) sorbitol, (b) mannitol, and (c) maltitol, in the 23.3% wt. NaCl deicing solution at different low temperatures.

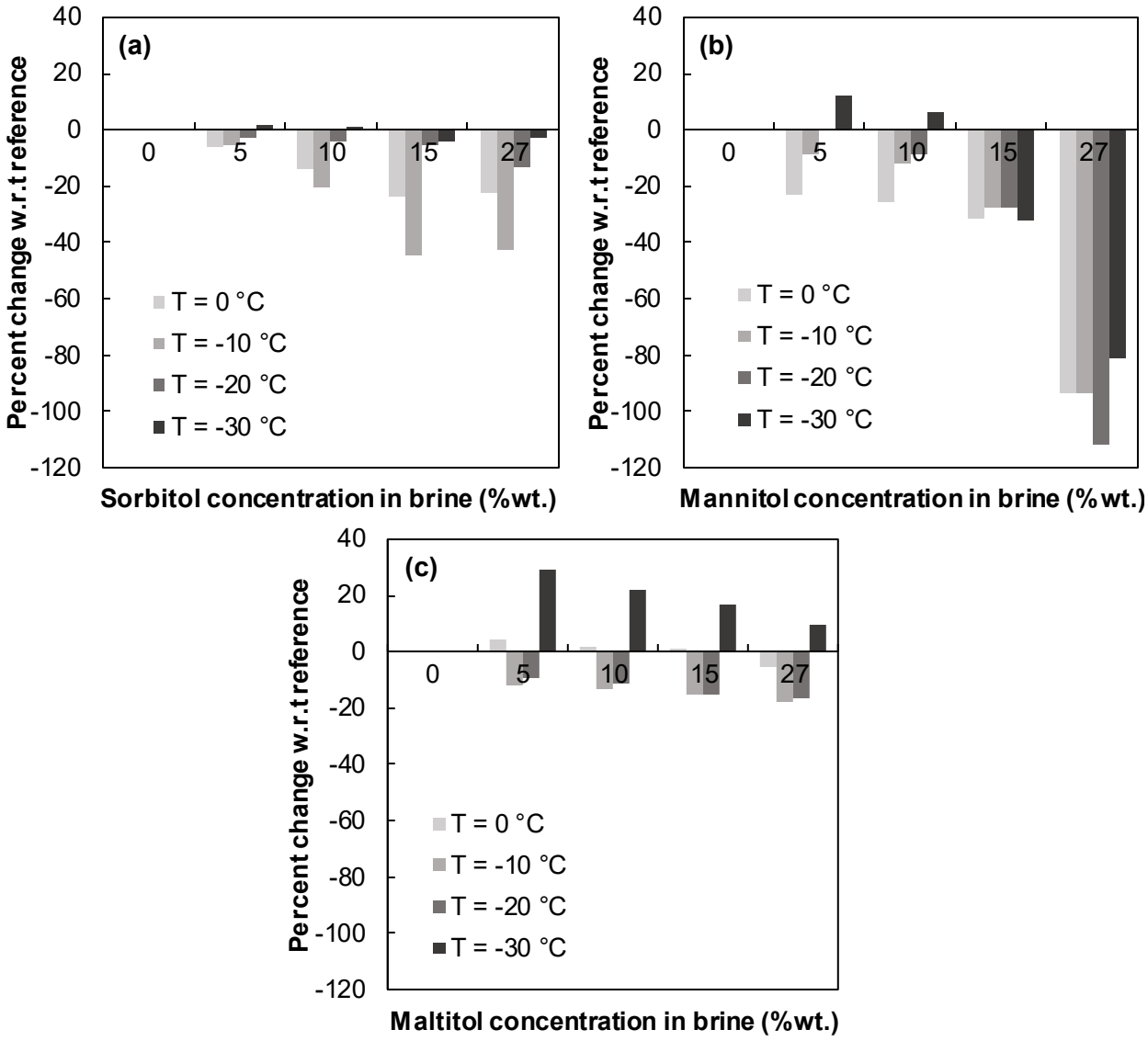

Figure 4.6. Percent decrease in the weight of ice cube immersed in (a) 23.3% wt. NaCl brine+sorbitol, (b) 23.3% wt. NaCl brine+mannitol, and (c) 23.3% wt. NaCl brine+maltitol solutions when compared to the traditional deicing solution (23.3% wt. NaCl brine), at different low temperatures.

4.2.2 Skid Resistance

The skid resistance of PCC pavements after the application of (23.3% wt. NaCl) and bio-based deicing solutions (23.3% wt. NaCl + 27.7% wt. sorbitol, 23.3% wt. NaCl + 27.7% wt. maltitol, and 23.3% wt. NaCl + 27.7% wt. mannitol) is determined in terms of BPN values using the procedure described in Section 4.1.2. The skid resistance test conducted for the optimum deicing solution combinations is depicted in Figure 4.7. The BPN values of salt brine deicer and bio-based deicing solution are provided in Table 4.1. The reduction in the average BPN values corresponding to the reference and bio-based deicing solutions is provided in Figure 4.8. As observed from Figure

4.8 and Table 4.1, the BPN values of the pavement surface decreased after the application of salt brine deicer and bio-based deicing solutions. The application of reference brine deicing solution on test pavement surface resulted in a 17% reduction in the average BPN values (skid resistance). The bio-based deicing solutions resulted in a slightly higher reduction in the BPN values (skid resistance) when compared to the salt brine deicer. An almost similar reduction in the BPN values in noticed corresponding to the three bio-based deicing combinations tested herein. The average BPN values of the pavement surface decreased by 32-35% after the application of the bio-based deicing solution (23.3% wt. NaCl + 27.7% polyol) (see Figure 4.8). The skid resistance of the mannitol-based deicing solution is also determined for 13.3% mannitol in the brine solution as no undissolved particles are present at this concentration. The average BPN values of the pavement surface decreased by 24% after the application of 13.3% mannitol + 23.3% wt. brine solution. This also shows that increasing the concentration of polyols in the deicing solutions leads to a decrease in the skid resistance of the pavement surface. The reduction in the skid resistance of the pavement surface after the application of bio-based deicing solutions may be attributed to the viscosity of the bio-based deicing solution. The viscosity of the bio-based deicing solutions is discussed in the next section.

Table 4.1.Average BPN values of the pavement surface before and after the treatment with deicer solution.

S. No.	Solution	BPN value											
		Before deicer application						After deicer application					
		1	2	3	4	5	Avg.	1	2	3	4	5	Avg.
1	23.3% Brine	112	115	115	115	115	114.4	95	95	94	95	94	94.6
2	23.3% Brine + 27.7% Sorbitol	116	113	113	113	114	113.8	84	75	75	75	75	76.8
3	23.3% Brine + 27.7% Maltitol	90	92	90	90	90	90.4	60	60	60	60	60	60
4	23.3% Brine + 27.7% Mannitol	103	100	100	98	100	100.2	70	68	68	68	68	68.4
5	23.3% Brine + 13.3% Mannitol	101	102	104	103	103	102.6	77	77	78	78	77	77.4

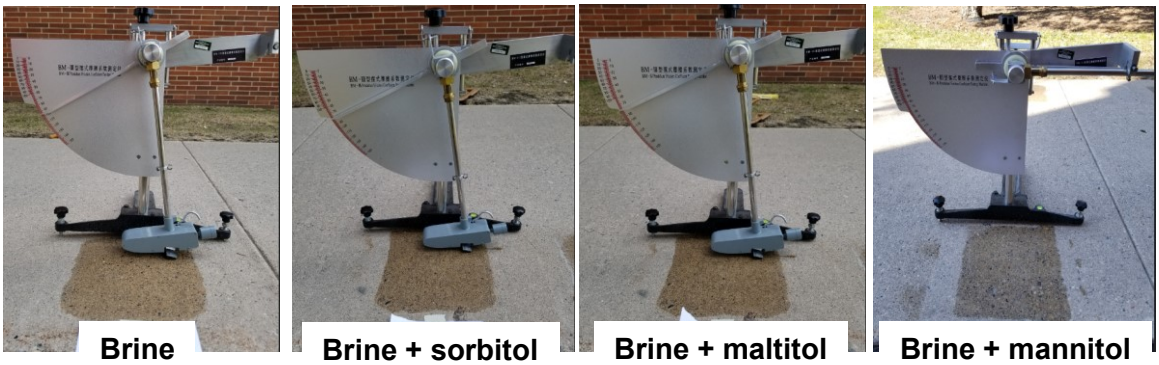

Figure 4.7.Skid resistance test on the PCC surface for all four optimal combinations of polyol and brine.

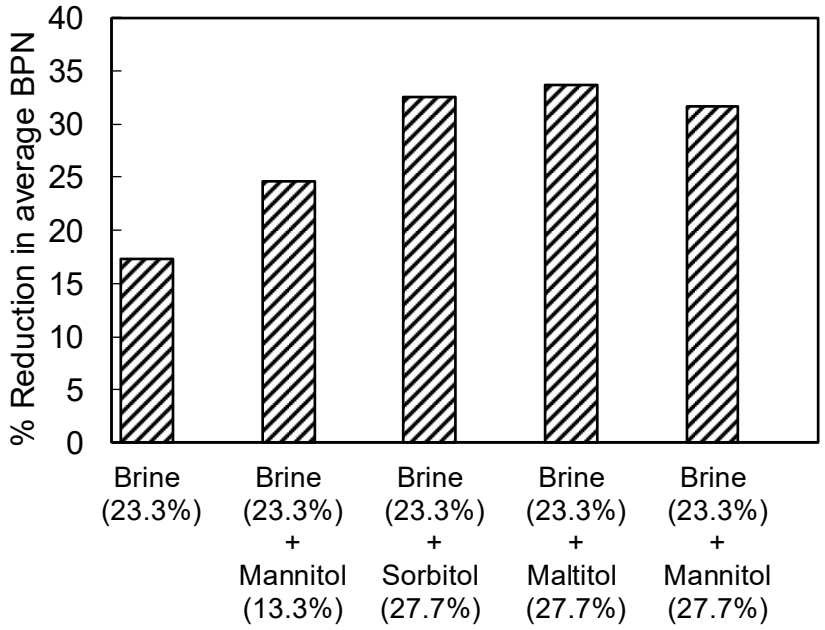

Figure 4.8.Reduction in average BPN value for various combinations of bio-based deicing solutions and salt brine deicer (brine).

4.2.3 Viscosity

The viscosity of the salt brine deicer (23.3% wt. NaCl) and bio-based deicing solutions (23.3% wt. NaCl + 27.7% wt. sorbitol, 23.3% wt. NaCl + 27.7% wt. maltitol, and 23.3% wt. NaCl + 13.3% mannitol) is determined using the procedure provided in Section 4.1.3. The viscosity of both reference and bio-based deicing solutions are provided in Table 4.2. From Table 4.2, it can be inferred that the viscosity of the salt brine deicer (23.3% wt. NaCl) increased with the addition of corn-based polyols (sorbitol or mannitol or maltitol). The addition of 27.7% wt. sorbitol and 27.7% wt. maltitol is observed to increase the viscosity of the salt brine deicer (23.3% wt. NaCl) by 50 % and 64% respectively. Similarly, the bio-based deicing solution with 13.3% wt. mannitol in 23.3% wt. NaCl exhibited a 21.4% increase in viscosity when compared to the viscosity of the salt brine deicer. Comparing the trends of viscosity and the trends of reduction in the average BPN values

(see Figure 4.8), it can be inferred that higher viscosity values resulted in a higher reduction in skid resistance of the pavement surfaces.

Table 4.2. The viscosity of deicer solutions (20.3°C).

S. No.	Solution	Viscosity (MPa.s)
1	23.3% Brine	1.143
2	23.3% Brine + 27.7% Sorbitol	1.714
3	23.3% Brine + 27.7% Maltitol	1.878
4	23.3% Brine + 13.3% Mannitol	1.388
*5	Tap water	0.979

Note: (*) indicates measurement performed for calibration.

4.2.4 Dissolved Oxygen

The average of the three replicates and the reduction in DO levels after 3 days is summarized in Table 4.3. Three-day Dissolved Oxygen test of river water mixed with various deicers. From Table 4.3, it is found that 23.3% of brine deicer did not affect the DO levels of raw water after 3 days. However, for deicer solutions prepared from the corn-based polyols+brine the DO levels were observed to drop. While sorbitol recorded the highest additional drop in DO level (12.36%), the mannitol was observed to record the least additional drop in DO level (2.3%). According to APHA (1992) (Apha 1992) guidelines, at least one sample dilution must meet the criteria of a residual DO of at least 1 mg/L and depletion of at least 2 mg/L to achieve a valid Biological Oxygen Demand (BOD) test. At this juncture, it is important to note that the DO test was performed only to acquire preliminary water quality results, which is not a complete indication of the acute toxicity of water bodies. Standard tests like BOD, COD, phytotoxicity, etc. may be required to obtain an overall evaluation of the influence of deicer on water bodies which is out of the scope of the current study and hence is not considered.

Table 4.3. Three-day Dissolved Oxygen test of river water mixed with various deicers

S. No	Deicer Solution		Dissolved Oxygen (mg/L)				
			1	2	3	Average	Consumed DO
1	Control sample (River water)	**Day 0**	6.85	6.99	6.77	6.87	1.43
		Day 3	5.33	5.29	5.69	5.44	
2	23.3% Brine	**Day 0**	6.89	6.93	6.71	6.84	1.42
		Day 3	5.5	5.29	5.47	5.42	
3	23.3% Brine + 27.7% Sorbitol	**Day 0**	6.59	6.45	6.31	6.45	2.14
		Day 3	4.12	4.4	4.4	4.31	
4		**Day 0**	6.5	6.6	6.2	6.43	1.89

	23.3% Brine + 27.7% Maltitol	***Day 3***	4.48	4.75	4.4	4.54	
5	23.3% Brine + 13.3% Mannitol	***Day 0***	6.46	6.61	6.4	6.49	1.50
		Day 3	5.26	4.96	4.75	4.99	

Note: 'Day 0' indicates the reading obtained immediately after the addition of deicer solution and 'Day 3' indicates the reading obtained after 72 hours of deicer addition.

4.3 Conclusions

Following are the important conclusions that can be drawn from this study:

1. The salt brine deicer mixed with bio-based additives exhibited superior ice melting capacity even at sub-freezing temperatures when compared to salt brine deicer alone.
   a. When 27.7% wt. mannitol is added to the salt brine deicer, 93%, 112%, and 81% increase in the ice melting is observed at -10 °C, -20 °C, and -30 °C, respectively when compared to the reference 23.3% wt. salt brine deicer.
   b. The addition of 27.7% wt. sorbitol resulted in a 43% and 13% increase in the ice melting capacity of the reference salt brine at -10 °C and -20 °C, respectively. However, at -30 °C, the addition of 27.7% wt. sorbitol to salt brine deicer did not improve the ice melting capacity.
   c. When 27.7% wt. maltitol is added to salt brine deicer, the ice melting capacity of the deicing solution increased by 17% at both -10 °C and -20 °C. However, at -30 °C, the addition of 27.7% wt. maltitol to salt brine deicer did not improve the ice melting capacity of the traditional salt brine deicer.
2. The average skid resistance of PCC pavement decreased by 17% after the application of salt brine deicer. The application of polyol-based deicers led to an average reduction of 33% in the skid resistance of the PCC pavement surface when compared to the skid resistance of the dry surface.
3. The addition of 27.7% sorbitol and 27.7% maltitol in the salt brine deicer results in average increase of 50% and 64%, respectively, in the viscosity of the salt brine deicer. Moreover, the bio-based deicers with high viscosities are also observed to result in the lower skid resistance of the PCC pavements.
4. The addition of polyols to the salt brine is observed to reduce the DO levels. The addition of 27.7% wt. sorbitol and 13.3% wt. mannitol to the traditional salt brine deicer resulted in 12.36% and 2.30% additional deterioration in DO when compared to salt brine alone. However the residual DO is significantly above 1 mg/ L which is recommended by the current standards.

CHAPTER 5
CONCLUSIONS AND RECOMMENDATIONS

The role of various corn-based polyols in enhancing the deicing characteristics of salt-brine solution is explored in this research. To this end, five different deicer characterization tests, namely freezing point depression, corrosion inhibition, ice melting, skid resistance, and dissolved oxygen were carried out to quantify the respective properties of the polyol-brine blends. All the tests were carried out in accordance with SHRP guidelines (Chappelow et al. 1992) whenever the appropriate recommendations are available. The compositions of the various polyols-brine blends and their properties obtained from the experiments are summarized in Table 5.1.

Table 5.1 Various combinations of polyols-brine employed in this study and their deicing characteristics

S. No	Test	Combination	Metric
1	Freezing point depression	23.3% Brine	-21.1°C
		23.3% Brine + 27.7% Sorbitol	-38.1°C
		23.3% Brine + 27.7% Maltitol	-35.6°C
		23.3% Brine + 13.3% Mannitol	-26.7°C
2	Corrosion inhibition	23.3% Brine	0.83mm/yr.
		23.3% Brine + 3% Sorbitol	0.06mm/yr.
		23.3% Brine + 2% Maltitol	0.06mm/yr.
		23.3% Brine + 3% Mannitol	0.09mm/yr.
3	Ice melting*	23.3% Brine + 27.7% Sorbitol	13%@ -20°C
		23.3% Brine + 27.7% Maltitol	17%@ -20°C
		23.3% Brine + 27.7% Mannitol	112%@ -20°C
4	Skid resistance	23.3% Brine	94.6 BPN
		23.3% Brine + 27.7% Sorbitol	76.8 BPN
		23.3% Brine + 27.7% Maltitol	60.0 BPN
		23.3% Brine + 27.7% Mannitol	68.4 BPN
		23.3% Brine + 13.3% Mannitol	77.4 BPN
5	Dissolved oxygen (3 days)	23.3% Brine	1.42 mg/ml
		23.3% Brine + 27.7% Sorbitol	2.14 mg/ml
		23.3% Brine + 27.7% Maltitol	1.89 mg/ml
		23.3% Brine + 13.3% Mannitol	1.50 mg/ml

Note: Asterik (*) indicates the percentage increase in the deicing characteristic when compared to 23.3 wt. % salt-brine alone.

5.1 Conclusions

The following are the conclusions drawn from this study.

1. Sorbitol exhibited the highest freezing point depression when mixed with the salt-brine solution among the polyols studied for all the deicing characteristics in this study. The

weight fraction of the constituents used for this combination is 27.77 wt.% of sorbitol + 23.3 wt.% salt-brine solution and, the freezing point depression obtained for this combination is -38.1°C.

2. The highest corrosion inhibition was observed when a blend of maltitol and the salt-brine solution was used. The weight fraction of the constituents used for this combination is 0.5-2 wt.% of maltitol + 23.3 wt.% salt-brine solution, and the corrosion rate obtained for this combination is 0.14-0.06 mm/yr (0.83 mm/yr for 23% salt brine).
3. The addition of mannitol to salt-brine solution improved the ice melting capacity 112% at the sub-freezing temperature of -20°C when compared to the salt-brine solution. The blend that produced the highest ice melting capacity is 27.77 wt.% of mannitol + 23.3 wt.% salt-brine.
4. While the decrease in the skid-resistance for salt-brine is around 17%, the skid resisence of polyol-salt blends can fall up to 33% when compared to the dry pavements.
5. The consumption of Dissolved Oxygen in the stream water was found not to exceed the recommended limit suggested by APHA guidelines (1992). The combination that resulted in the least dissolved oxygen is 13.33 wt.% of mannitol + 23.3 wt.% salt-brine, which is comparable to the 23.3 wt.% salt-brine alone.

5.2 Recommendations

Based on the experimental results, the following recommendations are provided

1. The combinations of polyol-brine blends in the decreasing order of freezing temperatures is provided in the funnel chart Figure 5.1.

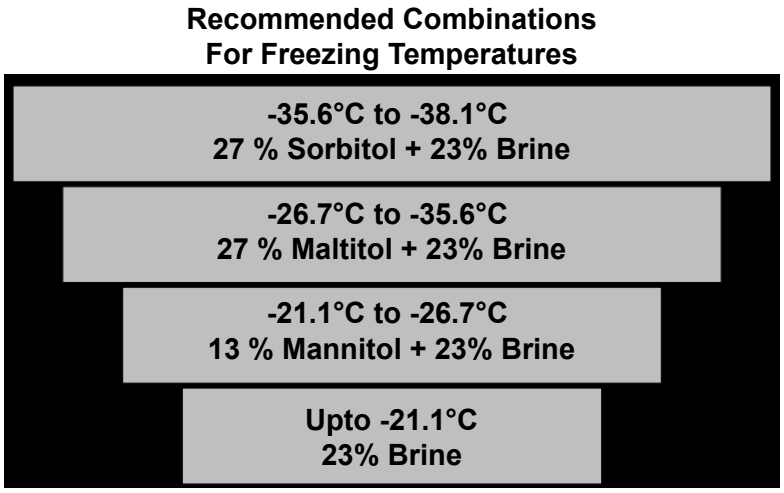

Figure 5.1. Recommended combinations for freezing point depression

2. The preferential order (first blend – highest priority) of polyol-brine blends for corrosion inhibition in concrete pavements, bridge decks, and airports are provided in funnel chart Figure 5.2.

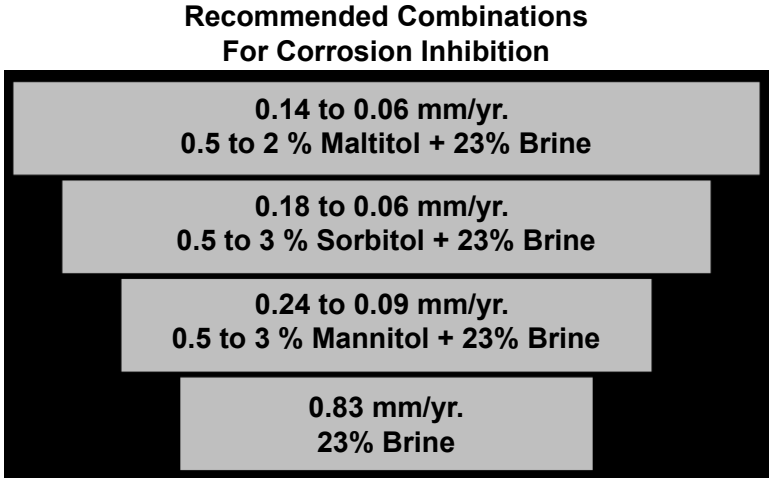

Figure 5.2. Recommended combinations for corrosion inhibition

3. The preferential order (first blend – highest priority) of various polyol-brine blends is provided in the funnel chart Figure 5.3.

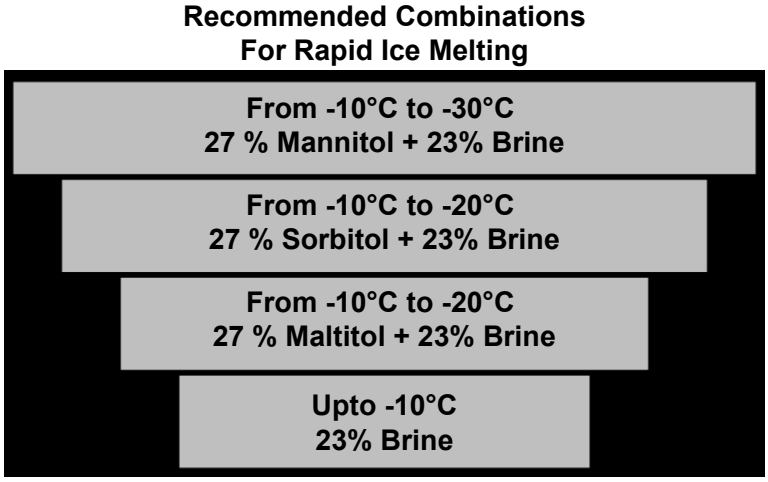

Figure 5.3. Recommended combinations for rapid ice melting

References

Administration, N. H. T. S. (2018). "FARS Encyclopedia."

Alcántara, J., Chico, B., Simancas, J., Díaz, I., and Morcillo, M. (2017). "Marine atmospheric corrosion of carbon steel: A review." *Materials*, 10(4), 406.

Aliyu, B., Osheku, C., Oyedeji, E., ADETORO, M., Okon, A., and Idoko, C. (2015). "Validating a novel theoretical expression for burn tine and average thrust in solid rocket motor design." *Advances in research*, 5, 1-11.

Amrhein, C., Strong, J. E., and Mosher, P. A. (1992). "Effect of deicing salts on metal and organic matter mobilization in roadside soils." *Environmental Science & Technology*, 26(4), 703-709.

Apha, A. (1992). "WPCF (American Public Health Association, American Waterworks Association, Water Pollution Control Federation)(1992) Standard methods for the examination of water and wastewater." *Standard methods for the examination of water and wastewater*, 17.

ASTM (2018). "*ASTM A572/A572M-18 Standard Specification for High-Strength Low-Alloy Columbium-Vanadium Structural Steel*.", ASTM International, West Conshohocken, PA.

ASTM (2018). "ASTM E303 – 93 Standard Test Method for Measuring Surface Frictional Properties Using the British Pendulum Tester."ASTM International.

ASTM, and International (2016). "ASTM B117-16 *S*tandard Practice for Operating Salt Spray (Fog) Apparatus." ASTM International, West Conshohocken, PA.

ASTM-G102-89-e1 (2015). "Standard Practice for Calculation of Corrosion Rates and Related Information from Electrochemical measurements." ASTM International.

Auleda, J. M., Raventós, M., Sánchez, J., and Hernández, E. (2011). "Estimation of the freezing point of concentrated fruit juices for application in freeze concentration." *Journal of Food Engineering*, 105(2), 289-294.

Awad, M., Saad, A., Shaaban, M., Jahdaly, B., and Hazazi, O. A. (2017). "New insight into the mechanism of the inhibition of corrosion of mild steel by some amino acids." *Int. J. Electrochem. Sci*, 12, 1657-1669.

Barclay, A., Sandall, P., and Shwide-Slavin, C. (2014). *The ultimate guide to sugars and sweeteners: Discover the taste, use, nutrition, science, and lore of everything from agave nectar to xylitol*, The Experiment.

Belch, A. C., Berkowitz, M., and McCammon, J. (1986). "Solvation structure of a sodium chloride ion pair in water." *Journal of the American Chemical Society*, 108(8), 1755-1761.

BeMiller, J. N. (2018). *Carbohydrate chemistry for food scientists*, Elsevier.

Berglund, K. A., Alizadeh, H., and Dunuwila, D. D. (2001). "Deicing compositions and methods of use." Google Patents.

Biresaw, G., and Mittal, K. L. (2011). *Surfactants in Tribology, 2 Volume Set*, CRC Press.

Bloomer, T. A. (2000). "Anti-freezing and deicing composition and method." Google Patents.

Bradt, C. B., Lehoux, R. R., Schwartz, M. I., and Spanos, D. (2014). "Deicing formulation utilizing co-products from lignocellulose to bio fuel process." Google Patents.

Brycki, B. E., Kowalczyk, I. H., Szulc, A., Kaczerewska, O., and Pakiet, M. "Organic Corrosion Inhibitors." *Corrosion Inhibitors, Principles and Recent Applications*, IntechOpen.

Butt, H.-J., Graf, K., and Kappl, M. (2013). *Physics and chemistry of interfaces*, John Wiley & Sons.

Bäckström, M., Karlsson, S., Bäckman, L., Folkeson, L., and Lind, B. (2004). "Mobilisation of heavy metals by deicing salts in a roadside environment." *Water research*, 38(3), 720-732.
Chappelow, C. C., McElroy, A. D., Blackburn, R. R., Darwin, D., de Noyelles, F. G., and Locke, C. E. (1992). "Handbook of test methods for evaluating chemical deicers." Strategic Highway Research Program.
Chappelow, C. C., McElroy, A. D., Blackburn, R. R., Darwin, D., de Noyelles, F. G., and Locke Jr, C. E. (1992). "Handbook of test methods for evaluating chemical deicers." Strategic Highway Research Program.
Christov, M., and Popova, A. (2004). "Adsorption characteristics of corrosion inhibitors from corrosion rate measurements." *Corrosion science*, 46(7), 1613-1620.
Consultants, P. S. (1993). "The Use of Selected Deicing Materials on Michigan Roads: Environmental and Economic Impacts." <https://www.michigan.gov/documents/ch2-deice_51438_7.pdf>.
Corsi, S. R., Graczyk, D. J., Geis, S. W., Booth, N. L., and Richards, K. D. (2010). "A fresh look at road salt: aquatic toxicity and water-quality impacts on local, regional, and national scales." *Environmental science & technology*, 44(19), 7376-7382.
Darwin, D., Browning, J., Gong, L., and Hughes, S. R. "Effects of deicers on concrete deterioration." American Concrete Institute.
Dewick, P. M. (2006). *Essentials of organic chemistry: for students of pharmacy, medicinal chemistry and biological chemistry*, John Wiley & Sons.
Dwyer, F. P. J., and Mellor, D. P. (1964). *Chelating agents and metal chelates*, Academic Press, New York.
E274M-15, A. E. (2020). "Standard Test Method for Skid Resistance of Paved Surfaces Using a Full-Scale Tire." ASTM International.
E1859/E1859M-11, A. (2015). "Standard Test Method for Friction Coefficient Measurements Between Tire and Pavement Using a Variable Slip Technique."ASTM International.
E1911-19, A. (2019). "Standard Test Method for Measuring Surface Frictional Properties Using the Dynamic Friction Tester."
Fay, L., and Akin, M. (2018). "Investigation of Alternative Deicers for Snow and Ice Control." Center for Environmentally Sustainable Transportation in Cold Climates.
Fay, L., Volkening, K., Gallaway, C., and Shi, X. "Performance and impacts of current deicing and anti-icing products: User perspective versus experimental data." *Proc., 87th Annual Meeting of the Transportation Research Board, Washington, DC*, Citeseer, 1-22.
FHWA (2018). "How Do Weather Events Impact Roads? - FHWA Road Weather Management." <https://ops.fhwa.dot.gov/weather/q1_roadimpact.htm>.
Fischel, M. (2001). "Evaluation of selected deicers based on a review of the literature." Colorado Department of Transportation.
Fischel, M. (2009). "Evaluation of Selected Deicers Based on a Review of the Literature —."
Freundlich, H. (1906). "Over the Adsorption in Solution." *Journal of Physical Chemistry*, 57(25), 385-471.
Gerbino-Bevins, B., Tuan, C. Y., and Mattison, M. (2012). "Evaluation of Ice-Melting Capacities of Deicing Chemicals." *Journal of Testing and Evaluation*, 40(6), 952-960.
Goff, D. (2018). "Theoretical Aspects of the Freezing Process." <https://www.uoguelph.ca/foodscience/book/export/html/1881>.
Groenewoud, W. M. (2001). *Characterisation of polymers by thermal analysis*, Elsevier.

Gucunski, N., Maher, A., Basily, B., La, H., Lim, R., Parvardeh, H., and Kee, S. (2013). "Robotic platform rabit for condition assessment of concrete bridge decks using multiple nde technologies." *HDKBR INFO Magazin*, 3(4), 5-12.

Guddat, S., Thevis, M., and Schänzer, W. (2008). "Identification and quantification of the osmodiuretic mannitol in urine for sports drug testing using gas chromatography-mass spectrometry." *European Journal of Mass Spectrometry*, 14(3), 127-133.

Hartley, R. A., and Wood, D. H. (2001). "Deicing solution." Google Patents.

Henry, J. J. (2000). *Evaluation of pavement friction characteristics*, Transportation Research Board.

Hodge, J., Nelson, E., and Moy, B. (1963). "Chelates in Agriculture, Metal Chelation by Glucose-Ammonia Derivatives." *Journal of Agricultural and Food Chemistry*, 11(2), 126-129.

HOLLAND, R. I. (1991). "Use of potentiodynamic polarization technique for corrosion testing of dental alloys." *European Journal of Oral Sciences*, 99(1), 75-85.

Hosking, J., and Woodford, G. (1976). "Measurement of skidding resistance. Part 1: guide to the use of SCRIM."

Hui, Y. H., and Sherkat, F. (2005). *Handbook of food science, technology, and engineering-4 volume Set*, CRC press.

IowaDoT (2018). "Office of Maintenance - Iowa Department of Transportation." <https://iowadot.gov/maintenance/winter-operations/materials>.

Izumi, I., Nakamura, T., and Sack, R. L. (1997). *Snow Engineering: Recent Advances: Proceedings of the third international conference, Sendai, Japan, 26-31 May 1996*, CRC Press.

Janke, G. A., and Johnson Jr, W. D. (1997). "Deicing composition and method." Google Patents.

Janke, G. A., and Johnson Jr, W. D. (1998). "Deicing composition and method." Google Patents.

Jayawardena, J., Vanniarachchi, M., and Wansapala, M. (2017). "Freezing point depression of different Sucrose solutions and coconut water." *International Journal of Food Science and Nutrition*, 2, 68-71.

Jones, D. A. (1996). *Principles and Prevention of Corrosion*, Prentice Hall.

Kaczerewska, O., Leiva-Garcia, R., Akid, R., Brycki, B., Kowalczyk, I., and Pospieszny, T. (2018). "Effectiveness of O-bridged cationic gemini surfactants as corrosion inhibitors for stainless steel in 3 M HCl: Experimental and theoretical studies." *Journal of Molecular Liquids*, 249, 1113-1124.

Kalsoom, U., Bennett, I., and Boyce, M. C. (2016). "A review of extraction and analysis: methods for studying osmoregulants in plants." *J Chromatogr Sep Tech*, 7(315), 2.

Kao, J. C., and Sung, W.-P. (2017). *Civil, Architecture and Environmental Engineering Volume 2: Proceedings of the International Conference ICCAE, Taipei, Taiwan, November 4-6, 2016*, CRC Press.

Kelley, M., Donley, A., Clark, S., and Clark, A. (2015). "Structure and dynamics of NaCl ion pairing in solutions of water and methanol." *The Journal of Physical Chemistry B*, 119(51), 15652-15661.

Kelly, R. G., Scully, J. R., Shoesmith, D., and Buchheit, R. G. (2002). *Electrochemical techniques in corrosion science and engineering*, CRC Press.

Kelting, D. L. (2010). *Review of effects and costs of road de-icing with recommendations for winter road management in the Adirondack Park*.

Kerti, J., Kardos, P., and Kalman, T. (2001). "Environmentally safe snow and ice dissolving liquid." Google Patents.

Ketcham, S., Minsk, L. D., Blackburn, R. R., and Fleege, E. J. (1996). "Manual of practice for an effective anti-icing program: a guide for highway winter maintenance personnel." United States. Federal Highway Administration.
Kim, Y.-S., and Kim, J.-G. (2017). "Corrosion behavior of pipeline carbon steel under different iron oxide deposits in the district heating system." *Metals*, 7(5), 182.
Kimbrough, D. (2006). "Salting roads: The solution for winter driving." *ChemMatters*, 14-16.
Klyosov, A. A., Philippidis, G. P., James, A. M., and Monovoukas, Y. A. (2000). "Liquid and solid de-icing and anti-icing compositions and methods for making same." Google Patents.
Koefod, R. S. (2000). "Deicer composition which includes a plant material which is a corrosion inhibitor." Google Patents.
Koefod, R. S., and Rose III, R. H. (2004). "Deicer and pre-wetting agent." Google Patents.
Kokkalis, A. G., and Panagouli, O. K. (1998). "Fractal evaluation of pavement skid resistance variations. I: Surface Wetting." *Chaos, Solitons & Fractals*, 9(11), 1875-1890.
Lai, C., Xie, B., Zou, L., Zheng, X., Ma, X., and Zhu, S. (2017). "Adsorption and corrosion inhibition of mild steel in hydrochloric acid solution by S-allyl-O, O′-dialkyldithiophosphates." *Results in physics*, 7, 3434-3443.
Langmuir, I. (1916). "The constitution and fundamental properties of solids and liquids. Part I. Solids." *Journal of the American chemical society*, 38(11), 2221-2295.
Lewis, M., Burkhardt, S., and Lewis, J. (2019). "Deicing composition comprising lignocellulosic byproducts." Google Patents.
Lgaz, H., Salghi, R., Bhat, K. S., Chaouiki, A., and Jodeh, S. (2017). "Correlated experimental and theoretical study on inhibition behavior of novel quinoline derivatives for the corrosion of mild steel in hydrochloric acid solution." *Journal of Molecular Liquids*, 244, 154-168.
Liu, Y. (2009). "Is the Free Energy Change of Adsorption Correctly Calculated?" *Journal of Chemical & Engineering Data*, 54(7), 1981-1985.
Liu, Y., Fwa, T., and Choo, Y. (2004). "Effect of surface macrotexture on skid resistance measurements by the British Pendulum Test." *Journal of Testing and Evaluation*, 32(4), 304-309.
Louhenkilpi, S. (2014). "Continuous Casting of Steel." *Treatise on Process Metallurgy*, S. Seetharaman, ed., Elsevier, Boston, 373-434.
Marshall, R. T., Goff, H. D., and Hartel, R. W. (2012). *Ice cream*, Springer.
Marzorati, S., Verotta, L., and Trasatti, S. (2019). "Green corrosion inhibitors from natural sources and biomass wastes." *Molecules*, 24(1), 48.
Mateega, R. E. (2013). "Rehabilitation of Historic Holmes Street Bridge." *STRUCTURE*, STRUCTURE Magazine, 3.
McCafferty, E. (2005). "Validation of corrosion rates measured by the Tafel extrapolation method." *Corrosion Science*, 47(12), 3202-3215.
McCafferty, E. (2010). *Introduction to Corrosion Science*, Springer Science & Business Media.
MPCA (2018). "Environmental impacts of road salt and other de-icing chemicals - Minnesota Stormwater Manual." <https://stormwater.pca.state.mn.us/index.php/Environmental_impacts_of_road_salt_and_other_de-icing_chemicals>.
Muthumani, A., Fay, L., Bergner, D., and Shi, X. (2015). "Understanding the Effectiveness of Non-Chloride Liquid Agricultural By-Products and Solid Complex Chloride/Mineral Products."

NASS/USDA (2018). "Ranking Of States That Produce The Most Corn." <http://beef2live.com/story-ranking-states-produce-corn-0-107129>.
Nazari, M. H., and Shi, X. (2019). "Developing Renewable Agro-Based Anti-Icers for Sustainable Winter Road Maintenance Operations." *Journal of Materials in Civil Engineering*, 31(12), 04019299.
NCGA (2018). "National Corn Growers Association - World of Corn 2018." <http://www.worldofcorn.com/#us-average-corn-yield>.
NHTSA (2018). "FARS Encyclopedia." <https://www-fars.nhtsa.dot.gov/Crashes/CrashesTime.aspx>.
Nixon, W. A., and Xiong, J. (2009). "Investigation of materials for the reduction and prevention of corrosion on highway maintenance equipment." Citeseer.
Pappas, L. S. (2006). *Ice Creams & Sorbets: Cool Recipes*, Chronicle Books LLC.
Peterson, O. (1995). "Chemical effects on cement mortar of calcium magnesium acetate as a deicing salt." *Cement and Concrete Research*, 25(3), 617-626.
Potera, C. (2005). "Making succinate more successful." National Institute of Environmental Health Sciences.
Public Sector Consultants, I. (1993). "The Use of Selected Deicing Materials on Michigan Roads: Environmental and Economic Impacts." <https://www.michigan.gov/documents/ch2-deice_51438_7.pdf>.
Rahman, M. S., Guizani, N., Al-Khaseibi, M., Al-Hinai, S. A., Al-Maskri, S. S., and Al-Hamhami, K. (2002). "Analysis of cooling curve to determine the end point of freezing." *Food Hydrocolloids*, 16(6), 653-659.
Rahman, M. S., Guizani, N., Al-Khaseibi, M., Ali Al-Hinai, S., Al-Maskri, S. S., and Al-Hamhami, K. (2002). "Analysis of cooling curve to determine the end point of freezing." *Food Hydrocolloids*, 16(6), 653-659.
Revie, R. W., and Uhlig, H. H. (2008). "Inhibitors and Passivators." *Corrosion and Corrosion Control*, 303-316.
Roberge, P. R. (2000). *Handbook of corrosion engineering*, McGraw-Hill.
Sajid, H. U., and Kiran, R. (2018). "Influence of corrosion and surface roughness on wettability of ASTM A36 steels." *Journal of Constructional Steel Research*, 144, 310-326.
Sajid, H. U., and Kiran, R. (2018). "Influence of high stress triaxiality on mechanical strength of ASTM A36, ASTM A572 and ASTM A992 steels." *Construction and Building Materials*, 176, 129-134.
Sajid, H. U., and Kiran, R. (2019). "Post-fire mechanical behavior of ASTM A572 steels subjected to high stress triaxialities." *Engineering Structures*, 191, 323-342.
Sajid, H. U., Naik, D. L., and Kiran, R. (2020). "Microstructure-mechanical Property Relationships for Post-fire Structural Steels." *ASCE Journal of Materials in Civil Engineering*.
Salt, N. R. C. C. o. t. C. C. o. R., and Deicing, C. M. A. f. H. (1991). *Highway deicing: comparing salt and calcium magnesium acetate*, Transportation Research Board.
Sanburn, M. R. a. J. (2018). "How Beet Juice Is Helping Keep Roads Safe This Winter." @TIME.
Shi, X. (2008). *Impact of airport pavement deicing products on aircraft and airfield infrastructure*, Transportation Research Board.
Shi, X., Fay, L., Gallaway, C., Volkening, K., Peterson, M. M., Pan, T., Creighton, A., Lawlor, C., Mumma, S., and Liu, Y. (2009). "Evaluation of alternative anti-icing and deicing compounds using sodium chloride and magnesium chloride as baseline deicers–Phase I." Colorado. Dept. of Transportation. Applied Research and Innovation Branch.

Shi, X., Fay, L., Yang, Z., Nguyen, T. A., and Liu, Y. (2009). "Corrosion of deicers to metals in transportation infrastructure: Introduction and recent developments." *Corrosion reviews*, 27(1-2), 23-52.
Shi, X., and Fu, L. (2018). *Sustainable Winter Road Operations*, John Wiley & Sons.
Shi, X., Li, Y., Jungwirth, S., Fang, Y., Seeley, N., and Jackson, E. (2012). "Identification and laboratory assessment of best practices to protect DOT equipment from the corrosive effect of chemical deicers." Washington State Department of Transportation.
Sliem, M. H., Afifi, M., Radwan, A. B., Fayyad, E. M., Shibl, M. F., Heakal, F. E.-T., and Abdullah, A. M. (2019). "AEO7 Surfactant as an Eco-Friendly Corrosion Inhibitor for Carbon Steel in HCl solution." *Scientific reports*, 9(1), 2319.
Srivastava, L. M. (2002). *Plant growth and development: hormones and environment*, Elsevier.
Standish, N. W., and Cross, G. G. (1965). "Deicer composition." Google Patents.
Stefan, H. G., Novotny, E., Sander, A., and Mohseni, O. (2008). "Study of Environmental Effects of De-Icing Salt on Water Quality in the Twin Cities Metropolitan Area, Minnesota."
Stewart, M. I. (2014). "Heat Transfer Theory." *Surface Production Operations*, M. I. Stewart, ed., Gulf Professional Publishing, Boston, 39-97.
sumsion, E. S., and Guthrie, S. "Physical and Chemical Effects of Deicers on Concrete Pavement: Literature Review." <https://www.udot.utah.gov/main/uconowner.gf?n=8081525197623431>.
Sumsion, E. S., and Guthrie, S. (2013). "Physical and Chemical Effects of Deicers on Concrete Pavement: Literature Review." <https://www.udot.utah.gov/main/uconowner.gf?n=8081525197623431>.
Talor, P., Gopalakrishnan, K., Verkade, J. G., Wadhwa, K., and Kim, S. (2010). "Development of an Improved Agricultural-Based Deicing Product."
Talor, P., Gopalakrishnan, K., Verkade, J. G., Wadhwa, K., and Kim, S. (2010). "f an Improved Agricultural-Based Deicing Product."
Telis, V., Telis-Romero, J., Sobral, P., and Gabas, A. (2007). "Freezing point and thermal conductivity of tropical fruit pulps: mango and papaya." *International Journal of Food Properties*, 10(1), 73-84.
URAJI, T., KOHNO, H., YOSHIMURA, H., SHIMOYAMADA, M., and WATANABE, K. (1996). "Freezing point depression of polyol-aqueous solutions in the high concentration range." *Food Science and Technology International, Tokyo*, 2(1), 38-42.
Villa-Vélez, H. A., Telis-Romero, J., Higuita, D. M. C., and Telis, V. R. N. (2012). "Effect of maltodextrin on the freezing point and thermal conductivity of uvaia pulp (Eugenia piriformis Cambess)." *Ciência e Agrotecnologia*, 36(1), 78-85.
Wambold, J. C., Meyer, W. E., and Henry, J. J. (1990). "New-Generation Skid Testers for the 1990s." *Surface Characteristics of Roadways: International Research and Technologies*, ASTM International.
Wang, K., Nelsen, D. E., and Nixon, W. A. (2006). "Damaging effects of deicing chemicals on concrete materials." *Cement and Concrete Composites*, 28(2), 173-188.
Wang, W.-y., Liu, B., and Kodur, V. (2012). "Effect of temperature on strength and elastic modulus of high-strength steel." *Journal of materials in civil engineering*, 25(2), 174-182.
Yang, B. Y., and Montgomery, R. (2003). "De-icers derived from corn steep water." *Bioresource technology*, 90(3), 265-273.

Zumbe, A., Lee, A., and Storey, D. (2001). "Polyols in confectionery: the route to sugar-free, reduced sugar and reduced calorie confectionery." *British Journal of nutrition*, 85(S1), S31-S45.